Dynamics of a 2D Piecewise Linear Braess Paradox Model: Effect of the Third Partition

International Journal of Bifurcation and Chaos

DYNAMICS OF A 2D PIECEWISE LINEAR BRAESS PARADOX MODEL: EFFECT OF THE THIRD PARTITION

VIKTOR AVRUTIN
DESP, University of Urbino, Italy,
Avrutin.Viktor@ist.uni-stuttgart.de

CHRISTOPH DIBAK
IPVS, University of Stuttgart, Germany,
Christoph.Dibak@ipvs.uni-stuttgart.de

ARIANNA DAL FORNO
DESt "Cognetti de Martiis", University of Torino,Torino, Italy,
arianna.dalforno@unito.it

UGO MERLONE
Department of Psychology, University of Torino, Torino, Italy,
ugo.merlone@unito.it

Received (to be inserted by publisher)

In this work we investigate the dynamics of a piecewise linear 2D discontinuous map modeling a simple network showing the Braess paradox. This paradox represents an example in which adding a new route to a specific congested transportation network makes all the travelers worse off in terms of their individual travel time. In the particular case in which the modeled network corresponds to a binary choice situation, the map is defined on two partitions and its dynamics has already been described. In the general case corresponding to a ternary choice, a third partition appears leading to a significantly more complex bifurcation structures formed by border collision bifurcations of stable cycles with points located in all three partitions. Considering a map taking a constant value on one of the partitions, we provide a first systematic description of possible dynamics for this case.

Keywords: piecewise smooth maps; discontinuous maps; border collision bifurcations; Braess paradox;

1. Introduction

The Braess paradox, initially introduced in [Braess, 1968], is an example of a counter-intuitive situation in which making an additional resource available decreases the overall performance of a system instead of increasing it. In particular, referring to selfish routing of agents in a network it is possible to show that adding edges to a network can increase the latency incurred by all of the traffic at equilibrium (an equivalent characterization in which edges are removed is presented in [Lin *et al.*, 2011]).
As pointed out by Korilis *et al.*, this is not a real paradox but rather an "instance of the Pareto inefficiency of non-cooperative equilibria" [Korilis *et al.*,

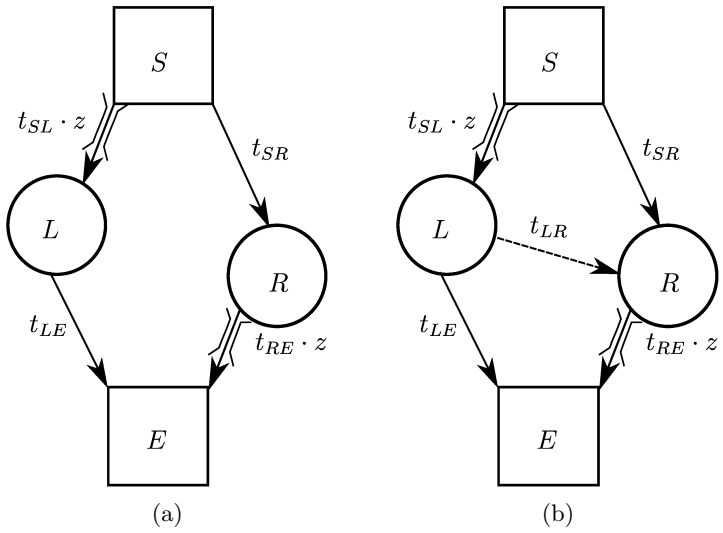

Fig. 1. Networks for the Braess paradox example (a) before and (b) after introducing an additional edge.

1999, p.215]. Nevertheless the original paper by Braess has received an impressive numbers of citations with applications to several fields such as transportation [Nagurney & Boyce, 2005], communication [Altman *et al.*, 2008], computer science [Roughgarden & Tardos, 2002], economic planning [Malkevitch, 2011] and even to outbreaks of global infectious diseases [Zhang *et al.*, 2013].

The Braess paradox can be illustrated by the example shown in Fig. 1. Assume, there is a unitary mass of commuters moving from Start (S) to End (E), and there are two symmetrical routes from S to E each of which consisting of a section of road and a bridge, as shown in Fig. 1(a). The time spent along segments $S \to R$ and $L \to E$ does not depend on traffic and takes $t_{LE} = t_{SR} = 27$ minutes. On the contrary, the bridges are bottlenecks: the time spent along segments $S \to L$ and $R \to E$ is proportional to the number of commuters, i.e., $t_{SL} \cdot z = t_{RE} \cdot z = 24z$ minutes, where $z \in [0, 1]$ is the fraction of the population using that segment. In this network there is a Nash equilibrium with commuters splitting in two equal groups at S, so that both roads take a total travel time of 39 minutes. Now we assume that a very fast road is built connecting L to R in $t_{LR} = 3$ minutes, as shown in Fig. 1(b). In the augmented network there is a new Nash equilibrium in which the entire population chooses route $S \to L \to R \to E$ with 51 minutes total travel time. Therefore, adding a link to a network with linear costs depending on congestion, when each user independently seeks the best possible route, the total travel time may increase.

Although a lot of interest has been devoted to several aspects of the Braess paradox, contributions analyzing it from the dynamical point of view are scant. For example, starting from the contributions [Bischi *et al.*, 2009a], [Bischi *et al.*, 2009b] on the dynamics of impulsive agents facing binary choices, [Dal Forno & Merlone, 2013a] analyzes the Braess paradox as a ternary choice problem and provides a first analysis of the border collision bifurcation curves. However, the complexity of the bifurcation structures appearing in this case has not been explained so far. The goal of the present paper is to analyze how the bifurcation structures are influences by introducing a third choice (the new link). In particular, the goal is to determine the regularities in the appearance of cycles with points located in all three partitions.

The paper is organized as follows. In Sec. 2 the model considered in this work is introduced. Starting from the network mentioned above a model in form of a piecewise linear discontinuous 2D map is developed. First, in Sec. 3 the behavior of this map is briefly described in the case when only two routes are available and the third route is still not introduced, i.e., in the binary choice situation. Thereafter, in Sec. 4 the main subject of the paper is addressed, namely the full network with three routes, corresponding to the ternary choice situation. The bifurcation structures appearing in this case turn out to be much more complex than in the binary choice situation, as the map is defined on three partitions instead of two. To explain this complexity, in Sec. 5 we consider a particular parameter

plane defined by the condition that the investigated map takes a constant value on one of its partitions. This property makes possible to predict which cycles exists in this parameter plane. Eventually, the obtained results are transferred back to the original parameter plane of interest, explaining a large part of its bifurcation structures (although not all of them). Additionally, in Sec. 6 we discuss some bifurcation phenomena which cannot be explained when considering only the map with a constant value on one partition. Sec. 7 concludes.

2. Model

A dynamic formulation of a population interacting on a network such as the one shown in Fig. 1 is derived in [Dal Forno & Merlone, 2013a] and [Dal Forno *et al.*, 2014]. For the sake of brevity we denote route $S{\to}L{\to}E$ with $\mathcal{L}$, route $S{\to}L{\to}R{\to}E$ with $\mathcal{M}$, and route $S{\to}R{\to}E$ with $\mathcal{R}$.
Compared to the basic network in Fig. 1(a), the new link in the augmented network in Fig. 1(a) makes a new possibility available: now the commuters have three choices, where the new one is route $\mathcal{M}$. Models with three choices in discrete time have been introduced in [Dal Forno *et al.*, 2012] and in continuous time in [Sandholm, 2010]. In this paper we analyze the dynamics when the travel time t_{LR} for the new route varies in a range that makes this link a dominant choice for some values of parameters, and a dominated choice for others.
We indicate by $x \in [0,1]$ the fraction of the unitary population choosing the route $\mathcal{L}$, and by $y \in [0,1]$ the fraction choosing the route $\mathcal{R}$. Consequently, the fraction of the population choosing the route $\mathcal{M}$ is $1-x-y \in [0,1]$. Therefore, the travel times on the routes $\mathcal{L}$, $\mathcal{M}$, and $\mathcal{R}$ are

$$t_{\mathcal{L}}(x,y) = t_{SL}(1-y) + t_{LE} \tag{1a}$$
$$t_{\mathcal{M}}(x,y) = t_{SL}(1-y) + t_{LR} + t_{RE}(1-x) \tag{1b}$$
$$t_{\mathcal{R}}(x,y) = t_{SR} + t_{RE}(1-x) \tag{1c}$$

respectively. In the numerical example presented above we obtain

$$t_{\mathcal{L}}(x,y) = 51 - 24y \tag{2a}$$
$$t_{\mathcal{M}}(x,y) = 51 - 24(x+y) \tag{2b}$$
$$t_{\mathcal{R}}(x,y) = 51 - 24x \tag{2c}$$

Since agents are interested to minimize their travel times, route $\mathcal{L}$ is the best choice when

$$t_{\mathcal{L}}(x,y) < t_{\mathcal{M}}(x,y) \quad \text{and} \quad t_{\mathcal{L}}(x,y) < t_{\mathcal{R}}(x,y) \tag{3}$$

This happens when the population is distributed along routes according to conditions

$$x < 1 - \frac{t_{LE} - t_{LR}}{t_{RE}} \tag{4a}$$
$$y < 1 - \frac{t_{SR} + t_{RE}\,(1-x) - t_{LE}}{t_{SL}} \tag{4b}$$

In the following, for the sake of simplicity, as it is common (see [Bazzan & Klüg, 2005; Rapoport *et al.*, 2006; Gisches & Rapoport, 2012]) we consider symmetric travel times and define:

$$t_{\text{road}} := t_{LE} = t_{SR} \tag{5a}$$
$$t_{\text{bridge}} := t_{SL} = t_{RE}, \tag{5b}$$

In this case, the conditions (4) become

$$x < 1 - \frac{t_{\text{road}} - t_{LR}}{t_{\text{bridge}}} \quad \text{and} \quad y > x \tag{6}$$

A similar reasoning can be applied to the routes $\mathcal{M}$ and $\mathcal{R}$. Proceeding in this way and introducing the abbreviation

$$k := 1 - \frac{t_{\text{road}} - t_{LR}}{t_{\text{bridge}}} \in \left[0, \tfrac{1}{2}\right] \tag{7}$$

we obtain three different sets of population distribution along the routes

$$\begin{aligned}\mathcal{D}_{\mathcal{L}} =& \big\{(x,y)^{\mathrm{T}} \in \mathcal{D} \mid \\ & t_{\mathcal{L}}(x,y) < \min\left(t_{\mathcal{M}}(x,y), t_{\mathcal{R}}(x,y)\right) \big\} \\ =& \{(x,y)^{\mathrm{T}} \in \mathcal{D} \mid (x<k) \text{ and } (x<y)\}\end{aligned} \tag{8a}$$

$$\begin{aligned}\mathcal{D}_{\mathcal{M}} =& \big\{(x,y)^{\mathrm{T}} \in \mathcal{D} \mid \\ & t_{\mathcal{M}}(x,y) < \min\left(t_{\mathcal{R}}(x,y), t_{\mathcal{R}}(x,y)\right) \big\} \\ =& \{(x,y)^{\mathrm{T}} \in \mathcal{D} \mid (x>k) \text{ and } (y>k)\}\end{aligned} \tag{8b}$$

$$\begin{aligned}\mathcal{D}_{\mathcal{R}} =& \big\{(x,y)^{\mathrm{T}} \in \mathcal{D} \mid \\ & t_{\mathcal{R}}(x,y) < \min\left(t_{\mathcal{L}}(x,y), t_{\mathcal{M}}(x,y)\right) \big\} \\ =& \{(x,y)^{\mathrm{T}} \in \mathcal{D} \mid (y<k) \text{ and } (x>y)\}\end{aligned} \tag{8c}$$

in which the best choice is given by route $\mathcal{L}$, route $\mathcal{M}$ and route $\mathcal{R}$, respectively.
Agents are homogeneous and minimize their next period travel time. At time $n{+}1$ the vector $(x_n, y_n)^{\mathrm{T}}$ becomes common knowledge, and each agent can estimate travel times $t_{\mathcal{L}}(x_n,y_n)$, $t_{\mathcal{M}}(x_n,y_n)$ and $t_{\mathcal{R}}(x_n,y_n)$. We assume that if at time n a fraction x_n chooses route $\mathcal{L}$ and a fraction y_n chooses route $\mathcal{R}$ and travel times are such that $t_{\mathcal{R}}(x_n,y_n) < t_{\mathcal{L}}(x_n,y_n)$ and $t_{\mathcal{R}}(x_n,y_n) < t_{\mathcal{M}}(x_n,y_n)$, then a fraction of the x_n agents who chose route $\mathcal{L}$ and a fraction of the $1-x_n-y_n$ agents who chose $\mathcal{M}$ will both switch to route $\mathcal{R}$ at next time period $n+1$. This is the same for all paths which give the smaller travel time. In other words, at any time n all the

agents decide their route for time $n+1$ comparing times $t_{\mathcal{L}}(x_n, y_n)$, $t_{\mathcal{M}}(x_n, y_n)$ and $t_{\mathcal{R}}(x_n, y_n)$.
As already mentioned, commuters may switch route whenever another route becomes more attractive; following [Dal Forno & Merlone, 2013a] we assume that not all the commuters switch to the new route, rather the fraction of those who actually switch is respectively $\delta_{\mathcal{L}} \in (0,1]$ for those switching to $\mathcal{L}$, $\delta_{\mathcal{M}} \in (0,1]$ for those switching to $\mathcal{M}$, and $\delta_{\mathcal{R}} \in (0,1]$ for those switching to $\mathcal{R}$. Finally, assume that agents are impulsive, that is, they switch routes even when the difference between travel times is extremely small, as in [Bischi *et al.*, 2009a].
In this way we obtain the following model reflecting the dynamics of the network described above. The model is given by the 2D piecewise linear map:

$$\begin{aligned}(x_{n+1}, y_{n+1})^{\mathrm{T}} &= \vec{f}(x_n, y_n) \\ &= (f^x(x_n, y_n), f^y(x_n, y_n))^{\mathrm{T}}\end{aligned} \tag{9}$$

with

$$f^x(x,y) = \begin{cases} f^x_{\mathcal{L}}(x,y) = (1-\delta_{\mathcal{L}})x + \delta_{\mathcal{L}} \\ \qquad\qquad \text{if } (x,y)^{\mathrm{T}} \in \mathcal{D}_{\mathcal{L}} \\ f^x_{\mathcal{M}}(x,y) = (1-\delta_{\mathcal{M}})x \\ \qquad\qquad \text{if } (x,y)^{\mathrm{T}} \in \mathcal{D}_{\mathcal{M}} \\ f^x_{\mathcal{R}}(x,y) = (1-\delta_{\mathcal{R}})x \\ \qquad\qquad \text{if } (x,y)^{\mathrm{T}} \in \mathcal{D}_{\mathcal{R}} \end{cases} \tag{10a}$$

$$f^y(x,y) = \begin{cases} f^y_{\mathcal{L}}(x,y) = (1-\delta_{\mathcal{L}})y \\ \qquad\qquad \text{if } (x,y)^{\mathrm{T}} \in \mathcal{D}_{\mathcal{L}} \\ f^y_{\mathcal{M}}(x,y) = (1-\delta_{\mathcal{M}})y \\ \qquad\qquad \text{if } (x,y)^{\mathrm{T}} \in \mathcal{D}_{\mathcal{M}} \\ f^y_{\mathcal{R}}(x,y) = (1-\delta_{\mathcal{R}})y + \delta_{\mathcal{R}} \\ \qquad\qquad \text{if } (x,y)^{\mathrm{T}} \in \mathcal{D}_{\mathcal{R}} \end{cases} \tag{10b}$$

The map is defined on the triangular domain

$$\mathcal{D} = \{(x,y)^{\mathrm{T}} \in \mathbb{R}^2_+ \mid x + y \leqslant 1\} \tag{11a}$$

which is in general subdivided in three partitions

$$\mathcal{D}_{\mathcal{L}} = \{(x,y)^{\mathrm{T}} \in \mathcal{D} \mid (x < k) \text{ and } (x < y)\} \tag{11b}$$
$$\mathcal{D}_{\mathcal{M}} = \{(x,y)^{\mathrm{T}} \in \mathcal{D} \mid (x > k) \text{ and } (y > k)\} \tag{11c}$$
$$\mathcal{D}_{\mathcal{R}} = \{(x,y)^{\mathrm{T}} \in \mathcal{D} \mid (y < k) \text{ and } (x > y)\} \tag{11d}$$

as shown in Fig. 2(a), where k is defined in Eq. (7). To shorten the notation, a point in a 4D parameter space is denoted in the following by

$$\vec{\Delta} = (\delta_{\mathcal{L}}, \delta_{\mathcal{M}}, \delta_{\mathcal{R}}, k)^{\mathrm{T}} \tag{12}$$

Additionally, below the following abbreviations are used

$$\varrho_{\mathcal{L}} = 1 - \delta_{\mathcal{L}}, \quad \varrho_{\mathcal{M}} = 1 - \delta_{\mathcal{M}}, \quad \varrho_{\mathcal{R}} = 1 - \delta_{\mathcal{R}} \tag{13}$$

As follows from the description of the model given above, the parameters of the map belong to the following ranges:

$$0 \leqslant k \leqslant \tfrac{1}{2} \tag{14a}$$
$$0 < \delta_{\mathcal{L}}, \delta_{\mathcal{M}}, \delta_{\mathcal{R}} \leqslant 1 \tag{14b}$$

Regarding the limiting values of the parameters, note that the parameter k determines the size of the partitions of the region $\mathcal{D}$, as given by Eqs. (11). When $k = 0$, the road M is preferred by all commuters, so that this this limiting value corresponds to the trivial case with only one choice available. On the other hand, when $k = \frac{1}{2}$, the road M is ruled out by the other roads because it is always too costly; so that this limiting value corresponds to a case with only two choices. As a consequence, the behavior of map (9) in case $k = 0$ is trivial, and also in the case $k = \frac{1}{2}$ map (9) has a much simpler dynamics than in the generic case $0 < k < \frac{1}{2}$.
Parameters δ_s with $s \in \{\mathcal{L}, \mathcal{M}, \mathcal{R}\}$ model the propensity of the commuters to change their choice. The larger δ_s, the larger the fraction of commuters will change the road. Thus, in the limiting case $\delta_s = 1$ all commuters who have previously chosen the road s will change to the new faster road available.
An example of the domain $\mathcal{D}$ on which the map (9) is defined and its partitions its $\mathcal{D}_{\mathcal{L}}$, $\mathcal{D}_{\mathcal{M}}$, $\mathcal{D}_{\mathcal{R}}$ is shown in Fig. 2(a). To summarize we state

Property 1. *For $k = 0$ map (9) is defined on the partition $\mathcal{D}_{\mathcal{M}}$ only, while the partitions $\mathcal{D}_{\mathcal{L}}$, $\mathcal{D}_{\mathcal{R}}$ have zero size. For $k = \frac{1}{2}$ map (9) is defined on two partitions $\mathcal{D}_{\mathcal{L}}$, $\mathcal{D}_{\mathcal{R}}$ only, as the partition $\mathcal{D}_{\mathcal{M}}$ has zero size. In this particular case the map models a **binary choice** problem. For $0 < k < \frac{1}{2}$ map (9) is defined on three partitions and models a **ternary choice** problem. The size of the partition $\mathcal{D}_{\mathcal{M}}$ increases for decreasing k.*

Note that map (9) is discontinuous along the boundaries

$$\partial_{\mathcal{LM}} = \{(x,y)^{\mathrm{T}} \in \mathcal{D} \mid x = k, k \leqslant y \leqslant 1 - k\} \tag{15a}$$
$$\partial_{\mathcal{MR}} = \{(x,y)^{\mathrm{T}} \in \mathcal{D} \mid k \leqslant x \leqslant 1 - k, y = k\} \tag{15b}$$
$$\partial_{\mathcal{LR}} = \{(x,y)^{\mathrm{T}} \in \mathcal{D} \mid 0 \leqslant x \leqslant k, y = x\} \tag{15c}$$

of the partitions $\mathcal{D}_{\mathcal{L}}$, $\mathcal{D}_{\mathcal{M}}$, $\mathcal{D}_{\mathcal{R}}$ (see Fig. 3). As the goal of the present paper is bifurcation analysis, and the values of the functions f^x, f^y at these boundaries do not influence the bifurcation structures but only the behavior at the bifurcation moment, we prefer not

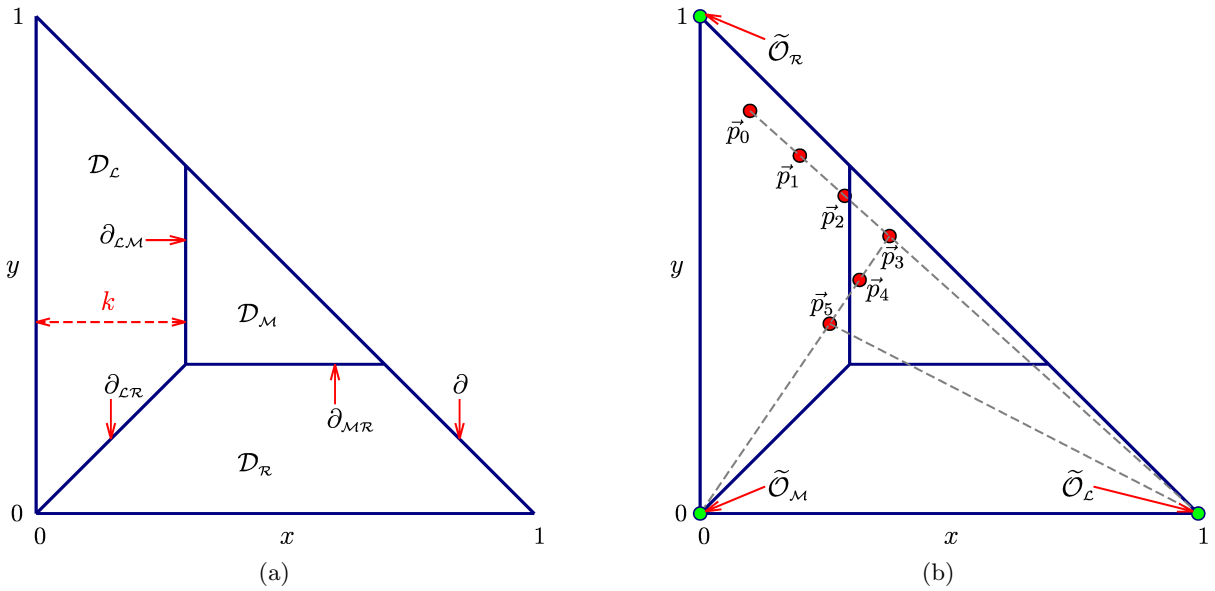

Fig. 2. (a) Domain of definition of map (9) and its partitions its $\mathcal{D}_\mathcal{L}$, $\mathcal{D}_\mathcal{M}$, $\mathcal{D}_\mathcal{R}$. (b) The first few points of an example-orbit of map (9) started in $\mathcal{D}_\mathcal{L}$. The lines along which the points are aligned are shown. $k = 0.3$.

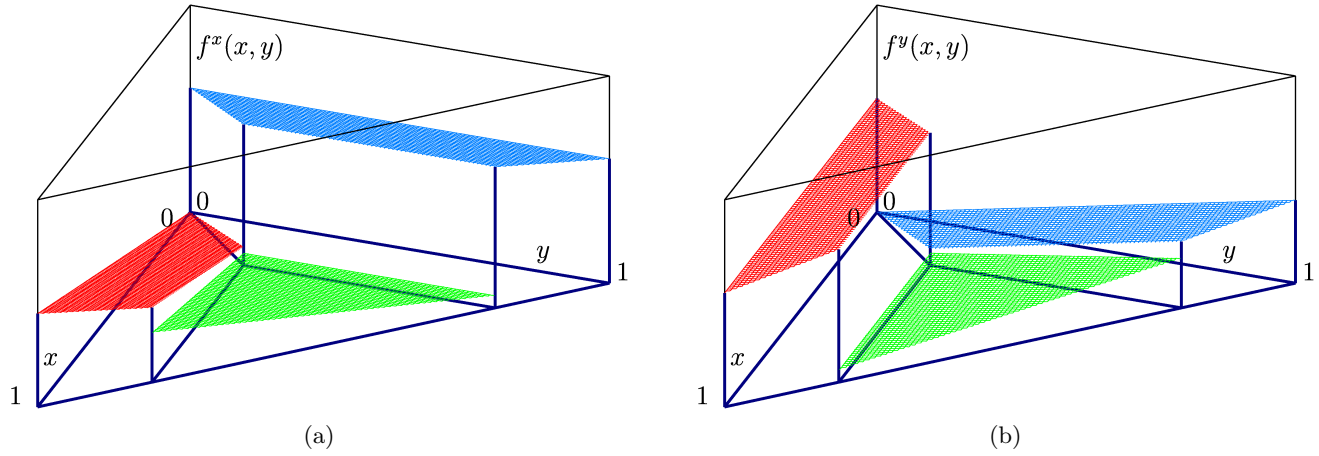

Fig. 3. Functions (a) $\vec{f}_\mathcal{L}$ and (b) $\vec{f}_\mathcal{R}$ at $\delta_\mathcal{L} = 0.6$, $\delta_\mathcal{M} = 0.7$, $\delta_\mathcal{R} = 0.55$, $k = 0.2$.

to define the map at boundaries, as this makes possible to preserve the symmetry of the phase space.

To understand the dynamics of map (9) it is worth to note that

Property 2. *Each of the functions*

$$\vec{f}_\mathcal{L}(x,y) = (f^x_\mathcal{L}(x,y), f^y_\mathcal{L}(x,y))^T \tag{16a}$$
$$\vec{f}_\mathcal{M}(x,y) = (f^x_\mathcal{M}(x,y), f^y_\mathcal{M}(x,y))^T \tag{16b}$$
$$\vec{f}_\mathcal{R}(x,y) = (f^x_\mathcal{R}(x,y), f^y_\mathcal{R}(x,y))^T \tag{16c}$$

is linear and ***contractive****. Unique and globally attracting fixed points of these functions are given by*

$$\widetilde{\mathcal{O}}_\mathcal{L} = (1,0)^T, \quad \widetilde{\mathcal{O}}_\mathcal{M} = (0,0)^T, \quad \widetilde{\mathcal{O}}_\mathcal{R} = (0,1)^T \tag{17}$$

respectively. For the function $\vec{f}$ these fixed points are ***virtual****.*

The contractiveness of $\vec{f}_\mathcal{L}$, $\vec{f}_\mathcal{M}$, $\vec{f}_\mathcal{R}$ follows immediately from Eqs. (14b) and (10). The fact that for any parameter value the fixed points are virtual (i.e., they are located outside the corresponding partition, $\widetilde{\mathcal{O}}_\mathcal{L} \notin \mathcal{D}_\mathcal{L}$, $\widetilde{\mathcal{O}}_\mathcal{M} \notin \mathcal{D}_\mathcal{M}$, $\widetilde{\mathcal{O}}_\mathcal{R} \notin \mathcal{D}_\mathcal{R}$) follows from Eqs. (14b) and (11). As a consequence, for the points of each orbit of map (9) are aligned in the following way:

Property 3. *Suppose, from $(m+1)$ subsequent points $\vec{p}_n, \ldots, \vec{p}_{n+m}$, $m \geqslant 1$, of an orbit of map (9) the first m points $\vec{p}_n, \ldots, \vec{p}_{n+m-1}$ belong to the same*

partition $\mathcal{D}_s$, with $s \in \{\mathcal{L}, \mathcal{M}, \mathcal{R}\}$. Then the points $\vec{p}_n, \ldots, \vec{p}_{n+m}$ belong to the straight line connecting the point $\vec{p}_n$ with the virtual fixed point $\widetilde{\mathcal{O}}_s$.

As the virtual fixed points $\widetilde{\mathcal{O}}_s$ are attractive, the direction of movement of an orbit along the lines mentioned above is towards the fixed point.
This property is illustrated in Fig. 2(b) showing an orbit started at a point $\vec{p}_0 \in \mathcal{D}_\mathcal{L}$. As one can see, the first three points of the orbit belong to $\mathcal{D}_\mathcal{L}$, and hence the points $\vec{p}_0$, $\vec{p}_1$, $\vec{p}_2$, $\vec{p}_3$ are aligned to a straight line towards the point $\widetilde{\mathcal{O}}_\mathcal{L}$. Then, as the orbit reaches the partition $\mathcal{D}_\mathcal{M}$, the next points $\vec{p}_3$, $\vec{p}_4$, $\vec{p}_5$ are aligned to a straight line towards the point $\widetilde{\mathcal{O}}_\mathcal{M}$, and so on.

The previous property applies for any orbit of map (9), both in transient and asymptotic phase of the dynamics. To explain the asymptotic behavior of map (9), the following property is useful:

Property 4. *Each cycle of map* (9) *is stable in its complete existence region. The bifurcations confining this region are* ***border collision bifurcations*** *occurring when one of the points of the cycle collides with one of the boundaries $\partial_{\mathcal{LM}}$, $\partial_{\mathcal{LR}}$, $\partial_{\mathcal{MR}}$.*

The stability of the cycle follows from the contractiveness of the functions $\vec{f}_s$, $s \in \{\mathcal{L}, \mathcal{M}, \mathcal{R}\}$. Indeed, let us consider a cycle of map (9), $N \geqslant 2$, with N_s points belonging to the partition $\mathcal{D}_s$, respectively. Then both eigenvalues of the cycle are equal to

$$\lambda = \varrho_\mathcal{L}^{N_\mathcal{L}} \varrho_\mathcal{M}^{N_\mathcal{M}} \varrho_\mathcal{R}^{N_\mathcal{R}} \tag{18}$$

and condition (14b) implies $0 \leqslant \lambda < 1$, i.e., the cycle is stable. As all fixed points of $\vec{f}$ are virtual, this implies that the only possible attracting sets of map (9) are stable cycles and – in limiting cases – Cantor-set attractors.

In the following, when referring to cycles, we use the standard notation based on the associated symbolic sequences. The symbolic sequence σ associated with an n-cycle, $n \geqslant 1$ has length n and consists of letters $\sigma_i \in \{\mathcal{L}, \mathcal{M}, \mathcal{R}\}$, $i = 0, \ldots, n-1$. The i-th letter of σ is $\mathcal{L}/\mathcal{M}/\mathcal{R}$ iff the i-th point of the cycle is located in the partition $\mathcal{D}_\mathcal{L}/\mathcal{D}_\mathcal{M}/\mathcal{D}_\mathcal{R}$, respectively. The cycle itself is denoted by $\mathcal{O}_\sigma$, and its i-th point by $\vec{p}_i^{\,\sigma} = (x_i^\sigma, y_i^\sigma)^{\mathrm{T}}$. The existence region of $\mathcal{O}_\sigma$ in the parameter space (which is by Property 4 also its stability region) is denoted by $\mathcal{P}_\sigma$. If a point of the cycle is located at the boundary between two partitions, i.e., at the moment of a border collision bifurcation, we associate with this cycle the symbolic sequence of the cycle existing before the bifurcation.

As in [Dal Forno & Merlone, 2013b], in the following we start our considerations with the bifurcation structure of the $(\delta_\mathcal{R}, \delta_\mathcal{L})$ parameter plane of map (9) for fixed values of the parameters related to the middle partition, i.e., $\delta_\mathcal{M}$ and k. This can be interpreted as investigation of the following question: A middle road with given properties has been introduced. What are possible effects of this act depending on the properties of the previously existing roads?
It is worth to emphasize the following symmetry of the $(\delta_\mathcal{R}, \delta_\mathcal{L})$ parameter plane of map (9):

Property 5. *Suppose, the point $(\delta_\mathcal{R}, \delta_\mathcal{L})^T = (a, b)^T$ belongs to the existence region of a cycle $\mathcal{O}_\sigma$ of map* (9)*. Then the point $(\delta_\mathcal{R}, \delta_\mathcal{L})^T = (b, a)^T$ belongs to the existence region of a cycle $\mathcal{O}_\varrho$, where the symbolic sequence ϱ results from σ by interchange all symbols $\mathcal{L}$ and $\mathcal{R}$.*

As a consequence, when symbolic sequences are neglected and only periods are considered, then for any values of $\delta_\mathcal{M}$ and k the bifurcation structure of the $(\delta_\mathcal{R}, \delta_\mathcal{L})$ parameter plane of map (9) is necessarily symmetric with respect to the diagonal $\delta_\mathcal{L} = \delta_\mathcal{R}$. Note that this symmetry does not depend on the symmetry of the network, rather it depends on symmetric travel costs, i.e., $t_{LE} = t_{SR}$ and $t_{SL}(z) \equiv t_{RE}(z)$ as in Fig. 1. For the sake of simplicity we assume that travel times are symmetrical.

3. Binary choice

Before considering the bifurcation structure of map (9) related to the ternary choice problem, let us first recall a few fact about the map and its bifurcation structures in the case that the map is related to the binary choice problem, i.e., for $k = \frac{1}{2}$ (see Property 1) A detailed study of this case is presented in [Bischi *et al.*, 2009a]. It can easily be seen that

Property 6. *In the particular case $k = \frac{1}{2}$ the asymptotic dynamics of map* (9) *takes place on the boundary of the region $\mathcal{D}$ given by the line*

$$\partial = \{(x, y)^T \in \mathbb{R}^2_+ \mid x + y = 1\} \tag{19}$$

Indeed, let us consider an orbit of map (9) started on an initial value $\vec{p}_0 \in \mathcal{D}$ which does not belong to the line ∂ (see Fig. 2). By Property 3 the distance between the points of the orbit and the line ∂ decreases in each iteration step. Therefore, the line ∂ is globally attracting and the asymptotic dynamics of map (9) takes place on this line. In fact, the

dynamics in this case can be described by a 1D map

$$\bar{x}_{n+1} = \begin{cases} g_{\mathcal{L}} = (1-\delta_{\mathcal{L}})\bar{x}_n + \delta_{\mathcal{L}} & \text{if } \bar{x}_n < \frac{1}{2} \\ g_{\mathcal{R}} = (1-\delta_{\mathcal{R}})\bar{x}_n & \text{if } \bar{x}_n > \frac{1}{2} \end{cases} \quad (20)$$

defined on the interval $[0,1]$. Clearly, each orbit and each invariant set of map (9) can be obtained from the corresponding orbit or invariant set of map (20) by $(x,y)^{\mathrm{T}} = (\bar{x}, 1-\bar{x})^{\mathrm{T}}$. The map (20) is a piecewise linear map with one border point. As the slopes on the left and on the right side of the border point are between zero and one by condition (14b), in the parameter space of map (20) (and therefore also of map (9)) the period adding structure can be observed, well-known both in flows [Lyubimov *et al.*, 1989; Homburg, 1996] and in maps [Leonov, 1959; Keener, 1980]. Recall that this structure is formed by stability regions of cycles, whose rotation numbers are organized by the Farey tree. Following the classification of the cycles involved in this structure according to their complexity levels, as introduced in [Leonov, 1959, 1960] (see also [Gardini *et al.*, 2010; Avrutin *et al.*, 2010]), the following two families of basic (also called maximal, principal, atomic, etc.) cycles

$$\mathcal{O}_1^{(1)} = \{\mathcal{O}_{\mathcal{L}\mathcal{R}^{n_1}} \mid n_1 \geqslant 1\} \quad (21a)$$

$$\mathcal{O}_2^{(1)} = \{\mathcal{O}_{\mathcal{R}\mathcal{L}^{n_1}} \mid n_1 \geqslant 1\} \quad (21b)$$

are referred to as cycles with complexity level one. In this notation the upper index $m \geqslant 1$ refers to the complexity level, and the lower index $j = 1, \ldots, 2^m$ is the index of a particular family in its complexity level. Families of cycles with a complexity level $m > 1$ can are defined recursively, based on the cycles with the complexity level $m-1$. More precisely, the symbolic sequences associated with cycles with the complexity level m can be obtained either by an appropriate concatenation of symbolic sequences associated with cycles with the complexity level $m-1$ (as described in [Gardini *et al.*, 2010]), or applying so-called symbolic replacements (as described in [Avrutin *et al.*, 2010]), which can also be used for an efficient calculation of the bifurcation curves. In both ways, the number of families is doubled in each step, so that there are 2^m families with the complexity level m, each of them with m indexes $n_1, \ldots, n_m$. For example, the families of complexity level $m = 2$ are

$$\mathcal{O}_1^{(2)} = \{\mathcal{O}_{\mathcal{L}\mathcal{R}^{n_1}(\mathcal{L}\mathcal{R}^{n_1+1})^{n_2}} \mid n_{1,2} \geqslant 1\} \quad (22a)$$

$$\mathcal{O}_2^{(2)} = \{\mathcal{O}_{\mathcal{L}\mathcal{R}^{n_1+1}(\mathcal{L}\mathcal{R}^{n_1})^{n_2}} \mid n_{1,2} \geqslant 1\} \quad (22b)$$

$$\mathcal{O}_3^{(2)} = \{\mathcal{O}_{\mathcal{R}\mathcal{L}^{n_1}(\mathcal{R}\mathcal{L}^{n_1+1})^{n_2}} \mid n_{1,2} \geqslant 1\} \quad (22c)$$

$$\mathcal{O}_4^{(2)} = \{\mathcal{O}_{\mathcal{R}\mathcal{L}^{n_1+1}(\mathcal{R}\mathcal{L}^{n_1})^{n_2}} \mid n_{1,2} \geqslant 1\} \quad (22d)$$

Note that the families of cycles given by Eqs. (21) and (22) correspond to the most simple case of the period adding structure. In other cases (in particular, when the involved cycles include points located in more than two partitions), the corresponding symbolic sequences can be obtained from these equations by replacing the letters $\mathcal{L}$ and $\mathcal{R}$ by appropriate symbolic sequences.

The bifurcation structure in the $(\delta_{\mathcal{R}}, \delta_{\mathcal{L}})$ parameter plane of map (9) for $k = \frac{1}{2}$ is illustrated in Fig. 4(a). As one can easily see in this figure, the complete period adding structure issues from an organizing center (a codimension-2 bifurcation point) at the origin $\delta_{\mathcal{R}} = \delta_{\mathcal{L}} = 0$ and covers the $(\delta_{\mathcal{R}}, \delta_{\mathcal{L}})$ parameter plane completely. Accordingly, the bifurcation scenario obtained by varying of parameters along the arc marked in Fig. 5(a), as shown in Fig. 4(b), is fully representative in the sense that no new cycles can appear when the radius of the arc changes.
To obtain an analytic description of the presented bifurcation structure recall that the boundaries of the existence regions of each cycle are given by border collision bifurcations (see Property 1) which occur when a point of a cycle collides with a border between partitions. In the case of the binary choice problem the only border is $\partial_{\mathcal{L}\mathcal{R}}$ (the point $\frac{1}{2}$ for map (20)). It can be shown that, as the functions $g_{\mathcal{L}}$ and $g_{\mathcal{R}}$ are both increasing, the basic cycles collide with the border by the first and the last point. Therefore, we obtain the following expressions for the border collision boundaries of the existence regions of basic cycles:

$$\begin{aligned} \xi_{\mathcal{L}\mathcal{R}^n}^{0,\partial_{\mathcal{L}\mathcal{R}}} &= \left\{\vec{\Delta} \mid x_0^{\mathcal{L}\mathcal{R}^n} = \tfrac{1}{2}\right\} \\ &= \left\{\vec{\Delta} \mid \delta_{\mathcal{L}} = \frac{1-\varrho_{\mathcal{R}}^n}{\varrho_{\mathcal{R}}^n}\right\} \end{aligned} \quad (23a)$$

$$\begin{aligned} \xi_{\mathcal{L}\mathcal{R}^n}^{n,\partial_{\mathcal{L}\mathcal{R}}} &= \left\{\vec{\Delta} \mid x_n^{\mathcal{L}\mathcal{R}^n} = \tfrac{1}{2}\right\} \\ &= \left\{\vec{\Delta} \mid \delta_{\mathcal{L}} = \frac{\varrho_{\mathcal{R}}(\varrho_{\mathcal{R}}^{-n}-1)}{(1+\delta_{\mathcal{R}})}\right\} \end{aligned} \quad (23b)$$

$$\begin{aligned} \xi_{\mathcal{R}\mathcal{L}^n}^{0,\partial_{\mathcal{L}\mathcal{R}}} &= \left\{\vec{\Delta} \mid x_0^{\mathcal{R}\mathcal{L}^n} = \tfrac{1}{2}\right\} \\ &= \left\{\vec{\Delta} \mid \delta_{\mathcal{R}} = \frac{1-\varrho_{\mathcal{L}}^n}{\varrho_{\mathcal{L}}^n}\right\} \end{aligned} \quad (23c)$$

$$\begin{aligned} \xi_{\mathcal{R}\mathcal{L}^n}^{n,\partial_{\mathcal{L}\mathcal{R}}} &= \left\{\vec{\Delta} \mid x_n^{\mathcal{R}\mathcal{L}^n} = \tfrac{1}{2}\right\} \\ &= \left\{\vec{\Delta} \mid \delta_{\mathcal{R}} = \frac{\varrho_{\mathcal{L}}(\varrho_{\mathcal{L}}^{-n}-1)}{1+\delta_{\mathcal{L}}}\right\} \end{aligned} \quad (23d)$$

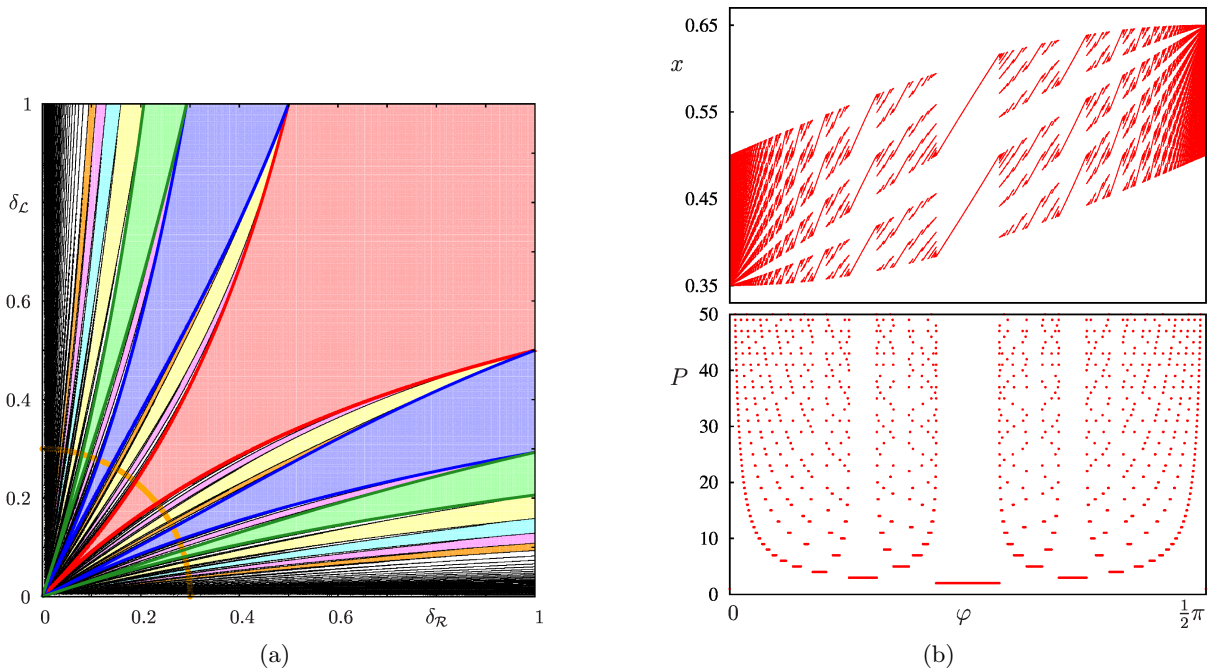

Fig. 4. (a) Bifurcation structure of the $(\delta_{\mathcal{R}}, \delta_{\mathcal{L}})$ parameter plane in the case of a binary choice ($k = \frac{1}{2}$). (b) Bifurcation scenario obtained by variation of $\delta_{\mathcal{R}}$, $\delta_{\mathcal{L}}$ along the arc indicated in (a). The angle φ is measured along the arc. Red curves show the boundaries of the region $\mathcal{P}_{\mathcal{LR}}$; blue curves – of the regions $\mathcal{P}_{\mathcal{LR}^2}$, $\mathcal{P}_{\mathcal{RL}^2}$, green curves – of the regions $\mathcal{P}_{\mathcal{LR}^3}$, $\mathcal{P}_{\mathcal{RL}^3}$. Regions corresponding to cycles with periods $P = 2, \ldots, 8$ are shown in colors as follows: $P = 2$ red, $P = 3$ blue, $P = 4$ green, $P = 5$ yellow, $P = 6$ cyan, $P = 7$ magenta, $P = 8$ orange.

Here and in the following the lower index in the notation used for a border collision bifurcation curve refers to the symbolic sequence of the cycles undergoing the bifurcation, the first upper index states which point of the cycle collides, and the second upper index which boundary is collided.

4. Ternary choice

4.1. *Numeric*

Examples of bifurcation structures in the $(\delta_{\mathcal{R}}, \delta_{\mathcal{L}})$ parameter plane for different values of $k < \frac{1}{2}$ are shown in Fig. 5. As follows from Property 5, the bifurcation structures are symmetric with respect to the diagonal $\delta_{\mathcal{L}} = \delta_{\mathcal{R}}$.

As one can see in Fig. 5, bifurcation structures obtained for different values of k are essentially different. Hereby the overall bifurcation structure is intrinsically two-dimensional and can not be investigated by considering 1D parameter paths, as it is possible in the case of a binary choice (see Fig. 4). For example, the bifurcation scenario shown in Fig. 6(a) is obtained by the variation of $\delta_{\mathcal{L}}$ and $\delta_{\mathcal{R}}$ along the diagonal of the parameter plane $(\delta_{\mathcal{R}}, \delta_{\mathcal{L}})$ marked in Fig. 5(b). The resulting bifurcation scenario resembles the usual period adding scenario. However, a striking feature of the presented scenario is that the bifurcation and the period diagrams seemingly do not match each other. For example, at the parameter value marked with A in Fig. 6(a), four points in the bifurcation diagram are visible, although the period diagram suggests that the period is three. As explained below (see Sec. 6), this is caused by the coexistence of cycles with the same period. However, it is also clear that the 1D bifurcation scenario shown in Fig. 6(a) does not reflect the complexity of the 2D bifurcation structure shown in Fig. 5(b).

Several features of the 2D bifurcation structures shown in Fig. 5 are remarkable. In particular, it is worth noticing a high number of bifurcation curves confining region associated with cycles with the same period. Clearly, to explain that and to understand the organizing principles of the observed bifurcation structures it is necessary to identify which cycles may be involved in and which border collision bifurcation curves may define the boundaries of their existence regions.

Another unusual phenomenon is that among the periodicity regions accumulating to the origin of the $(\delta_{\mathcal{R}}, \delta_{\mathcal{L}})$ parameter space there are regions associated with low periods. This is clearly visible in

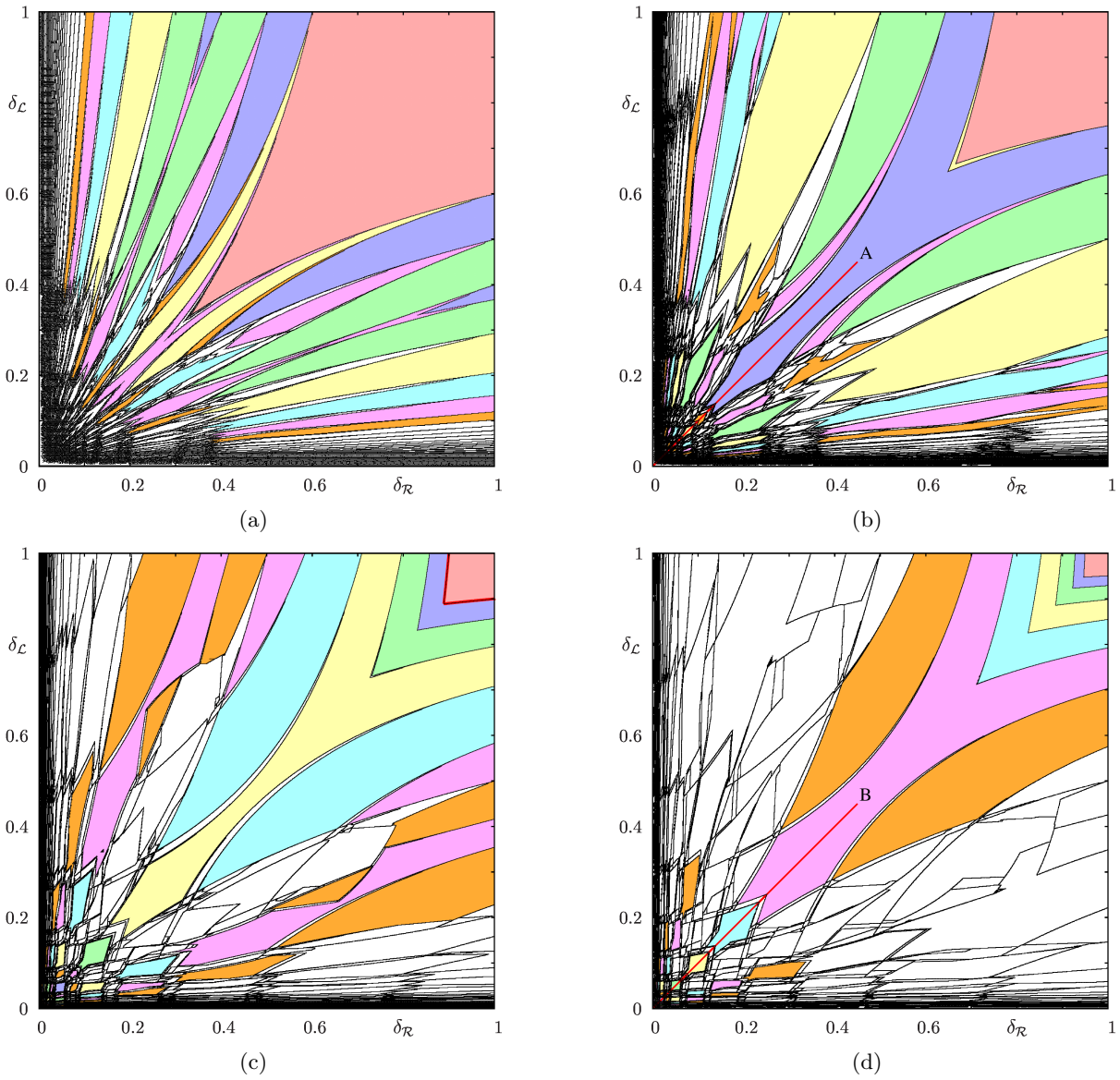

Fig. 5. Bifurcation structure of the $(\delta_{\mathcal{R}}, \delta_{\mathcal{L}})$ parameter plane in the case of a ternary choice. $\delta_{\mathcal{M}} = 0.3$, (a) $k = 0.4$, (b) $k = 0.25$, (c) $k = 0.1$, (d) $k = 0.05$. Bifurcation scenarios observed as parameters $(\delta_{\mathcal{R}}, \delta_{\mathcal{L}})$ change along the red lines marked with A and B in (b) and (d) are shown in Fig. 6(a) and (b), respectively. The regions are colored as in Fig. 4.

the bifurcation scenario shown in Fig. 6(b) which corresponds to the diagonal of the parameter plane $(\delta_{\mathcal{R}}, \delta_{\mathcal{L}})$ shown in Fig. 5(d). By contrast to Fig. 6(a) in which an increase of the periodicity of attractors for parameters tending to the accumulation point of the cascade can be observed, in Fig. 6(b) also a sequence of regions with decreasing periods can be seen. The question arises whether this sequence is finite or not and what is the difference between the observed cascade and the usual period adding scenario.

4.2. *Cycles on two partitions*

As the functions $\vec{f}_{\mathcal{L}}$, $\vec{f}_{\mathcal{M}}$, $\vec{f}_{\mathcal{R}}$ are linear, a cycle of map (9) cannot be located completely in one partition. When all three partitions $\mathcal{D}_{\mathcal{L}}$, $\mathcal{D}_{\mathcal{M}}$, $\mathcal{D}_{\mathcal{R}}$ are present, i.e., for $k < \frac{1}{2}$, it is possible that the cycle is located on two partitions only, however

Property 7. *If all points of a cycle of map* (9) *are located in two partitions only, then these partitions are* $\mathcal{D}_{\mathcal{L}}$ *and* $\mathcal{D}_{\mathcal{R}}$.

Indeed, suppose that all points of a cycle are located in the partitions $\mathcal{D}_{\mathcal{L}}$ and $\mathcal{D}_{\mathcal{M}}$. Then by Property 3 the y-values of these points decrease in each step,

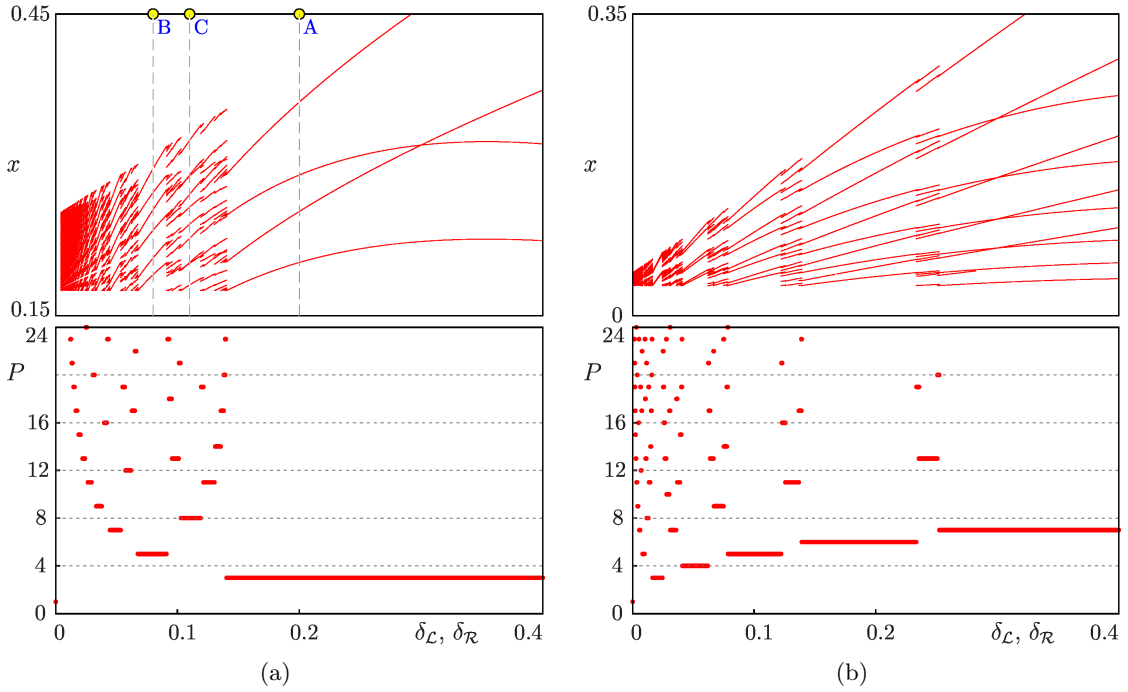

Fig. 6. Bifurcation scenario observed by variation of parameters along the diagonal of the $(\delta_{\mathcal{R}}, \delta_{\mathcal{L}})$ parameter plane at $\delta_{\mathcal{M}} = 0.3$ and (a) $k = 0.25$; (b) $k = 0.05$. The corresponding parameter paths are marked as red lines in Figs. 5(b) and (d), respectively. The attractors at the parameter values marked with A, B, and C are shown in Fig. 18(a), (b) and (c), respectively.

which is not possible. A similar reasoning applies also for partitions $\mathcal{D}_{\mathcal{R}}$ and $\mathcal{D}_{\mathcal{M}}$ and the x values of the points. As the dynamics inside the partitions $\mathcal{D}_{\mathcal{L}}$, $\mathcal{D}_{\mathcal{R}}$ does not change when the middle partition is introduced, no other cycles with all points located in these partitions can appear for $k < \frac{1}{2}$, as in the case $k = \frac{1}{2}$ described above. Due to the same reasons as before, the cycles are located on the line ∂. However, as for $k < \frac{1}{2}$ a portion in the middle of ∂ belongs to the middle partition $\mathcal{D}_{\mathcal{M}}$, the conditions of the border collision bifurcations confining the existence regions of the cycles change. Now the point of the cycle which is located before the bifurcation in the partition $\mathcal{D}_{\mathcal{L}}$ collides with the boundary $\partial_{\mathcal{LM}}$, and the one located before the bifurcation in the partition $\mathcal{D}_{\mathcal{R}}$ collides with the boundary $\partial_{\mathcal{MR}}$. As a consequence, we obtain for example the following expressions for the border collision bifurcation curves of basic cycles:

$$\begin{aligned}\xi_{\mathcal{LR}^n}^{0,\partial_{\mathcal{LM}}} &= \left\{\vec{\Delta} \mid x_0^{\mathcal{LR}^n} = k\right\} \\ &= \left\{\vec{\Delta} \mid \delta_{\mathcal{L}} = \frac{1-k\varrho_{\mathcal{R}}^n}{(1-k)\varrho_{\mathcal{R}}^n}\right\} \qquad (24a)\\ \xi_{\mathcal{LR}^n}^{n,\partial_{\mathcal{MR}}} &= \left\{\vec{\Delta} \mid x_n^{\mathcal{LR}^n} = 1-k\right\} \\ = \left\{\vec{\Delta} \mid \delta_{\mathcal{L}} = \frac{(1-k)(\varrho_{\mathcal{R}}^{1-n} - \varrho_{\mathcal{R}})}{k\varrho_{\mathcal{R}} + \delta_{\mathcal{R}}}\right\} &\qquad (24b)\end{aligned}$$

$$\begin{aligned}\xi_{\mathcal{RL}^n}^{0,\partial_{\mathcal{MR}}} &= \left\{\vec{\Delta} \mid x_0^{\mathcal{RL}^n} = 1-k\right\} \\ = \left\{\vec{\Delta} \mid \delta_{\mathcal{R}} = \frac{(1-k)(\varrho_{\mathcal{L}}^{1-n} - \varrho_{\mathcal{L}})}{k\varrho_{\mathcal{L}} + \delta_{\mathcal{L}}}\right\} &\qquad (24c)\\ \xi_{\mathcal{RL}^n}^{n,\partial_{\mathcal{LM}}} &= \left\{\vec{\Delta} \mid x_n^{\mathcal{RL}^n} = k\right\} \\ = \left\{\vec{\Delta} \mid \delta_{\mathcal{R}} = \frac{1-k\varrho_{\mathcal{L}}^n}{(1-k)\varrho_{\mathcal{L}}^n}\right\} &\qquad (24d)\end{aligned}$$

(for details on the appearance of period adding structures in a map defined on three partitions we refer to [Panchuk *et al.*, 2013]). Note also that not all of the cycles existing for $k = \frac{1}{2}$ exist also for $k < \frac{1}{2}$. Indeed,

Property 8. *A cycle with all points located in the partitions $\mathcal{D}_{\mathcal{L}}$, $\mathcal{D}_{\mathcal{R}}$ exists for $k < \frac{1}{2}$ only if the distance between its points located most close to the boundaries is larger than the size of the portion of the line ∂ covered by the partition $\mathcal{D}_{\mathcal{M}}$, i.e., larger than $(1-2k)\sqrt{2}$.*

As the size of the portion of ∂ belonging to the partition $\mathcal{D}_{\mathcal{M}}$ increases for decreasing k, the cycles existing for $k = \frac{1}{2}$ disappear one after each other for decreasing k. This is illustrated in Fig. 7, in which the existence regions of basic cycles are shown for four different values of k. As one can see, for $k = 0.48$ the cycles $\mathcal{O}_{\mathcal{LR}^n}$ and $\mathcal{O}_{\mathcal{RL}^n}$ exist for $n = 1, .., 9$, for

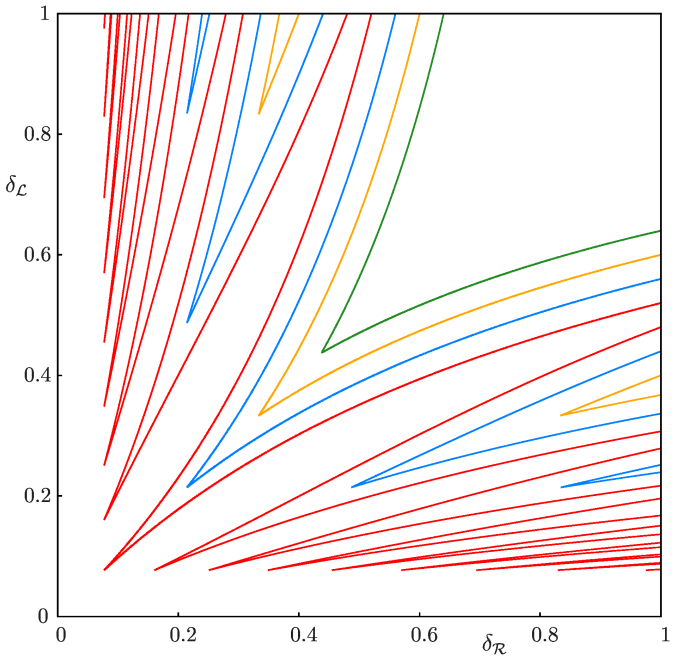

Fig. 7. Existence regions of basic cycles $\mathcal{O}_{\mathcal{LR}^n}$ and $\mathcal{O}_{\mathcal{RL}^n}$ for $k = 0.48$ (red curves), $k = 0.44$ (blue curves), $k = 0.40$ (orange curves), $k = 0.36$ (green curves). As one can see, instead of infinite families of basic cycles existing in the case of binary choice (i.e., for $k = \frac{1}{2}$), for $k = 0.48$ only 17 basic cycles exist, for $k = 0.44$ only 5, for $k = 0.40$ only 3, and for $k = 0.36$ only one.

$k = 0.44$ they exist for $n = 1, .., 3$, for $k = 0.40$ for $n = 1, 2$, and finally for $k = 0.36$ the only existing basic cycle is $\mathcal{O}_{\mathcal{LR}}$.

4.3. *Cycles on three partitions: possible bifurcations*

Let us start the consideration of cycles with points located on all three partitions with the most simple case, namely with cycles of period 3. Obviously, there are only two such cycles, namely $\mathcal{O}_{\mathcal{LRM}}$ and $\mathcal{O}_{\mathcal{RLM}}$. Moreover, among them only one needs to be considered, as by Property 5 the bifurcations structures in the $(\delta_{\mathcal{R}}, \delta_{\mathcal{L}})$ parameter plane associated with these cycles are symmetric to each other with respect to the line $\delta_{\mathcal{L}} = \delta_{\mathcal{R}}$. Hence, in the following we consider the bifurcations structures of the cycle $\mathcal{O}_{\mathcal{LRM}}$.

As already mentioned (see Property 4), the boundaries of the existence region $\mathcal{P}_{\mathcal{LRM}}$ of the cycle $\mathcal{O}_{\mathcal{LRM}}$ are given by border collision bifurcation curves. As there are three points of the cycle $\vec{p}_0^{\,\mathcal{LRM}} \in \mathcal{D}_{\mathcal{L}}$, $\vec{p}_1^{\,\mathcal{LRM}} \in \mathcal{D}_{\mathcal{R}}$, $\vec{p}_2^{\,\mathcal{LRM}} \in \mathcal{D}_{\mathcal{M}}$ and three boundaries between partitions $\partial_{\mathcal{LM}}$, $\partial_{\mathcal{LR}}$, $\partial_{\mathcal{MR}}$, the question arises which points of the cycle can undergo collisions with which boundaries. Seemingly, there are six possibilities for border collision bifurcations: $\xi^{0,\partial_{\mathcal{LM}}}_{\mathcal{LRM}}$, $\xi^{0,\partial_{\mathcal{LR}}}_{\mathcal{LRM}}$, $\xi^{1,\partial_{\mathcal{LR}}}_{\mathcal{LRM}}$, $\xi^{1,\partial_{\mathcal{MR}}}_{\mathcal{LRM}}$, $\xi^{2,\partial_{\mathcal{LM}}}_{\mathcal{LRM}}$, and $\xi^{2,\partial_{\mathcal{MR}}}_{\mathcal{LRM}}$. However,

Property 9. *The point $\vec{p}_1^{\,\mathcal{LRM}}$ of the cycle $\mathcal{O}_{\mathcal{LRM}}$ cannot collide with the boundary $\partial_{\mathcal{LR}}$. The point $\vec{p}_2^{\,\mathcal{LRM}}$ cannot collide with the boundary $\partial_{\mathcal{MR}}$.*

The proof follows a pure geometric reasoning. Indeed, by Property 3 the function $\vec{f}_{\mathcal{R}}$ maps the point $\vec{p}_1^{\,\mathcal{LRM}}$ towards the point $(0, 1)^{\mathrm{T}}$. If the bifurcation $\xi^{1,\partial_{\mathcal{LR}}}_{\mathcal{LRM}}$, would be possible, immediately before the bifurcation the point $\vec{p}_1^{\,\mathcal{LRM}}$ would be located arbitrary close to the boundary $\partial_{\mathcal{LR}}$ and hence it would be mapped on a point in the partition $\mathcal{D}_{\mathcal{L}}$. However, as $\vec{p}_1^{\,\mathcal{LRM}}$ belongs to the cycle $\mathcal{O}_{\mathcal{LRM}}$, it must be mapped on the point $\vec{p}_2^{\,\mathcal{LRM}}$ which belongs to $\mathcal{D}_{\mathcal{M}}$. Hence, the bifurcation $\xi^{1,\partial_{\mathcal{MR}}}_{\mathcal{LRM}}$ cannot occur. Similarly, one can show that the point $\vec{p}_2^{\,\mathcal{LRM}}$ cannot collide with the boundary $\partial_{\mathcal{MR}}$ because close to this boundary it would be mapped towards the origin by $\vec{f}_{\mathcal{M}}$ on a point in $\mathcal{D}_{\mathcal{R}}$, whereas it must be mapped on $\vec{p}_0^{\,\mathcal{LRM}} \in \mathcal{D}_{\mathcal{L}}$.

The remaining four border collisions are possible. Straight forwardly, the corresponding expressions can be obtained:

$$\begin{aligned} \xi^{0,\partial_{\mathcal{LR}}}_{\mathcal{LRM}} &= \left\{ \vec{\Delta} \mid x_0^{\mathcal{LRM}} = y_0^{\mathcal{LRM}} \right\} \\ &= \left\{ \vec{\Delta} \mid \delta_{\mathcal{L}} = \frac{\delta_{\mathcal{R}}}{1 - \delta_{\mathcal{R}}} \right\} \end{aligned} \tag{25a}$$

$$\xi^{0,\partial_{\mathcal{LM}}}_{\mathcal{LRM}} = \left\{\vec{\Delta} \mid x_0^{\mathcal{LRM}} = k\right\} = \left\{\vec{\Delta} \mid \delta_{\mathcal{L}} = \frac{k(\delta_{\mathcal{M}} + \delta_{\mathcal{R}}\varrho_{\mathcal{M}})}{\varrho_{\mathcal{R}}(1 - k\varrho_{\mathcal{M}})}\right\} \tag{25b}$$

$$\xi^{1,\partial_{\mathcal{MR}}}_{\mathcal{LRM}} = \left\{\vec{\Delta} \mid y_1^{\mathcal{LRM}} = k\right\} = \left\{\vec{\Delta} \mid \delta_{\mathcal{L}} = \frac{\delta_{\mathcal{R}}\varrho_{\mathcal{M}} - k(\delta_{\mathcal{M}} + \delta_{\mathcal{R}}\varrho_{\mathcal{M}})}{\varrho_{\mathcal{M}}(\delta_{\mathcal{R}} + k\varrho_{\mathcal{R}})}\right\} \tag{25c}$$

$$\xi^{2,\partial_{\mathcal{MR}}}_{\mathcal{LRM}} = \left\{\vec{\Delta} \mid x_2^{\mathcal{LRM}} = k\right\} = \left\{\vec{\Delta} \mid \delta_{\mathcal{L}} = \frac{k(\delta_{\mathcal{R}} + \delta_{\mathcal{M}}\varrho_{\mathcal{R}})}{\varrho_{\mathcal{R}}(1 - k\varrho_{\mathcal{M}})}\right\} \tag{25d}$$

The occurrence of these bifurcations in the $(\delta_{\mathcal{R}}, \delta_{\mathcal{L}})$ parameter plane for different values of the parameter k is illustrated in Fig. 9. As one can see, for large values of k (sufficiently close to $k = \frac{1}{2}$, i.e., when the partition $\mathcal{D}_{\mathcal{M}}$ is small enough) there are four regions associated with 3-cycles (see Fig. 9(a)). Two of these cycles have points in two partitions only ($\mathcal{O}_{\mathcal{LR}^2}$ and $\mathcal{O}_{\mathcal{RL}^2}$). As described in Sec. 4.2, when k decreases, the corresponding existence regions $\mathcal{P}_{\mathcal{LR}^2}$ and $\mathcal{P}_{\mathcal{RL}^2}$ decrease in size and disappear (so, in Fig. 9(b) they are much smaller than in Fig. 9(a), and in Fig. 9(c) they do not exist any longer). By contrast, the regions $\mathcal{P}_{\mathcal{LRM}}$ and $\mathcal{P}_{\mathcal{RLM}}$, which do not exist for $k = \frac{1}{2}$, increase in size when k decreases. As illustrated in Figs. 9(a) and (b), for large values of k the region $\mathcal{P}_{\mathcal{LRM}}$ is confined by three boundaries: a portion of the line $\delta_{\mathcal{L}} = 1$ and the border collision bifurcation curves $\xi^{0,\partial_{\mathcal{CR}}}_{\mathcal{LRM}}$, $\xi^{0,\partial_{\mathcal{LM}}}_{\mathcal{LRM}}$. When k decreases, the shape of the region becomes more complicated, as one more boundary appears, namely the bifurcation curve $\xi^{1,\partial_{\mathcal{MR}}}_{\mathcal{LRM}}$ (see Fig. 9(c)). It is worth noticing that after the curve $\xi^{0,\partial_{\mathcal{LM}}}_{\mathcal{LRM}}$ crosses the diagonal $\delta_{\mathcal{L}} = \delta_{\mathcal{R}}$, there is a region in the plane $(\delta_{\mathcal{L}}, \delta_{\mathcal{R}})$ in which the cycles $\mathcal{O}_{\mathcal{LRM}}$ and $\mathcal{O}_{\mathcal{RLM}}$ coexist. As a next step, for further decreasing k the boundaries of the region $\mathcal{P}_{\mathcal{LRM}}$ becomes a five, given by the border collision bifurcation curve $\xi^{2,\partial_{\mathcal{MR}}}_{\mathcal{LRM}}$ (see Fig. 9(d)). Note that the symmetry described by Property 5 implies that this bifurcation curve coincides with the border collision bifurcation curve $\xi^{2,\partial_{\mathcal{LM}}}_{\mathcal{RLM}}$ confining the existence region of the cycle $\mathcal{O}_{\mathcal{RLM}}$. The region $\mathcal{P}_{\mathcal{LRM}}$ remains confined by five boundaries until for further decreasing k the curves $\xi^{1,\partial_{\mathcal{MR}}}_{\mathcal{LRM}}$ and $\xi^{2,\partial_{\mathcal{MR}}}_{\mathcal{LRM}}$ not cross the diagonal $\delta_{\mathcal{L}} = \delta_{\mathcal{R}}$ and each other. Fig. 9(e) shows the shape of the region $\mathcal{P}_{\mathcal{LRM}}$ immediately before this codimension-2 bifurcation. After this bifurcation, the region $\mathcal{P}_{\mathcal{LRM}}$ is split in two parts, as shown in Fig. 9(f). Note that for decreasing k both parts of the region $\mathcal{P}_{\mathcal{LRM}}$ decrease in size but do not vanish.

5. Map with a constant value on one partition

5.1. *Basic idea*

It has been described in the previous paragraph how the region $\mathcal{P}_{\mathcal{LRM}}$ in the $(\delta_{\mathcal{R}}, \delta_{\mathcal{L}})$ parameter plane is transformed when k is varied. Clearly, a similar description is possible for any other cycle. However, to understand the organizing principles of the $(\delta_{\mathcal{R}}, \delta_{\mathcal{L}})$ parameter plane it is preferable not to describe the existence of each particular cycle separately, but to identify some reasonable families of cycles whose existence regions are transformed in a similar way. To obtain such kind of description let us note first that for any k one of the boundaries of the region $\mathcal{P}_{\mathcal{LRM}}$ is given by a portion of the line $\delta_{\mathcal{L}} = 1$ (see Fig. 9). It is evident from Fig. 5 that the bifurcation structures of the $(\delta_{\mathcal{R}}, \delta_{\mathcal{L}})$ parameter plane is up to far extent dominated by regions originating from this line. Therefore, as an intermediate step, let us change the parameter plane under consideration. In order to identify groups of cycles whose existence regions in the $(\delta_{\mathcal{R}}, \delta_{\mathcal{L}})$ parameter plane originate (for a fixed k) from the line $\delta_{\mathcal{L}} = 1$ we consider the bifurcation structure of the $(\delta_{\mathcal{R}}, k)$ parameter plane for a fixed value $\delta_{\mathcal{L}} = 1$. The reason why this mode of operation simplifies the considerations is the following

Property 10. *For $\delta_{\mathcal{L}} = 1$ the function $\vec{f}$ is constant on the partition $\mathcal{D}_{\mathcal{L}}$.*

For $\delta_{\mathcal{L}} = 1$ we straightforwardly obtain from Eq. (9)

$$\vec{f}_{\mathcal{L}}(x, y) = ((1 - \delta_{\mathcal{L}})x + \delta_{\mathcal{L}}, (1 - \delta_{\mathcal{L}})y)^{\mathrm{T}} = (1, 0)^{\mathrm{T}} \tag{26}$$

This property has numerous consequences. First of all,

Property 11. *For $\delta_{\mathcal{L}} = 1$, each cycle of map (9) contains exactly one point in the partition $\mathcal{D}_{\mathcal{L}}$.*

It follows from Property 7, that each cycles contains at least one point in $\mathcal{D}_{\mathcal{L}}$. To proof that this point is unique, let us assume that there exists a cycle with more than one point in $\mathcal{D}_{\mathcal{L}}$. Each of these points is mapped onto the same point $(1, 0)^{\mathrm{T}}$. However, a cycle cannot contain the same point more than once, so the point in $\mathcal{D}_{\mathcal{L}}$ must be unique. Accordingly,

Property 12. *For $\delta_{\mathcal{L}} = 1$, each cycle of map (9) is superstable.*

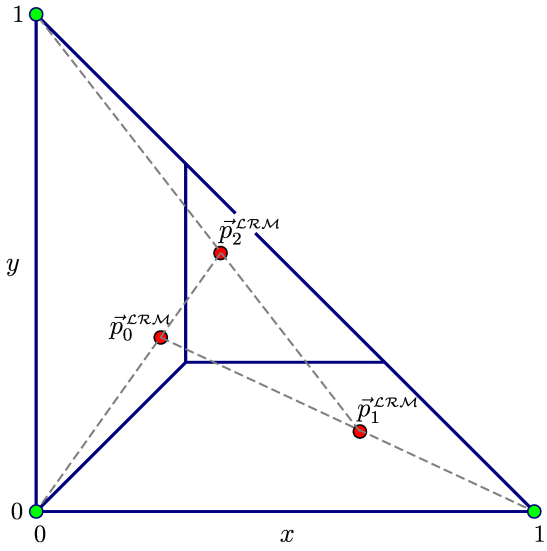

Fig. 8. 3-cycle $\mathcal{O}_{\mathcal{LRM}}$ (schematic). Dashed lines show the alignment of the points of the cycle and the virtual fixed points $\widetilde{\mathcal{O}}_{\mathcal{L}}$, $\widetilde{\mathcal{O}}_{\mathcal{M}}$, $\widetilde{\mathcal{O}}_{\mathcal{R}}$ as described by Property 3. This alignment implies that the border collision bifurcations $\xi_{\mathcal{LRM}}^{0,\partial_{\mathcal{LM}}}$, $\xi_{\mathcal{LRM}}^{0,\partial_{\mathcal{LR}}}$, $\xi_{\mathcal{LRM}}^{1,\partial_{\mathcal{MR}}}$, and $\xi_{\mathcal{LRM}}^{2,\partial_{\mathcal{LM}}}$ are possible, while the border collision bifurcations $\xi_{\mathcal{LRM}}^{1,\partial_{\mathcal{LR}}}$ and $\xi_{\mathcal{LRM}}^{2,\partial_{\mathcal{MR}}}$ cannot occur.

Indeed, it follows from Eq. (18) with $N_{\mathcal{L}} = 1$ that at $\delta_{\mathcal{L}} = 1$ the cycle has two zero eigenvalues.

For simplicity, we unify the notation used below for cycles existing at $\delta_{\mathcal{L}} = 1$:

Property 13. *For $\delta_{\mathcal{L}} = 1$, each n-cycle $\mathcal{O}_\sigma$ of map (9) can be written as*

$$\vec{p}_0{}^{\sigma} \in \mathcal{D}_{\mathcal{L}} \tag{27a}$$
$$\vec{p}_1{}^{\sigma} = (1,0)^{T} \in \mathcal{D}_{\mathcal{R}} \tag{27b}$$

and, for $n \geqslant 3$,

$$\vec{p}_2{}^{\sigma} = (1-\delta_{\mathcal{R}}, \delta_{\mathcal{R}})^{T} \in \partial \tag{27c}$$

The symbolic sequence σ associated with the cycle starts with the prefix $\sigma_0\sigma_1 = \mathcal{LR}$, and for $n \geqslant 3$ the remaining letters $\sigma_2, \ldots, \sigma_{n-1}$ are $\mathcal{M}$ and $\mathcal{R}$.

Considering the simplest example of 3-cycles, it was shown in the previous section that the regions $\mathcal{P}_{\mathcal{LRM}}$ and $\mathcal{P}_{\mathcal{RLM}}$ in the $(\delta_{\mathcal{R}}, \delta_{\mathcal{L}})$ parameter plane may overlap, which leads to the coexistence of $\mathcal{O}_{\mathcal{LRM}}$ and $\mathcal{O}_{\mathcal{RLM}}$. For $\delta_{\mathcal{L}} = 1$ this is not possible:

Property 14. *For $\delta_{\mathcal{L}} = 1$, two cycles of map (9) cannot coexist.*

Clearly, if two cycles would coexist, each of them would contain the point $(1,0)^{\mathrm{T}}$, which is not possible.

Clearly, similar properties can also be stated for the $(\delta_{\mathcal{L}}, k)$ parameter plane and $\delta_{\mathcal{R}} = 1$. The structure of the 3D parameter space $(\delta_{\mathcal{R}}, \delta_{\mathcal{L}}, k)$ is shown in Fig. 10(a). As shown in this figure, the regions origination from the lines $\delta_{\mathcal{L}} = 1$ or $\delta_{\mathcal{R}} = 1$ in the $(\delta_{\mathcal{L}}, \delta_{\mathcal{R}})$ parameter plane for any given value of k can be identified by considering the corresponding line in the $(\delta_{\mathcal{L}}, k)$ or $(\delta_{\mathcal{L}}, k)$ parameter plane, respectively.

As stated by Property 13, for $\delta_{\mathcal{L}} = 1$ the symbolic sequence associated with any cycle existing at these parameter values starts with the letter $\sigma_0 = \mathcal{L}$ and the remaining letters $\sigma_1, \ldots, \sigma_{n-1}$ are $\mathcal{M}$ and $\mathcal{R}$. The key point to understand the bifurcation structure of the $(\delta_{\mathcal{R}}, k)$ parameter plane at $\delta_{\mathcal{L}} = 1$ is to count the number of letters $\mathcal{R}$ among these letters. This number is shown in Fig. 10(b). As one can see, the value $N_{\mathcal{R}}$ increases monotonously for decreasing values of $\delta_{\mathcal{R}}$. For example, if $\delta_{\mathcal{R}} > \frac{1}{2}$, only one letter $\mathcal{R}$ appears in the symbolic sequences. In the following we consider families of cycles of map (9) grouped according to the number of letters $\mathcal{R}$ in the associated symbolic sequences.

5.2. *One letter $\mathcal{R}$ in the symbolic sequence*

As a first step, let us consider cycles of map (9) which

(i) have points in all three partitions $\mathcal{D}_{\mathcal{L}}$, $\mathcal{D}_{\mathcal{M}}$, $\mathcal{D}_{\mathcal{R}}$;
(ii) exist for $\delta_{\mathcal{L}} = 1$
(iii) have only one letter $\mathcal{R}$ in the associated symbolic sequence.

Recall that by Property 13 the first two letters of the symbolic sequence σ associated with a cycle ex-

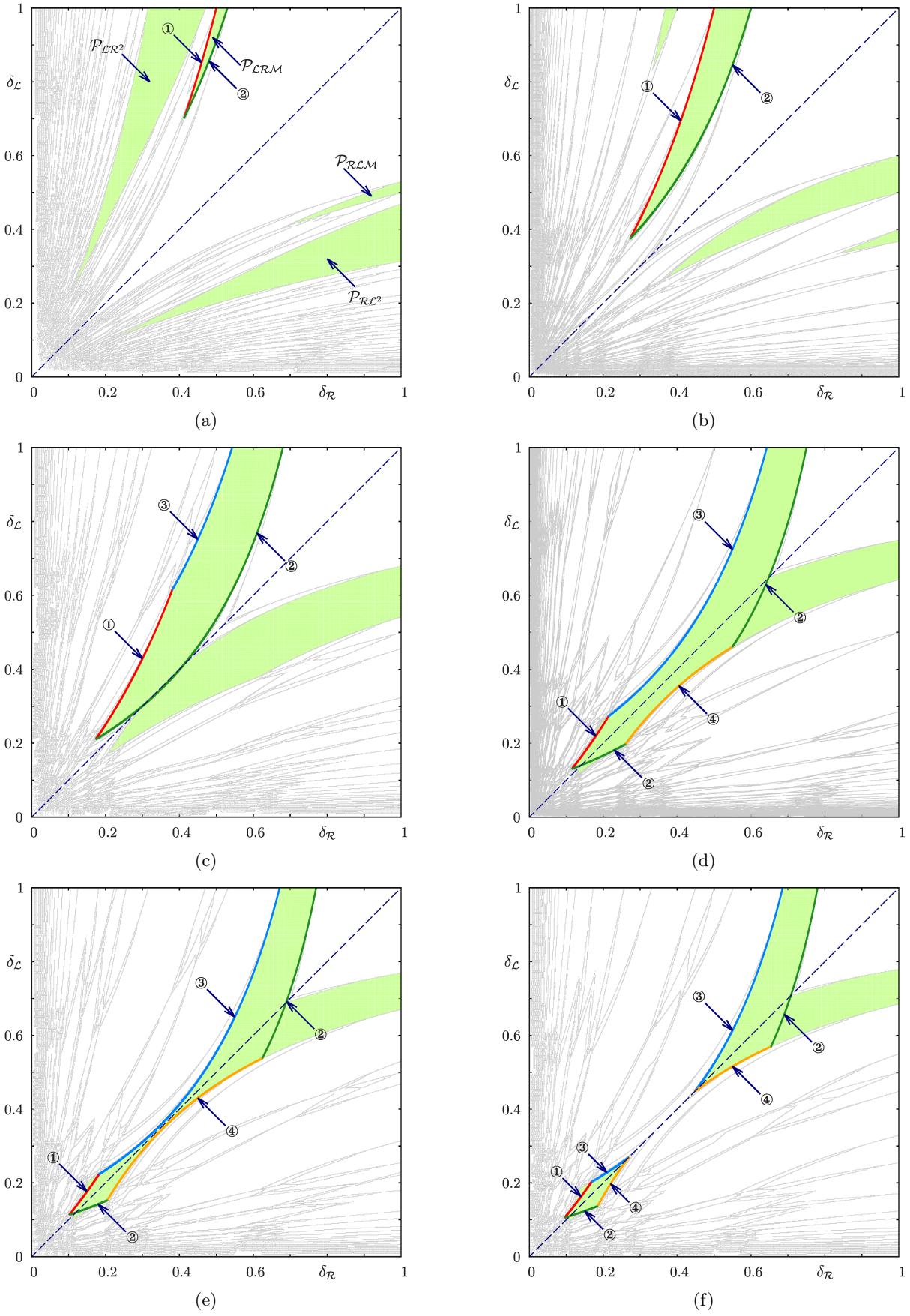

Fig. 9. Appearance of the border collision bifurcations $\xi^{0,\partial_{\mathcal{LR}}}_{\mathcal{LRM}}$, $\xi^{0,\partial_{\mathcal{LM}}}_{\mathcal{LRM}}$, $\xi^{1,\partial_{\mathcal{MR}}}_{\mathcal{LRM}}$, and $\xi^{2,\partial_{\mathcal{MR}}}_{\mathcal{LRM}}$ confining the existence region $\mathcal{P}_{\mathcal{LRM}}$ of the 3-cycle $\mathcal{O}_{\mathcal{LRM}}$ for decreasing values of k. In the figures the corresponding bifurcation curves are labeled with ①, ②, ③, and ④, respectively. Existence regions of 3-cycles are shown in light-green and labeled in (a). Parameter values: $\delta_{\mathcal{M}} = 0.3$, (a) $k = 0.47$, (b) $k = 0.40$, (c) $k = 0.32$, (d) $k = 0.25$, (e) $k = 0.23$ (f) $k = 0.22$.

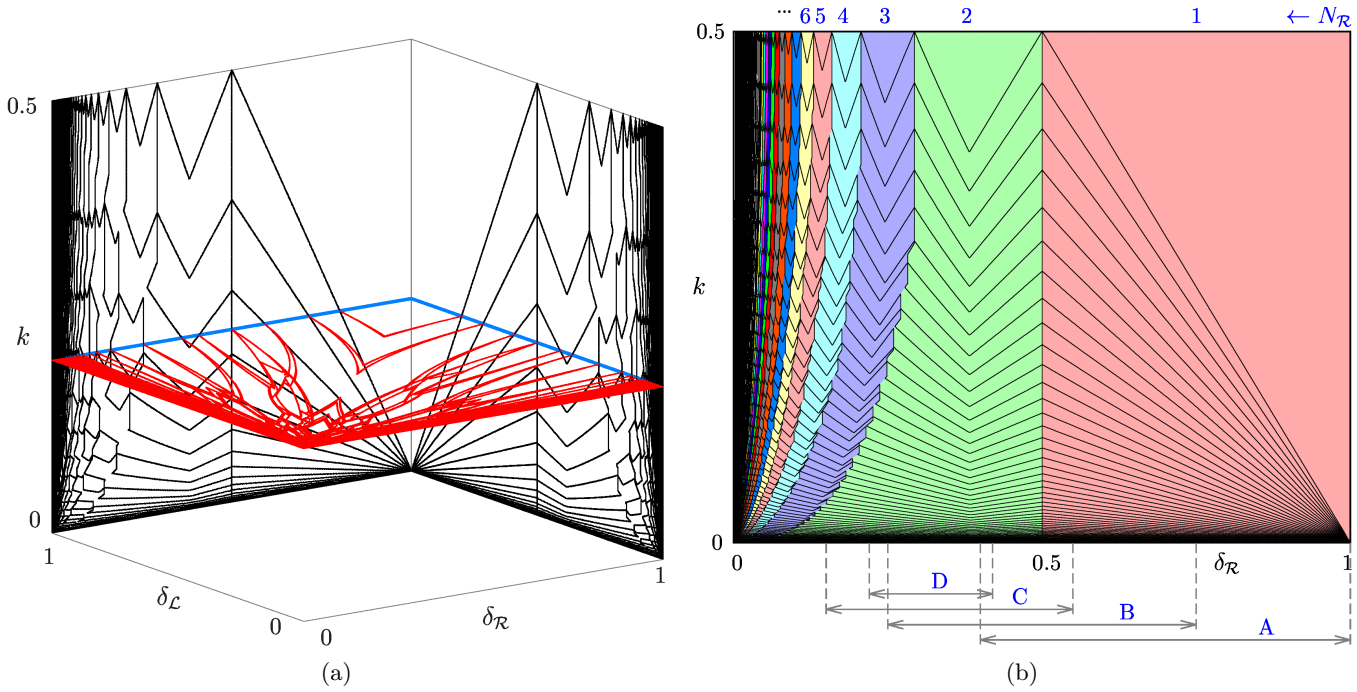

Fig. 10. (a) Bifurcation structure of the 3D parameter space $(\delta_{\mathcal{R}}, \delta_{\mathcal{L}}, k)$ of map (9) at $\delta_{\mathcal{M}} = 0.3$. The planes $(\delta_{\mathcal{R}}, \delta_{\mathcal{L}})$ with $k = 0.2$, $(\delta_{\mathcal{R}}, k)$ with $\delta_{\mathcal{L}} = 1$, and $(\delta_{\mathcal{L}}, k)$ with $\delta_{\mathcal{R}} = 1$ are shown. (b) Bifurcation structure of the parameter plane $(\delta_{\mathcal{R}}, k)$ of map (9) at $\delta_{\mathcal{L}} = 1$, $\delta_{\mathcal{M}} = 0.1$. The regions with different numbers $N_{\mathcal{R}}$ in the symbolic sequences associated with cycles are indicated by different colors. Note that in this numerically calculated figure the regions corresponding to cycles with the same period are not distinguished. The same parameter plane in the ranges of $\delta_{\mathcal{R}}$ indicated by A, B, C, and D is shown in more details in Figs. 11(b), 13(b), 15(b), and 16(b), respectively.

isting at $\delta_{\mathcal{L}} = 1$ are $\sigma_0 = \mathcal{L}$ and $\sigma_1 = \mathcal{R}$. The remaining part of σ cannot contain the letter $\mathcal{L}$ (by Property 13), neither the letter $\mathcal{R}$ (by the assumption that σ contains only one $\mathcal{R}$). Hence, the remaining letters can be only $\mathcal{M}$, i.e., there exists only one family of cycles which satisfy conditions (i) – (iii), namely

$$\{\mathcal{O}_{\mathcal{LRM}^n} \mid n \geqslant 1\} \tag{28}$$

The mechanism leading to the occurrence of cycles belonging to this family is illustrated in Fig. 11(a). As described by the Property 13, the first point of the cycle $\vec{p}_0^{\,\mathcal{LRM}^n}$ belongs to the partition $\mathcal{D}_{\mathcal{L}}$ and the second point is $\vec{p}_1^{\,\mathcal{LRM}^n} = (1, 0)^{\mathrm{T}} \in \mathcal{D}_{\mathcal{R}}$. The next point $\vec{p}_2^{\,\mathcal{LRM}^n}$ belongs to the partition $\mathcal{D}_{\mathcal{M}}$ and to the line ∂. By Property 3, the sequence of the points following $\vec{p}_2^{\,\mathcal{LRM}^n}$ (including the point $\vec{p}_0^{\,\mathcal{LRM}^n}$) is aligned along a straight line towards the point $\widetilde{\mathcal{O}}_{\mathcal{M}} = (0, 0)^{\mathrm{T}}$. Note that the points $\vec{p}_i^{\,\mathcal{LRM}^n}$, $i = 2, \ldots, n+1$ are necessarily located above the diagonal $y = x$, since otherwise the point $\vec{p}_{n+1}^{\,\mathcal{LRM}^n}$ cannot be mapped on a point in $\mathcal{D}_{\mathcal{L}}$.

From Fig. 11(a) the conditions of the bifurcations confining the existence region of a cycle $\mathcal{O}_{\mathcal{LRM}^n}$, $n \geqslant 1$, can be deduced. In general, i.e., not only for $\delta_{\mathcal{L}} = 1$, the existence conditions of this cycle and the the resulting from these conditions bifurcation boundaries which confine the corresponding existence region are described by

Property 15. *A sufficient condition for the existence of the cycle* $\mathcal{O}_{\mathcal{LRM}^n}$, $n \geqslant 1$, *is*

$$\vec{p}_0^{\,\mathcal{LRM}^n} \in \mathcal{D}_{\mathcal{L}} \tag{29a}$$
$$\vec{p}_1^{\,\mathcal{LRM}^n} \in \mathcal{D}_{\mathcal{R}} \tag{29b}$$
$$\vec{p}_{n+1}^{\,\mathcal{LRM}^n} \in \mathcal{D}_{\mathcal{M}} \tag{29c}$$

Only the following points of the cycle can collide the following boundaries:

- *The point* $\vec{p}_0^{\,\mathcal{LRM}^n}$ *can collide the boundaries* $\partial_{\mathcal{LM}}$ *and* $\partial_{\mathcal{LR}}$.
- *The point* $\vec{p}_1^{\,\mathcal{LRM}^n}$ *can collide the boundary* $\partial_{\mathcal{MR}}$.
- *The point* $\vec{p}_{n+1}^{\,\mathcal{LRM}^n}$ *can collide the boundary* $\partial_{\mathcal{LM}}$.

Obviously, conditions (29) are necessary for the existence of the cycle $\mathcal{O}_{\mathcal{LRM}^n}$. These conditions are also sufficient since Property 3 implies that condition (29c) guarantees that the points $\vec{p}_2^{\,\mathcal{LRM}^n}$, …, $\vec{p}_n^{\,\mathcal{LRM}^n}$ are located in the partition $\mathcal{D}_{\mathcal{M}}$. Accordingly, these points cannot collide any boundary, as

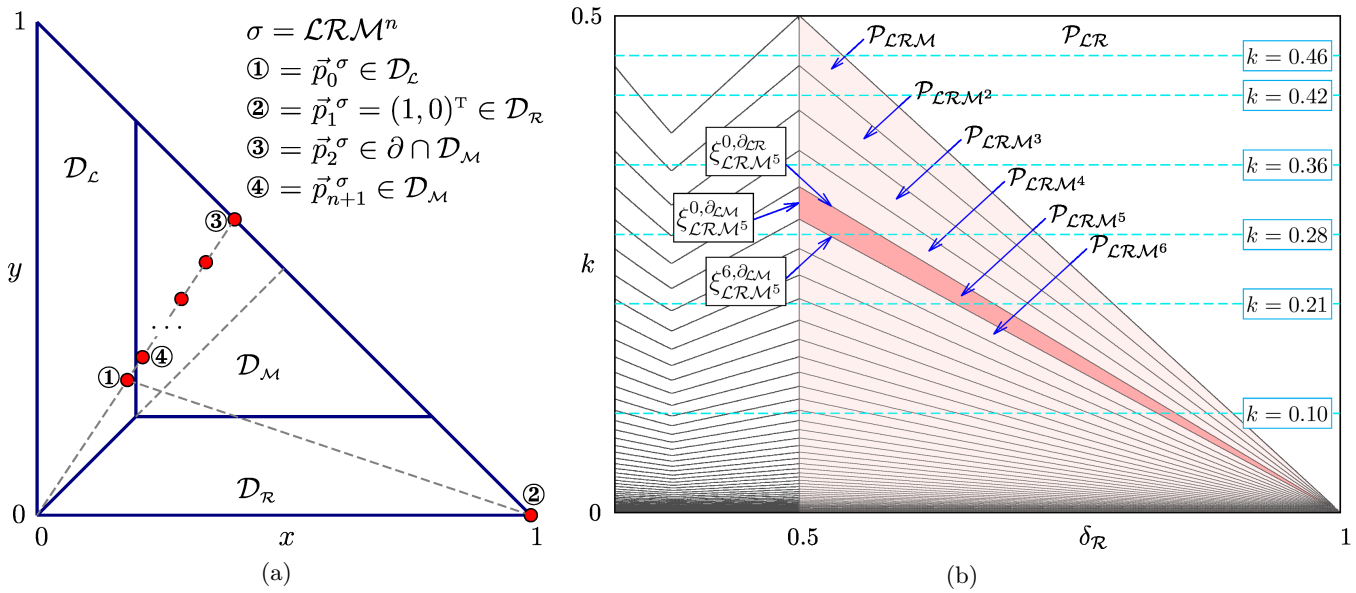

Fig. 11. (a) Mechanism leading to the appearance of cycles $\mathcal{O}_{\mathcal{LRM}^n}$, $n \geqslant 1$, of map (9) at $\delta_\mathcal{L} = 1$. (b) Regions $\mathcal{P}_{\mathcal{LRM}^n}$, $n \geqslant 1$, in the $(\delta_\mathcal{R}, k)$ parameter plane at $\delta_\mathcal{L} = 1$. As an example, the border collision bifurcation curves confining the existence region $\mathcal{P}_{\mathcal{LRM}^5}$ of the 7-cycle $\mathcal{O}_{\mathcal{LRM}^5}$ are labeled. The values of k corresponding to Fig. 12 are marked. $\delta_\mathcal{M} = 0.1$.

if the point $\vec{p}_i^{\,\mathcal{LRM}^n} \in \mathcal{D}_\mathcal{M}$, $i = 2, \ldots, n$ approaches a boundary, the $\vec{p}_{i+1}^{\,\mathcal{LRM}^n}$ is necessarily located outside $\mathcal{D}_\mathcal{M}$, i.e., the cycle $\mathcal{O}_{\mathcal{LRM}^n}$ cannot exist. The reasons why the point $\vec{p}_1^{\,\mathcal{LRM}^n}$ cannot collide the boundary $\partial_{\mathcal{LM}}$ and why the point $\vec{p}_{n+1}^{\,\mathcal{LRM}^n}$ cannot collide the boundary $\partial_{\mathcal{MR}}$ are the same as in the particular case $n = 1$ (i.e., the cycle $\mathcal{O}_{\mathcal{LRM}}$), as explained by Property 9. Therefore, for each $n \geqslant 1$ the cycle $\mathcal{O}_{\mathcal{LRM}^n}$ can undergo only the border collision bifurcations mentioned above. The expressions for these bifurcations can be obtained straightforwardly:

$$\begin{aligned}\xi^{0,\partial_{\mathcal{LM}}}_{\mathcal{LRM}^n} &= \left\{\vec{\Delta} \mid x_0^{\mathcal{LRM}^n} = k\right\} \\ &= \left\{\vec{\Delta} \mid \delta_\mathcal{L} = k\frac{1-\varrho_\mathcal{R}\varrho_\mathcal{M}^n}{(1-k)\varrho_\mathcal{R}\varrho_\mathcal{M}^n}\right\}\end{aligned} \tag{30a}$$

$$\begin{aligned}\xi^{0,\partial_{\mathcal{LR}}}_{\mathcal{LRM}^n} &= \left\{\vec{\Delta} \mid x_0^{\mathcal{LRM}^n} = y_0^{\mathcal{LRM}^n}\right\} \\ &= \left\{\vec{\Delta} \mid \delta_\mathcal{L} = \frac{\delta_\mathcal{R}}{1-\delta_\mathcal{R}}\right\}\end{aligned} \tag{30b}$$

$$\begin{aligned}\xi^{1,\partial_{\mathcal{MR}}}_{\mathcal{LRM}^n} &= \left\{\vec{\Delta} \mid y_1^{\mathcal{LRM}^n} = k\right\} \\ &= \left\{\vec{\Delta} \mid \delta_\mathcal{L} = \frac{\varrho_\mathcal{M}^n(k\varrho_\mathcal{R}+\delta_\mathcal{R}) - k}{\varrho_\mathcal{M}^n(k\varrho_\mathcal{R}+\delta_\mathcal{R})}\right\}\end{aligned} \tag{30c}$$

$$\begin{aligned}\xi^{n+1,\partial_{\mathcal{LM}}}_{\mathcal{LRM}^n} &= \left\{\vec{\Delta} \mid x_{n+1}^{\mathcal{LRM}^n} = k\right\} \\ &= \left\{\vec{\Delta} \mid \delta_\mathcal{L} = \frac{k(1-\varrho_\mathcal{R}\varrho_\mathcal{M}^n)}{\varrho_\mathcal{R}\varrho_\mathcal{M}^{n-1}(1-k\varrho_\mathcal{M})}\right\}\end{aligned} \tag{30d}$$

Note that in the particular case $\delta_\mathcal{L} = 1$ the bifurcation $\xi^{1,\partial_{\mathcal{MR}}}_{\mathcal{LRM}^n}$, $n \geqslant 1$, cannot occur, as the point $\vec{p}_1^{\,\mathcal{LRM}^n}$ is necessarily equal $(1,0)^\mathrm{T}$. As one can see in Fig. 11(b), the regions $\mathcal{P}_{\mathcal{LRM}^n}$ in the $(\delta_\mathcal{R}, k)$ parameter plane with $\delta_\mathcal{L} = 1$ are confined by the curves of border collision bifurcations $\xi^{0,\partial_{\mathcal{LM}}}_{\mathcal{LRM}^n}$, $\xi^{0,\partial_{\mathcal{LR}}}_{\mathcal{LRM}^n}$, and $\xi^{n+1,\partial_{\mathcal{LM}}}_{\mathcal{LRM}^n}$. From Eqs. (30a), (30b) and (30d) with $\delta_\mathcal{L} = 1$ we obtain that in this plain the corresponding bifurcation curves are given by straight lines:

$$\xi^{0,\partial_{\mathcal{LM}}}_{\mathcal{LRM}^n}\Big|_{\delta_\mathcal{L}=1} = \left\{\vec{\Delta} \mid k = \varrho_\mathcal{R}\varrho_\mathcal{M}^n\right\} \tag{31a}$$

$$\xi^{0,\partial_{\mathcal{LR}}}_{\mathcal{LRM}^n}\Big|_{\delta_\mathcal{L}=1} = \left\{\vec{\Delta} \mid \delta_\mathcal{R} = \tfrac{1}{2}\right\} \tag{31b}$$

$$\xi^{n+1,\partial_{\mathcal{LM}}}_{\mathcal{LRM}^n}\Big|_{\delta_\mathcal{L}=1} = \left\{\vec{\Delta} \mid k = \varrho_\mathcal{R}\varrho_\mathcal{M}^{n-1}\right\} \tag{31c}$$

The regions $\mathcal{P}_{\mathcal{LRM}^n}$, $n \geqslant 0$, in the $(\delta_\mathcal{R}, k)$ parameter plane with $\delta_\mathcal{L} = 1$ are shown in Fig. 11(b). As one can see, the portion of the $(\delta_\mathcal{R}, k)$ parameter plane with $\delta_\mathcal{L} = 1$, $\delta_\mathcal{R} > \frac{1}{2}$ below the region $\mathcal{P}_{\mathcal{LR}}$ is completely covered by the regions $\mathcal{P}_{\mathcal{LRM}^n}$. This can easily be seen, since it follows from Eqs. (31a) and (31c) that

$$\xi^{n+1,\partial_{\mathcal{LM}}}_{\mathcal{LRM}^n}\Big|_{\delta_\mathcal{L}=1} \equiv \xi^{0,\partial_{\mathcal{LM}}}_{\mathcal{LRM}^{n+1}}\Big|_{\delta_\mathcal{L}=1} \tag{32}$$

For the transfer of the obtained results to the $(\delta_\mathcal{R}, \delta_\mathcal{L})$ parameter plane the following property is important:

Property 16.

(a) For $\delta_{\mathcal{L}} = 1$, any $\delta_{\mathcal{M}}$ and any $n \geqslant 0$ there exists a non-empty region $\mathcal{P}_{\mathcal{LRM}^n}$ in the $(\delta_{\mathcal{R}}, k)$ parameter plane.

(b) For $\delta_{\mathcal{L}} = 1$ and any $0 < k^* < \frac{1}{2}$ there exists a number $n_{\max} \geqslant 1$ so that the line $k = k^*$ in the $(\delta_{\mathcal{R}}, k)$ parameter plane intersects the regions $\mathcal{P}_{\mathcal{LRM}^n}$ for $0 \leqslant n \leqslant n_{\max}$, and does not intersects the regions $\mathcal{P}_{\mathcal{LRM}^n}$ for $n > n_{\max}$. For decreasing values of k the number $n_{\max}$ increases.

This property follows immediately from Eqs. (31).

The transfer of the results from the $(\delta_{\mathcal{R}}, k)$ parameter plane with $\delta_{\mathcal{L}} = 1$ to the $(\delta_{\mathcal{R}}, \delta_{\mathcal{L}})$ parameter plane is illustrated in Fig. 12. As one can see in Fig. 11(b), the line $k = 0.46$ intersects only the regions $\mathcal{P}_{\mathcal{LR}}$ and $\mathcal{P}_{\mathcal{LRM}}$. Accordingly, as one can see in Fig. 12(a), in the $(\delta_{\mathcal{R}}, \delta_{\mathcal{L}})$ parameter plane only these two regions from the family (28) appear. Decreasing k (i.e., increasing the size of the middle partition $\mathcal{D}_{\mathcal{M}}$) we observe how the region $\mathcal{P}_{\mathcal{LRM}^2}$ appears (Fig. 12(b)), then the region $\mathcal{P}_{\mathcal{LRM}^3}$ (Fig. 12(c)). Additionally, it can be seen in Fig. 12(d) that a fourth bifurcation boundary confining the existence region of the cycle $\mathcal{O}_{\mathcal{LRM}}$ appears, namely the border collision bifurcation $\xi^{1,\partial_{\mathcal{MR}}}_{\mathcal{LRM}}$. Obviously, this bifurcation cannot occur for $\delta_{\mathcal{L}} = 1$, since it is defined by the condition (29b). The effect of this bifurcation has already been described in detail in Sec. 4.3: first the region $\mathcal{P}_{\mathcal{LRM}}$ becomes one additional boundary and then it becomes split in two parts. As one can see in Figs. 12(e) and (f), the same effect can be observed for further regions $\mathcal{P}_{\mathcal{LRM}^n}$, $n \geqslant 2$. In Fig. 12(e) the regions $\mathcal{P}_{\mathcal{LRM}}$ and $\mathcal{P}_{\mathcal{LRM}^2}$ are split in two parts, and in Fig. 12(f) the region $\mathcal{P}_{\mathcal{LRM}^3}$ is split as well. To simplify the notation, we denote in the following the part of the region $\mathcal{P}_{\mathcal{LRM}^n}$ connected with the line $\delta_{\mathcal{L}} = 1$ as its main part, and the disconnected part as a $\mathcal{P}_{\mathcal{LRM}^n}$-island. Then we conclude:

Property 17.

(a) For each value of k there exist a number $n_{\max}$ such that the regions $\mathcal{P}_{\mathcal{LRM}^n}$ in the $(\delta_{\mathcal{R}}, \delta_{\mathcal{L}})$ parameter plane exist for all $n = 0, \ldots, n_{\max}$. The number $n_{\max}$ increases with decreasing k.

(b) There exists a number $n'_{\max} < n_{\max}$ such that the $\mathcal{P}_{\mathcal{LRM}^n}$-islands exist for all $n = 0, \ldots, n'_{\max}$. The number $n'_{\max}$ increases with decreasing k. For each n the size of the $\mathcal{P}_{\mathcal{LRM}^n}$-island decreases with decreasing k. The islands with lower periodicity are located in the $(\delta_{\mathcal{R}}, \delta_{\mathcal{L}})$ parameter place closer to the origin.

(c) For each n, there is a non-empty region in the $(\delta_{\mathcal{R}}, \delta_{\mathcal{L}})$ parameter plane between the regions $\mathcal{P}_{\mathcal{LRM}^n}$ and $\mathcal{P}_{\mathcal{LRM}^{n+1}}$.

The statement 17(a) follows immediately from the Property 16(b), the other statements can be proved by direct calculations.

5.3. *Two letters $\mathcal{R}$ in the symbolic sequence*

As shown above, there exists only one family of cycles existing in the parameter plane $\delta_{\mathcal{L}} = 1$ with a single point in the partition $\mathcal{D}_{\mathcal{R}}$. Indeed, as the corresponding symbolic sequence has necessarily the prefix $\mathcal{LR}$, the remaining suffix can contain only letters $\mathcal{M}$. As a next step let us consider cycles which

(i) have points in all three partitions $\mathcal{D}_{\mathcal{L}}$, $\mathcal{D}_{\mathcal{M}}$, $\mathcal{D}_{\mathcal{R}}$;
(ii) exist for $\delta_{\mathcal{L}} = 1$
(iii) have two letters $\mathcal{R}$ in the associated symbolic sequence.

As before, the associated symbolic sequence has the prefix $\mathcal{LR}$, but the suffix in this case contains not only letters $\mathcal{M}$ but also one letter $\mathcal{R}$. Obviously, there are only three possibilities, at which position in this suffix the letter $\mathcal{R}$ can be located, namely at the end, at the beginning or in the middle. Accordingly, we can define the following three families of cycles:

$$\{\mathcal{O}_{\mathcal{LRM}^n\mathcal{R}} \mid n \geqslant 1\} \tag{33a}$$

$$\{\mathcal{O}_{\mathcal{LR}^2\mathcal{M}^n} \mid n \geqslant 1\} \tag{33b}$$

$$\{\mathcal{O}_{\mathcal{LRM}^{n_1}\mathcal{RM}^{n_2}} \mid n_1, n_2 \geqslant 1\} \tag{33c}$$

Note that from a formal point of view it is possible to extend the definition of the family (33c) by the cases $n_1 = 0$ and $n_2 = 0$, which correspond to the families (33b) and (33a), respectively. However, as shown below, it is preferable to keep these families separately, since the mechanisms leading to the appearance of these cycles and therefore also the bifurcations confining their existence regions differ.

5.3.1. *Family* $\{\mathcal{O}_{\mathcal{LRM}^n\mathcal{R}} \mid n \geqslant 1\}$

The mechanism leading to the appearance of cycles forming the family (33a) at $\delta_{\mathcal{L}} = 1$ is illustrated in Fig. 13. Clearly, the first two points of the cycle are $\vec{p}_0^{\,\mathcal{LRM}^{n_{\mathcal{R}}}} \in \mathcal{D}_{\mathcal{L}}$ and $\vec{p}_1^{\,\mathcal{LRM}^{n_{\mathcal{R}}}} \in \mathcal{D}_{\mathcal{R}} = (1, 0)^{\mathrm{T}}$. As in the case of the family (28), the next point $\vec{p}_2^{\,\mathcal{LRM}^{n_{\mathcal{R}}}}$ belongs to the partition $\mathcal{D}_{\mathcal{M}}$, however, by contrast to the previous case, it is necessarily located below the diagonal $y = x$. The following points $\vec{p}_i^{\,\mathcal{LRM}^{n_{\mathcal{R}}}}$,

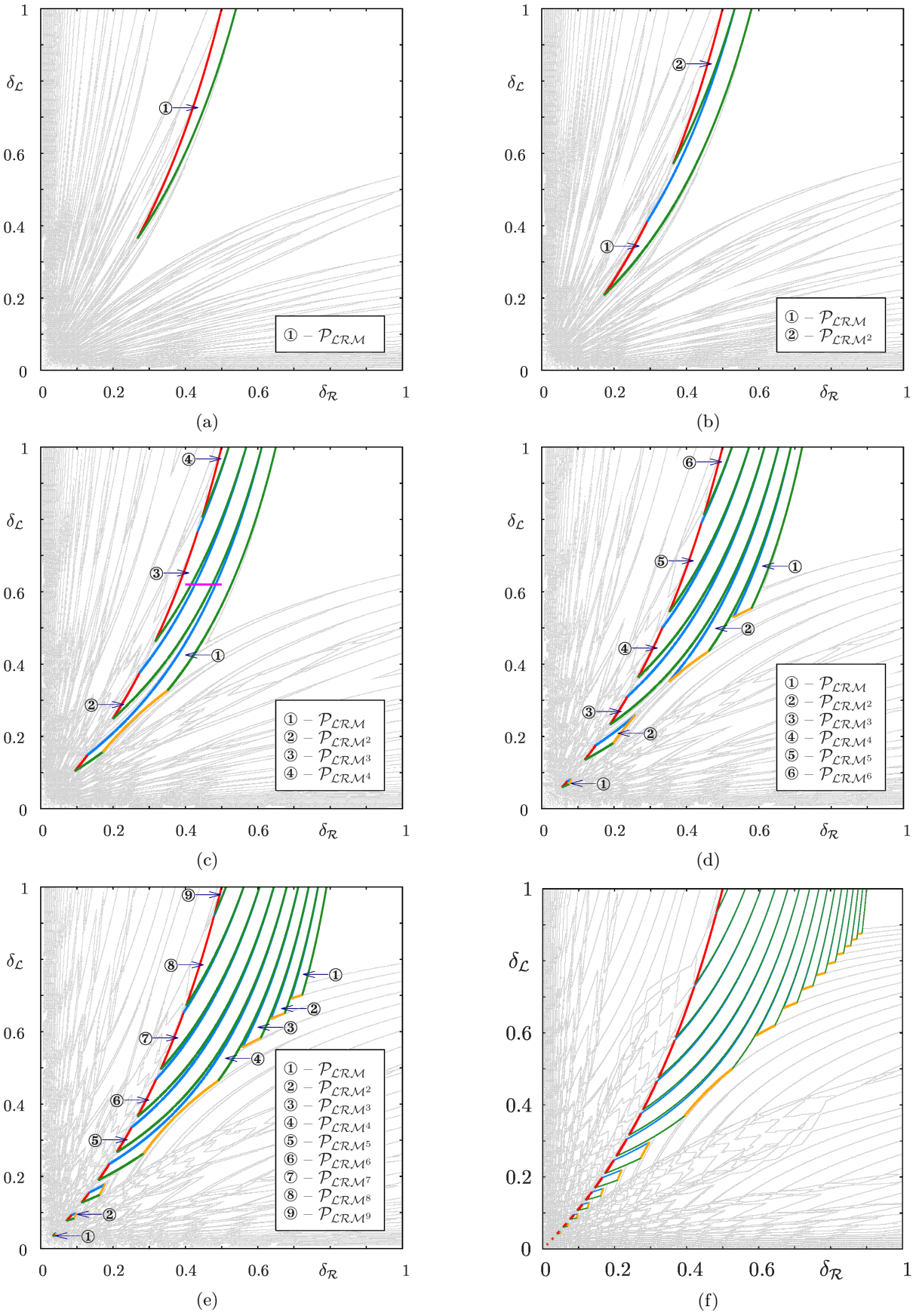

Fig. 12. Bifurcation structure of the $(\delta_{\mathcal{R}}, \delta_{\mathcal{L}})$ parameter plane at $\delta_{\mathcal{M}} = 0.1$ and (a) $k = 0.46$, (b) $k = 0.42$, (c) $k = 0.35$, (d) $k = 0.28$, (e) $k = 0.21$, (f) $k = 0.10$. The regions $\mathcal{P}_{\mathcal{LRM}^n}$, (a) $n = 1$ (b) $n = 1, 2$, (c) $n = 1, \ldots, 4$, (d) $n = 1, \ldots, 6$, (e) $n = 1, \ldots, 9$, (f) $n = 1, \ldots, 16$, are shown. The bifurcation curves $\xi^{0,\partial_{\mathcal{LM}}}_{\mathcal{LRM}^n}$ are shown red, $\xi^{0,\partial_{\mathcal{LR}}}_{\mathcal{LRM}^n}$ blue, $\xi^{1,\partial_{\mathcal{MR}}}_{\mathcal{LRM}^n}$ orange and $\xi^{n+1,\partial_{\mathcal{LM}}}_{\mathcal{LRM}^n}$ green. The corresponding lines in the $(\delta_{\mathcal{R}}, k)$ parameter plane are marked in Fig. 11(b). The bifurcation scenario along the line marked in (c) is shown in Fig. 17.

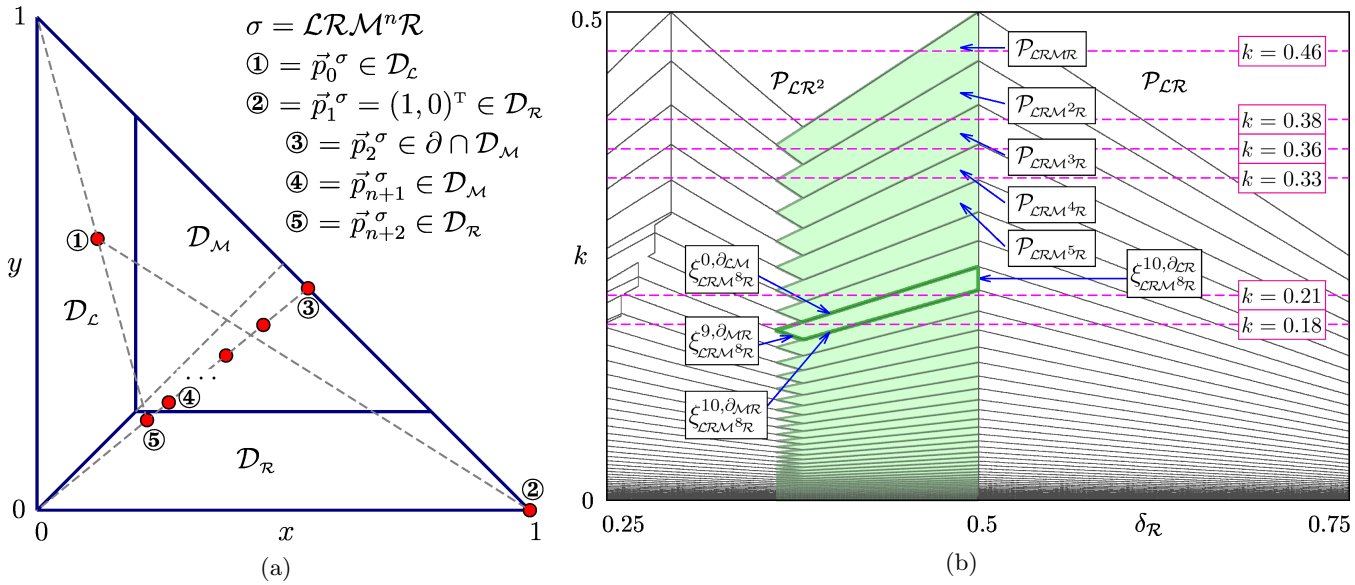

Fig. 13. (a) Mechanism leading to the appearance of cycles $\mathcal{O}_{\mathcal{LRM}^n\mathcal{R}}$, $n \geqslant 1$, of map (9) at $\delta_\mathcal{L} = 1$. (b) Regions $\mathcal{P}_{\mathcal{LRM}^n\mathcal{R}}$, $n \geqslant 1$, in the $(\delta_\mathcal{R}, k)$ parameter plane. As an example, the border collision bifurcation curves confining the existence region $\mathcal{P}_{\mathcal{LRM}^8\mathcal{R}}$ of the 11-cycle $\mathcal{O}_{\mathcal{LRM}^8\mathcal{R}}$ are labeled. The values of k corresponding to Fig. 14 are marked. $\delta_\mathcal{M} = 0.1$.

$i = 3, \ldots, n+2$ are aligned along the straight line towards the origin. Among these points all except for the last one are located in the partition $\mathcal{D}_\mathcal{M}$ and the last one in the partition $\mathcal{D}_\mathcal{R}$. Therefore,

Property 18. *A sufficient condition for the existence of the cycle $\mathcal{O}_{\mathcal{LRM}^n\mathcal{R}}$, $n \geqslant 1$, is*

$$\vec{p}_0^{\,\mathcal{LRM}^n\mathcal{R}} \in \mathcal{D}_\mathcal{L} \tag{34a}$$
$$\vec{p}_1^{\,\mathcal{LRM}^n\mathcal{R}} \in \mathcal{D}_\mathcal{R} \tag{34b}$$
$$\vec{p}_{n+1}^{\,\mathcal{LRM}^n\mathcal{R}} \in \mathcal{D}_\mathcal{M} \tag{34c}$$
$$\vec{p}_{n+2}^{\,\mathcal{LRM}^n\mathcal{R}} \in \mathcal{D}_\mathcal{R} \tag{34d}$$

The following points of the cycle can collide the following boundaries:

- *The point $\vec{p}_0^{\,\mathcal{LRM}^n\mathcal{R}}$ can collide the boundary $\partial_\mathcal{LM}$.*
- *The point $\vec{p}_0^{\,\mathcal{LRM}^n\mathcal{R}}$ can collide the boundary $\partial_\mathcal{LR}$.*
- *The point $\vec{p}_1^{\,\mathcal{LRM}^n\mathcal{R}}$ can collide the boundary $\partial_\mathcal{MR}$.*
- *The point $\vec{p}_{n+1}^{\,\mathcal{LRM}^n\mathcal{R}}$ can collide the boundary $\partial_\mathcal{MR}$.*
- *The point $\vec{p}_{n+2}^{\,\mathcal{LRM}^n\mathcal{R}}$ can collide the boundary $\partial_\mathcal{MR}$.*
- *The point $\vec{p}_{n+2}^{\,\mathcal{LRM}^n\mathcal{R}}$ can collide the boundary $\partial_\mathcal{LR}$.*

To demonstrate that no other border collision bifurcations are possible note that the condition $\vec{p}_{n+1}^{\,\mathcal{LRM}^n\mathcal{R}} \in \mathcal{D}_\mathcal{M}$ implies $\vec{p}_i^{\,\mathcal{LRM}^n\mathcal{R}} \in \mathcal{D}_\mathcal{M}$ for $i = 2, \ldots, n$, so that these points cannot collide a boundary. Similarly, the point $\vec{p}_1^{\,\mathcal{LRM}^n\mathcal{R}}$ cannot collide the boundary $\partial_\mathcal{LR}$, as $\vec{p}_2^{\,\mathcal{LRM}^n\mathcal{R}} \in \mathcal{D}_\mathcal{R}$, while a point approaching the boundary $\partial_\mathcal{LR}$ must be mapped in $\mathcal{D}_\mathcal{L}$.

Straight forward calculations lead to the following expressions of the border collision bifurcations of the cycles $\mathcal{O}_{\mathcal{LRM}^n\mathcal{R}}$:

$$\xi^{0,\partial_\mathcal{LM}}_{\mathcal{LRM}^n\mathcal{R}} = \left\{\vec{\Delta} \mid x_0^{\mathcal{LRM}^n\mathcal{R}} = k\right\} = \left\{\vec{\Delta} \mid \delta_\mathcal{L} = \frac{1-\varrho_\mathcal{M}^n\varrho_\mathcal{R}^2}{(1-k)\varrho_\mathcal{M}^n\varrho_\mathcal{R}^2}\right\} \tag{35a}$$

$$\xi^{0,\partial_\mathcal{LR}}_{\mathcal{LRM}^n\mathcal{R}} = \left\{\vec{\Delta} \mid x_0^{\mathcal{LRM}^n\mathcal{R}} = y_0^{\mathcal{LRM}^n\mathcal{R}}\right\} = \left\{\vec{\Delta} \mid \delta_\mathcal{L} = \frac{\delta_\mathcal{R}(1+\varrho_\mathcal{M}^n\varrho_\mathcal{R})}{\varrho_\mathcal{M}^n(1-\delta_\mathcal{R})^2}\right\} \tag{35b}$$

$$\xi^{1,\partial_\mathcal{MR}}_{\mathcal{LRM}^n\mathcal{R}} = \left\{\vec{\Delta} \mid y_1^{\mathcal{LRM}^n\mathcal{R}} = k\right\} = \left\{\vec{\Delta} \mid \delta_\mathcal{L} = \frac{\delta_\mathcal{R} + \varrho_\mathcal{M}^n\varrho_\mathcal{R}(\delta_\mathcal{R}+k\varrho_\mathcal{R}) - k}{\delta_\mathcal{R} + \varrho_\mathcal{M}^n\varrho_\mathcal{R}(\delta_\mathcal{R}+k\varrho_\mathcal{R})}\right\} \tag{35c}$$

$$\xi^{n+1,\partial_\mathcal{MR}}_{\mathcal{LRM}^n\mathcal{R}} = \left\{\vec{\Delta} \mid y_{n+1}^{\mathcal{LRM}^n\mathcal{R}} = k\right\} = \left\{\vec{\Delta} \mid \delta_\mathcal{L} = \frac{\varrho_\mathcal{M}^{n-1}(\delta_\mathcal{R}(1+\varrho_\mathcal{R}) + k\varrho_\mathcal{R}^2\varrho_\mathcal{M}) - k}{\varrho_\mathcal{M}^{n-1}(\delta_\mathcal{R}\varrho_\mathcal{R} + k\varrho_\mathcal{R}^2\varrho_\mathcal{M})}\right\} \tag{35d}$$

$$\xi^{n+2,\partial_\mathcal{MR}}_{\mathcal{LRM}^n\mathcal{R}} = \left\{\vec{\Delta} \mid y_{n+2}^{\mathcal{LRM}^n\mathcal{R}} = k\right\} = \left\{\vec{\Delta} \mid \delta_\mathcal{L} = \frac{\varrho_\mathcal{M}^n(\delta_\mathcal{R}(1+\varrho_\mathcal{R}) + k\varrho_\mathcal{R}^2) - k}{\varrho_\mathcal{M}^n(\delta_\mathcal{R}\varrho_\mathcal{R} + k\varrho_\mathcal{R}^2)}\right\} \tag{35e}$$

$$\xi^{n+2,\partial_\mathcal{LR}}_{\mathcal{LRM}^n\mathcal{R}} = \left\{\vec{\Delta} \mid x_{n+2}^{\mathcal{LRM}^n\mathcal{R}} = y_{n+2}^{\mathcal{LRM}^n\mathcal{R}}\right\} = \left\{\vec{\Delta} \mid \delta_\mathcal{L} = \frac{\delta_\mathcal{R}(2-\delta_\mathcal{R})}{1-\delta_\mathcal{R}^2}\right\} \tag{35f}$$

For the particular case $\delta_\mathcal{L} = 1$ the bifurcations $\xi^{0,\partial_\mathcal{LR}}_{\mathcal{LRM}^n\mathcal{R}}$ and $\xi^{1,\partial_\mathcal{MR}}_{\mathcal{LRM}^n\mathcal{R}}$ cannot occur. To show that the point $\vec{p}_0^{\,\mathcal{LRM}^n\mathcal{R}}$ cannot collide $\partial_\mathcal{LR}$ note that in the

case $\delta_{\mathcal{L}} = 1$ the condition $\vec{p}_2^{\,\mathcal{LRM}^{n_{\mathcal{R}}}} = (1-\delta_{\mathcal{R}}, \delta_{\mathcal{R}})^{\mathrm{T}} \in \mathcal{D}_{\mathcal{M}}$ implies $\delta_{\mathcal{R}} > k$. Therefore, $y_{n+2}^{\mathcal{LRM}^{n_{\mathcal{R}}}} > k$, since $y_{n+2}^{\mathcal{LRM}^{n_{\mathcal{R}}}} = y_{n+1}^{\mathcal{LRM}^{n_{\mathcal{R}}}} + \delta_{\mathcal{R}}$, and $y_{n+1}^{\mathcal{LRM}^{n_{\mathcal{R}}}} > 0$. As any point $(x,y)^{\mathrm{T}} \in \partial_{\mathcal{LR}}$ satisfies $x = y < k$, a collision of the point $\vec{p}_0^{\,\mathcal{LRM}^{n_{\mathcal{R}}}}$ with $\partial_{\mathcal{LR}}$ is not possible.
For the other bifurcations we obtain form Eqs. (35):

$$\xi^{0,\partial_{\mathcal{LM}}}_{\mathcal{LRM}^n\mathcal{R}}\Big|_{\delta_{\mathcal{L}}=1} = \left\{\vec{\Delta} \mid k = \varrho_{\mathcal{M}}^n \varrho_{\mathcal{R}}^2\right\} \tag{36a}$$

$$\xi^{n+1,\partial_{\mathcal{MR}}}_{\mathcal{LRM}^n\mathcal{R}}\Big|_{\delta_{\mathcal{L}}=1} = \left\{\vec{\Delta} \mid k = \varrho_{\mathcal{M}}^{n-1} \delta_{\mathcal{R}}\right\} \tag{36b}$$

$$\xi^{n+2,\partial_{\mathcal{MR}}}_{\mathcal{LRM}^n\mathcal{R}}\Big|_{\delta_{\mathcal{L}}=1} = \left\{\vec{\Delta} \mid k = \varrho_{\mathcal{M}}^{n} \delta_{\mathcal{R}}\right\} \tag{36c}$$

$$\xi^{n+2,\partial_{\mathcal{LR}}}_{\mathcal{LRM}^n\mathcal{R}}\Big|_{\delta_{\mathcal{L}}=1} = \left\{\vec{\Delta} \mid \delta_{\mathcal{R}} = 1\right\} \tag{36d}$$

Obviously, the regions $\mathcal{P}_{\mathcal{LRM}^n\mathcal{R}}$ and $\mathcal{P}_{\mathcal{LRM}^{n+1}\mathcal{R}}$ are adjacent in the $(\delta_{\mathcal{R}}, k)$ parameter plane with $\delta_{\mathcal{L}} = 1$, since it follows from Eqs. (36b) and (36c) that

$$\xi^{n+2,\partial_{\mathcal{MR}}}_{\mathcal{LRM}^{n+1}\mathcal{R}}\Big|_{\delta_{\mathcal{L}}=1} = \xi^{n+2,\partial_{\mathcal{MR}}}_{\mathcal{LRM}^n\mathcal{R}}\Big|_{\delta_{\mathcal{L}}=1} \tag{37}$$

The bifurcation structure formed by the regions $\mathcal{P}_{\mathcal{LRM}^n\mathcal{R}}$ in the $(\delta_{\mathcal{R}}, k)$ parameter plane is shown in Fig. 13(b). Similar to Property 16, Eqs. (36) imply:

Property 19.
(a) For $\delta_{\mathcal{L}} = 1$, any $\delta_{\mathcal{M}}$ and any $n \geqslant 0$ there exists a non-empty region $\mathcal{P}_{\mathcal{LRM}^n\mathcal{R}}$ in the $(\delta_{\mathcal{R}}, k)$ parameter plane.
(b) For $\delta_{\mathcal{L}} = 1$ and any $0 < k^* < \frac{1}{2}$ there exist numbers $n_{\max} > n_{min} \geqslant 1$ so that the line $k = k^*$ in the $(\delta_{\mathcal{R}}, k)$ parameter plane intersects the regions $\mathcal{P}_{\mathcal{LRM}^n\mathcal{R}}$ for $n_{\min} \leqslant n \leqslant n_{\max}$, and does not intersects the regions $\mathcal{P}_{\mathcal{LRM}^n}$ for $n < n_{\min}$ and $n > n_{\max}$. For decreasing values of k both numbers $n_{\min}$ and $n_{\max}$ increase.

In other words, the family (33a) similar to family (28) is represented in the $(\delta_{\mathcal{R}}, k)$ parameter plane for each value of $\delta_{\mathcal{M}}$ by an infinite family of regions $\mathcal{P}_{\mathcal{LRM}^n\mathcal{R}}$, among which only a finite number of regions are intersected by the line $k = k^*$ for each k^*. The difference between the families (28) and (33a) regards their regions intersected by this line for decreasing k. Recall that by Property 16(b), when a particular region $\mathcal{P}_{\mathcal{LRM}^n}$ becomes intersected by this line for some value k^*, it remains intersected by all smaller values of k^* as well. By contrast, according to Property 22(b), when k^* is decreased, each particular region $\mathcal{P}_{\mathcal{LRM}^n\mathcal{R}}$ becomes first intersected by the line $k = k^*$ and then it becomes not intersected.

The presented results explain the bifurcation structure formed by the regions $\mathcal{P}_{\mathcal{LRM}^n\mathcal{R}}$ in the $(\delta_{\mathcal{R}}, \delta_{\mathcal{L}})$ parameter plane. The development of this structure for decreasing values of k^* is shown in Fig. 14. It follows from Fig. 13, that the regions for decreasing values of k^* the regions $\mathcal{P}_{\mathcal{LRM}^n\mathcal{R}}$ for increasing $n \geqslant 1$ appear after each other (similar to the regions $\mathcal{P}_{\mathcal{LRM}^n}$ discussed above). By contrast to the regions $\mathcal{P}_{\mathcal{LRM}^n}$ they can also disappear.
As one can see in Fig. 14(a), for a large value of k^* the line $k = k^*$ in the $(\delta_{\mathcal{R}}, k)$ parameter plane with $\delta_{\mathcal{L}} = 1$ intersects only the region $\mathcal{P}_{\mathcal{LRMR}}$. The boundaries of this region in the $(\delta_{\mathcal{R}}, \delta_{\mathcal{L}})$ parameter plane are given by the border collision bifurcation curves $\xi^{0,\partial_{\mathcal{LM}}}_{\mathcal{LRMR}}$ and $\xi^{3,\partial_{\mathcal{LR}}}_{\mathcal{LRMR}}$. Indeed, it can easily be seen in Fig. 13(b) that when for decreasing k^* a region $\mathcal{P}_{\mathcal{LRM}^n\mathcal{R}}$ appears in the $(\delta_{\mathcal{R}}, \delta_{\mathcal{L}})$ parameter plane, then at the beginning it is confined by the border collision bifurcation curves $\xi^{0,\partial_{\mathcal{LM}}}_{\mathcal{LRM}^n\mathcal{R}}$ and $\xi^{n+2,\partial_{\mathcal{LR}}}_{\mathcal{LRM}^n\mathcal{R}}$. Then, with decreasing k^* the region becomes more boundaries, namely first the border collision bifurcation curve $\xi^{n+2,\partial_{\mathcal{MR}}}_{\mathcal{LRM}^n\mathcal{R}}$ appears, and then $\xi^{0,\partial_{\mathcal{MR}}}_{\mathcal{LRM}^n\mathcal{R}}$. So, for example in Fig. 14(b) the region $\mathcal{P}_{\mathcal{LRMR}}$ is confined by four border collision bifurcation curves, namely, $\xi^{0,\partial_{\mathcal{LM}}}_{\mathcal{LRMR}}$, $\xi^{3,\partial_{\mathcal{LR}}}_{\mathcal{LRMR}}$, $\xi^{3,\partial_{\mathcal{MR}}}_{\mathcal{LRMR}}$, and $\xi^{0,\partial_{\mathcal{MR}}}_{\mathcal{LRMR}}$. The next region $\mathcal{P}_{\mathcal{LRM}^2\mathcal{R}}$ is confined by three border collision bifurcation curves, namely, $\xi^{0,\partial_{\mathcal{LM}}}_{\mathcal{LRM}^2\mathcal{R}}$, $\xi^{4,\partial_{\mathcal{LR}}}_{\mathcal{LRM}^2\mathcal{R}}$, and $\xi^{4,\partial_{\mathcal{MR}}}_{\mathcal{LRM}^2\mathcal{R}}$. Finally, the "newborn" region $\mathcal{P}_{\mathcal{LRM}^3\mathcal{R}}$ is still confined by two curves only, namely, $\xi^{0,\partial_{\mathcal{LM}}}_{\mathcal{LRM}^3\mathcal{R}}$, $\xi^{4,\partial_{\mathcal{LR}}}_{\mathcal{LRM}^3\mathcal{R}}$.
When k^* is further decreased, the regions $\mathcal{P}_{\mathcal{LRM}^n\mathcal{R}}$ become split in two parts. The mechanism leading to that is the same as in the case of the regions $\mathcal{P}_{\mathcal{LRM}^n}$ (the border collision bifurcation curves $\xi^{0,\partial_{\mathcal{LM}}}_{\mathcal{LRM}^n\mathcal{R}}$, $\xi^{4,\partial_{\mathcal{LR}}}_{\mathcal{LRM}^n\mathcal{R}}$ become tangent to each other). In Fig. 14(c) the $\mathcal{P}_{\mathcal{LRMR}}$-island is already created. Note that the main part of $\mathcal{P}_{\mathcal{LRMR}}$ is already shrunk and its boundaries are now defined by the border collision bifurcation curves $\xi^{0,\partial_{\mathcal{LM}}}_{\mathcal{LRMR}}$, $\xi^{3,\partial_{\mathcal{MR}}}_{\mathcal{LRMR}}$. For further decreasing k^* the main part of the region $\mathcal{P}_{\mathcal{LRMR}}$ disappears completely, as one can see in Fig. 14(d), and only the $\mathcal{P}_{\mathcal{LRMR}}$-island remains. The same phenomenon occurs for the regions $\mathcal{P}_{\mathcal{LRM}^n\mathcal{R}}$ for higher values of n. So, for example, Fig. 14(d) shows the regions $\mathcal{P}_{\mathcal{LRM}^2\mathcal{R}}$ immediately before it splits in two parts.
In the transformations of the bifurcation structure described above only four border collision bifurcation boundaries of the regions $\mathcal{P}_{\mathcal{LRM}^n\mathcal{R}}$ are involved. When k^* becomes small enough, also the

fifth border collision bifurcation boundary $\xi^{1,\partial_{\mathcal{MR}}}_{\mathcal{LRM}^n\mathcal{R}}$ appears, which leads to a significant change in the bifurcation structure. As one can see in Fig. 14(e), a both the main parts of the regions $\mathcal{P}_{\mathcal{LRM}^n\mathcal{R}}$ and the $\mathcal{P}_{\mathcal{LRM}^n\mathcal{R}}$-islands become this new boundary. As a consequence, the islands decrease in size and moreover, some of them disappears, as illustrated in Fig. 14(f).
To summarize, the following result can be stated for the regions $\mathcal{P}_{\mathcal{LRM}^n\mathcal{R}}$:

Property 20.
(a) For each value of k there exist numbers $n_{\min}$, $n_{\max}$ such that the main parts of the regions $\mathcal{P}_{\mathcal{LRM}^n\mathcal{R}}$ exist in the $(\delta_{\mathcal{R}}, \delta_{\mathcal{L}})$ parameter plane for all $n = n_{\min}, \dots, n_{\max}$.
(b) The $\mathcal{P}_{\mathcal{LRM}^n\mathcal{R}}$-islands may exist for some (but not necessarily for all) $n = 1, \dots, n_{\max}$. Islands with lower periodicity are located in the $(\delta_{\mathcal{R}}, \delta_{\mathcal{L}})$ parameter place closer to the origin.

This Property follows from Eqs. (35). Comparing Properties 17 and 20 one can see immediately that the results obtained for the family (33a) are not so strong as similar results which hold for the family (28). In particular, the existence of islands depends on the particular value of k and can not be deduced from the existence of the corresponding main parts of the corresponding $\mathcal{P}_{\mathcal{LRM}^n\mathcal{R}}$ region. Note also that in the example discussed above the border collision bifurcation curves $\xi^{0,\partial_{\mathcal{LR}}}_{\mathcal{LRM}^n\mathcal{R}}$, $n \geqslant 1$, are not involved. It can be shown that for larger values of $\delta_{\mathcal{M}}$ these bifurcations appear and lead to disappearance of some $\mathcal{P}_{\mathcal{LRM}^n\mathcal{R}}$-islands.

5.3.2. *Family* $\{\mathcal{O}_{\mathcal{LR}^2\mathcal{M}^n} \mid n \geqslant 1\}$

The appearance of cycles forming the family (33b) at $\delta_{\mathcal{L}} = 1$ is illustrated in Fig. 15. As before, the first two points of the cycle correspond to the prefix $\mathcal{LR}$ in the associated symbolic sequence: The point $\vec{p}_0^{\,\mathcal{LRM}^{n_{\mathcal{R}}}}$ is located in the partition $\mathcal{D}_{\mathcal{L}}$ and hence the next point $\vec{p}_1^{\,\mathcal{LRM}^{n_{\mathcal{R}}}}$ is $(1,0)^{\mathrm{T}} \in \mathcal{D}_{\mathcal{R}}$. However, the value $\delta_{\mathcal{R}}$ is now not large enough to map the point $(1,0)^{\mathrm{T}}$ in the partition $\mathcal{D}_{\mathcal{M}}$ so that next point $\vec{p}_2^{\,\mathcal{LRM}^{n_{\mathcal{R}}}} \in \partial$ is also located in $\mathcal{D}_{\mathcal{R}}$ and only the following point $\vec{p}_3^{\,\mathcal{LRM}^{n_{\mathcal{R}}}} \in \partial$ belongs to $\mathcal{D}_{\mathcal{M}}$. Moreover, to prevent the appearance of a third letter $\mathcal{R}$ in the associated symbolic sequence it is necessary to require that point $\vec{p}_3^{\,\mathcal{LRM}^{n_{\mathcal{R}}}}$ is located above the diagonal $y = x$. The following points $\vec{p}_i^{\,\mathcal{LRM}^{n_{\mathcal{R}}}}$, $i = 4, \dots, n+2$ are aligned along the straight line towards the origin and are located in the partition $\mathcal{D}_{\mathcal{M}}$.

Therefore,

Property 21. *A sufficient condition for the existence of the cycle $\mathcal{O}_{\mathcal{LR}^2\mathcal{M}^n}$, $n \geqslant 1$, is*

$$\vec{p}_0^{\,\mathcal{LRM}^{n_{\mathcal{R}}}} \in \mathcal{D}_{\mathcal{L}} \tag{38a}$$
$$\vec{p}_2^{\,\mathcal{LRM}^{n_{\mathcal{R}}}} \in \mathcal{D}_{\mathcal{R}} \tag{38b}$$
$$\vec{p}_{n+2}^{\,\mathcal{LRM}^{n_{\mathcal{R}}}} \in \mathcal{D}_{\mathcal{M}} \tag{38c}$$

The following points of the cycle can collide the following boundaries:
- *The point $\vec{p}_0^{\,\mathcal{LR}^2\mathcal{M}^n}$ can collide the boundary $\partial_{\mathcal{LR}}$.*
- *The point $\vec{p}_0^{\,\mathcal{LR}^2\mathcal{M}^n}$ can collide the boundary $\partial_{\mathcal{LM}}$.*
- *The point $\vec{p}_2^{\,\mathcal{LR}^2\mathcal{M}^n}$ can collide the boundary $\partial_{\mathcal{MR}}$.*
- *The point $\vec{p}_{n+2}^{\,\mathcal{LR}^2\mathcal{M}^n}$ can collide the boundary $\partial_{\mathcal{LM}}$.*

To demonstrate that conditions (38) are sufficient for the existence of the cycle $\mathcal{O}_{\mathcal{LR}^2\mathcal{M}^n}$ note that by condition (38b) the point $\vec{p}_1^{\,\mathcal{LR}^2\mathcal{M}^n}$ is located in the partition $\mathcal{D}_{\mathcal{R}}$. Similarly, condition (38c) implies that the points $\vec{p}_i^{\,\mathcal{LR}^2\mathcal{M}^n}$, $i = 3, \dots, n+1$ are located in the partition $\mathcal{D}_{\mathcal{M}}$.

The expressions for the border collision bifurcations of the cycle $\mathcal{O}_{\mathcal{LR}^2\mathcal{M}^n}$, $n \geqslant 1$, is can be calculated straightforwardly:

$$\begin{aligned}\xi^{0,\partial_{\mathcal{LR}}}_{\mathcal{LR}^2\mathcal{M}^n} &= \left\{\vec{\Delta} \mid x_0^{\mathcal{LR}^2\mathcal{M}^n} = y_0^{\mathcal{LR}^2\mathcal{M}^n}\right\} \\ &= \left\{\vec{\Delta} \mid \delta_{\mathcal{L}} = \frac{\delta_{\mathcal{R}}(2-\delta_{\mathcal{R}})}{\varrho_{\mathcal{R}}^2}\right\}\end{aligned} \tag{39a}$$

$$\begin{aligned}\xi^{0,\partial_{\mathcal{LM}}}_{\mathcal{LR}^2\mathcal{M}^n} &= \left\{\vec{\Delta} \mid x_0^{\mathcal{LR}^2\mathcal{M}^n} = k\right\} \\ &= \left\{\vec{\Delta} \mid \delta_{\mathcal{L}} = \frac{k(1-\varrho_{\mathcal{M}}^n\varrho_{\mathcal{R}}^2)}{(1-k)\varrho_{\mathcal{M}}^n\varrho_{\mathcal{R}}^2}\right\}\end{aligned} \tag{39b}$$

$$\begin{aligned}\xi^{2,\partial_{\mathcal{MR}}}_{\mathcal{LR}^2\mathcal{M}^n} &= \left\{\vec{\Delta} \mid y_2^{\mathcal{LR}^2\mathcal{M}^n} = k\right\} \\ &= \left\{\vec{\Delta} \mid \delta_{\mathcal{L}} = \frac{\delta_{\mathcal{R}} + \varrho_{\mathcal{M}}^n\varrho_{\mathcal{R}}(\delta_{\mathcal{R}} + k\varrho_{\mathcal{R}}) - k}{\varrho_{\mathcal{M}}^n\varrho_{\mathcal{R}}(\delta_{\mathcal{R}} + k\varrho_{\mathcal{R}})}\right\}\end{aligned} \tag{39c}$$

$$\begin{aligned}\xi^{n+2,\partial_{\mathcal{LM}}}_{\mathcal{LR}^2\mathcal{M}^n} &= \left\{\vec{\Delta} \mid x_{n+2}^{\mathcal{LR}^2\mathcal{M}^n} = k\right\} \\ &= \left\{\vec{\Delta} \mid \delta_{\mathcal{L}} = \frac{1-\varrho_{\mathcal{M}}^n\varrho_{\mathcal{R}}^2}{\varrho_{\mathcal{M}}^{n-1}\varrho_{\mathcal{R}}^2(1-k\varrho_{\mathcal{M}})}\right\}\end{aligned} \tag{39d}$$

From Eqs. (39) the expressions of the corresponding border collision bifurcation curves in the $(\delta_{\mathcal{R}}, k)$ parameter plane can easily be obtained:

$$\xi^{0,\partial_{\mathcal{LR}}}_{\mathcal{LR}^2\mathcal{M}^n}\Big|_{\delta_{\mathcal{L}}=1} = \left\{\vec{\Delta} \mid \delta_{\mathcal{R}} = 1 - \tfrac{\sqrt{2}}{2}\right\} \tag{40a}$$

$$\xi^{0,\partial_{\mathcal{LM}}}_{\mathcal{LR}^2\mathcal{M}^n}\Big|_{\delta_{\mathcal{L}}=1} = \left\{\vec{\Delta} \mid k = \varrho_{\mathcal{M}}^n\varrho_{\mathcal{R}}^2\right\} \tag{40b}$$

$$\xi^{2,\partial_{\mathcal{MR}}}_{\mathcal{LR}^2\mathcal{M}^n}\Big|_{\delta_{\mathcal{L}}=1} = \left\{\vec{\Delta} \mid k = \delta_{\mathcal{R}}\right\} \tag{40c}$$

$$\xi^{n+2,\partial_{\mathcal{LM}}}_{\mathcal{LR}^2\mathcal{M}^n}\Big|_{\delta_{\mathcal{L}}=1} = \left\{\vec{\Delta} \mid k = \varrho_{\mathcal{M}}^{n-1}\varrho_{\mathcal{R}}^2\right\} \tag{40d}$$

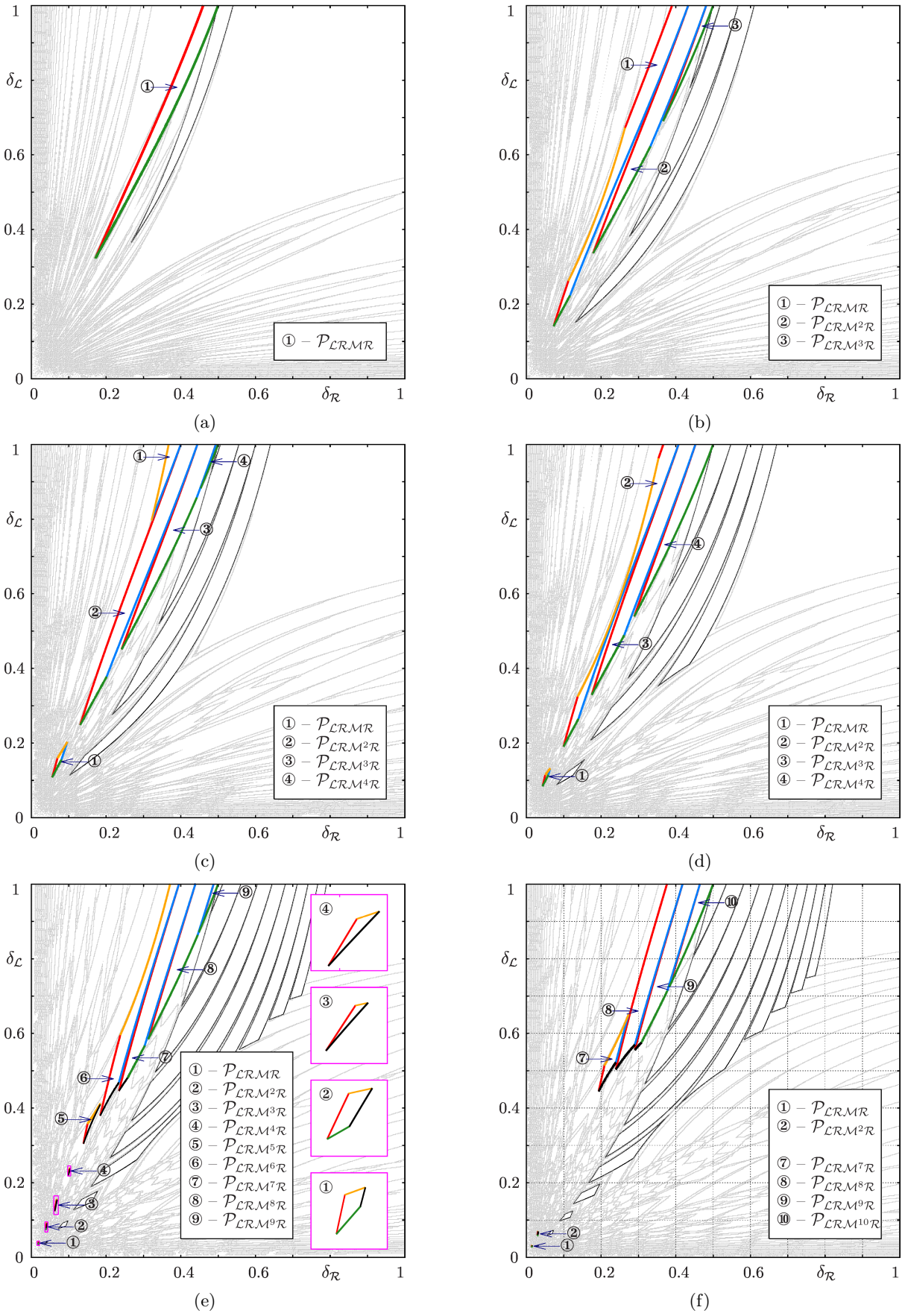

Fig. 14. Bifurcation structure of the $(\delta_{\mathcal{R}}, \delta_{\mathcal{L}})$ parameter plane at $\delta_{\mathcal{M}} = 0.1$ and (a) $k = 0.46$, (b) $k = 0.39$, (c) $k = 0.36$, (d) $k = 0.33$, (e) $k = 0.21$, (f) $k = 0.18$. The regions $\mathcal{P}_{\mathcal{LRM}^n\mathcal{R}}$ with (a) $n = 1$ (b) $n = 1, 2, 3$, (c) $n = 1, \ldots, 4$, (d) $n = 1, \ldots, 4$, (e) $n = 1, \ldots, 9$, (f) $n = 1, 2, 7, 8, 9, 10$, are show. The bifurcation curves $\xi^{0,\partial_{\mathcal{LM}}}_{\mathcal{LRM}^n\mathcal{R}}$ are shown orange, $\xi^{1,\partial_{\mathcal{MR}}}_{\mathcal{LRM}^n\mathcal{R}}$ black, $\xi^{n+1,\partial_{\mathcal{MR}}}_{\mathcal{LRM}^n\mathcal{R}}$ red, $\xi^{n+2,\partial_{\mathcal{MR}}}_{\mathcal{LRM}^n\mathcal{R}}$ blue, and $\xi^{n+2,\partial_{\mathcal{LR}}}_{\mathcal{LRM}^n\mathcal{R}}$ green. The corresponding lines in the $(\delta_{\mathcal{R}}, k)$ parameter plane are marked in Fig. 13(b).

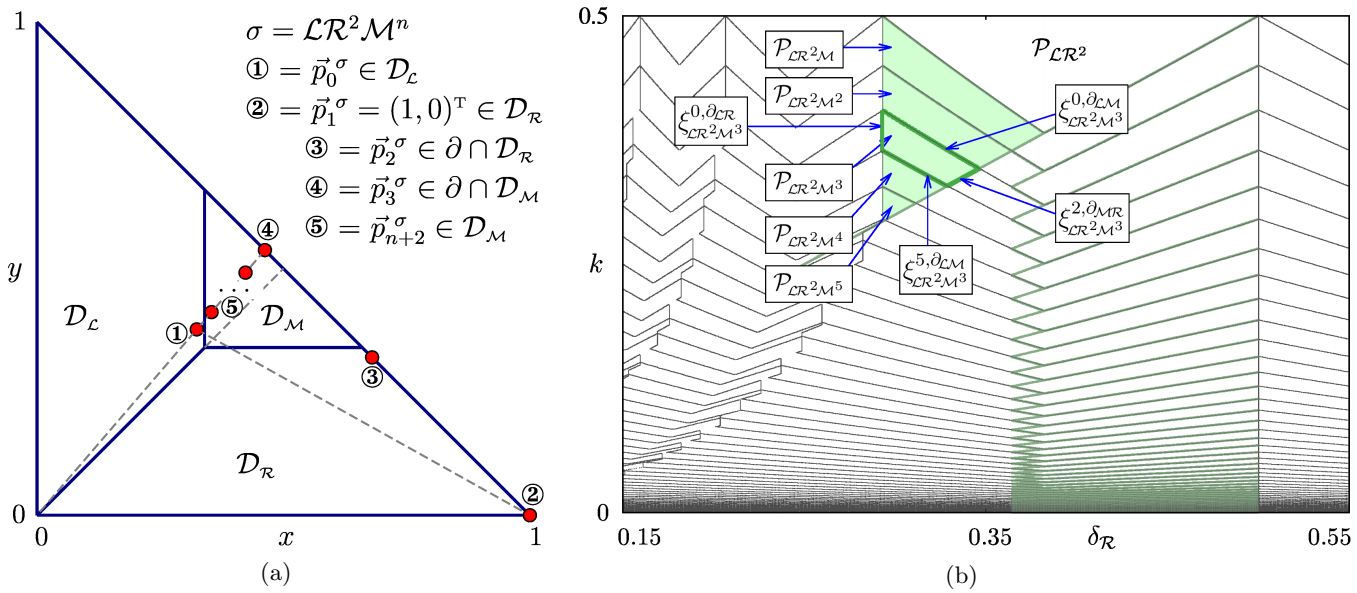

(a) (b)

Fig. 15. (a) Mechanism leading to the appearance of cycles $\mathcal{O}_{\mathcal{LR}^2\mathcal{M}^n}$, $n \geqslant 1$, of map (9) at $\delta_{\mathcal{L}} = 1$. (b) Regions $\mathcal{P}_{\mathcal{LR}^2\mathcal{M}^n}$, $n = 1, \ldots, 5$, in the $(\delta_{\mathcal{R}}, k)$ parameter plane. As an example, the border collision bifurcation curves confining the existence region $\mathcal{P}_{\mathcal{LR}^2\mathcal{M}^3}$ of the 6-cycle $\mathcal{O}_{\mathcal{LR}^2\mathcal{M}^3}$ are labeled. $\delta_{\mathcal{M}} = 0.1$.

As follows from Eqs. (40b) and (40d), the regions $\mathcal{P}_{\mathcal{LR}^2\mathcal{M}^n}$ and $\mathcal{P}_{\mathcal{LR}^2\mathcal{M}^{n+1}}$ are adjacent in the $(\delta_{\mathcal{R}}, k)$ parameter plane with $\delta_{\mathcal{L}} = 1$, since

$$\xi^{n+3,\partial_{\mathcal{LM}}}_{\mathcal{LR}^2\mathcal{M}^{n+1}}\Big|_{\delta_{\mathcal{L}}=1} = \xi^{0,\partial_{\mathcal{LM}}}_{\mathcal{LR}^2\mathcal{M}^{n}}\Big|_{\delta_{\mathcal{L}}=1} \tag{41}$$

The regions $\mathcal{P}_{\mathcal{LR}^2\mathcal{M}^n}$ in the bifurcation structure of the $(\delta_{\mathcal{R}}, k)$ parameter plane with $\delta_{\mathcal{L}} = 1$ are shown in Fig. 15(b). It follows from Eqs. (40) that the family (33b) differs from the families (28) and (33a) in the following respect:

Property 22.

(a) For $\delta_{\mathcal{L}} = 1$ and any $\delta_{\mathcal{M}}$ there exists a number $N_{\max} \geqslant 1$ such that non-empty regions $\mathcal{P}_{\mathcal{LR}^2\mathcal{M}^n}$ in the $(\delta_{\mathcal{R}}, k)$ parameter plane exist for $n = 1, \ldots, N_{\max}$ and do not exist for $n > N_{\max}$.

(b) For $\delta_{\mathcal{L}} = 1$ and any $n \geqslant 1$ there exists a value of $\delta_{\mathcal{M}}$ such that a non-empty regions $\mathcal{P}_{\mathcal{LR}^2\mathcal{M}^n}$ in the $(\delta_{\mathcal{R}}, k)$ parameter plane exist.

(c) For $\delta_{\mathcal{L}} = 1$ and any $1 - \frac{\sqrt{2}}{2} < k^* < \frac{1}{2}$ there exist numbers $N_{\max} \geqslant n_{\max} > n_{min} \geqslant 1$ so that the line $k = k^*$ in the $(\delta_{\mathcal{R}}, k)$ parameter plane intersects the regions $\mathcal{P}_{\mathcal{LR}^2\mathcal{M}^n}$ for $n_{\min} \leqslant n \leqslant n_{\max}$, and does not intersects the regions $\mathcal{P}_{\mathcal{LR}^2\mathcal{M}^n}$ for $n < n_{\min}$ and $n > n_{\max}$. For $k^* \geqslant \frac{\sqrt{2}}{2}$ the line $k = k^*$ in the $(\delta_{\mathcal{R}}, k)$ parameter plane does not intersects any of the regions $\mathcal{P}_{\mathcal{LR}^2\mathcal{M}^n}$.

By contrast to the families (28) and (33a) which correspond to infinite sequences of regions in the $(\delta_{\mathcal{R}}, k)$ parameter plane with $\delta_{\mathcal{L}} = 1$ for each $\delta_{\mathcal{M}}$, the family (33b) correspond to a finite sequence of regions in this plane. However, by Property 22(b), in the 3D parameter space $(\delta_{\mathcal{R}}, k, \delta_{\mathcal{M}})$ this sequence is infinite. Indeed, this can easily be shown taking into account that the border collision bifurcation curves $\xi^{0,\partial_{\mathcal{LR}}}_{\mathcal{LR}^2\mathcal{M}^n}$ and $\xi^{2,\partial_{\mathcal{MR}}}_{\mathcal{LR}^2\mathcal{M}^n}$ in the $(\delta_{\mathcal{R}}, k)$ parameter plane with $\delta_{\mathcal{L}} = 1$ do not depend on $\delta_{\mathcal{M}}$, whereas the distance between the border collision bifurcation curves $\xi^{0,\partial_{\mathcal{LM}}}_{\mathcal{LR}^2\mathcal{M}^n}$ and $\xi^{n+2,\partial_{\mathcal{LM}}}_{\mathcal{LR}^2\mathcal{M}^n}$ decreases for decreasing $\delta_{\mathcal{M}}$.

5.3.3. *Family* $\{\mathcal{O}_{\mathcal{LRM}^{n_1}\mathcal{RM}^{n_2}} \mid n_{1,2} \geqslant 1\}$

The appearance of a cycle belonging to the family (33c) at $\delta_{\mathcal{L}} = 1$ is illustrated in Fig. 16. As one cal see, the first two points $\vec{p}_0{}^{\sigma}$, $\vec{p}_1{}^{\sigma}$ of a cycle $\mathcal{O}_{\sigma}$, $\sigma = \mathcal{LRM}^{n_1}\mathcal{RM}^{n_2}$, $n_{1,2} > 0$, (corresponding to the prefix $\mathcal{LR}$ in the associated symbolic sequence σ) are located in the same way as it is for all other cycles considered before. The next point $\vec{p}_2{}^{\sigma}$ is necessarily located at the line ∂ below its intersection with the diagonal $y = x$. Accordingly, the point $\vec{p}_{n_1+2}{}^{\sigma}$ (which follows a sequence of n_1 points $\vec{p}_2{}^{\sigma}, \ldots, \vec{p}_{n_1+1}{}^{\sigma}$ located in $\mathcal{D}_{\mathcal{M}}$) belongs to the partition $\mathcal{D}_{\mathcal{R}}$. This is similar to the mechanism leading to the appearance of the cycles family (33a). The difference is that the point $\vec{p}_{n_1+2}{}^{\sigma}$ is mapped not in $\mathcal{D}_{\mathcal{L}}$ but in $\mathcal{D}_{\mathcal{M}}$, so that the point $\vec{p}_{n_1+3}{}^{\sigma}$ starts the next sequence of n_2 points in the partition $\mathcal{D}_{\mathcal{M}}$. This point

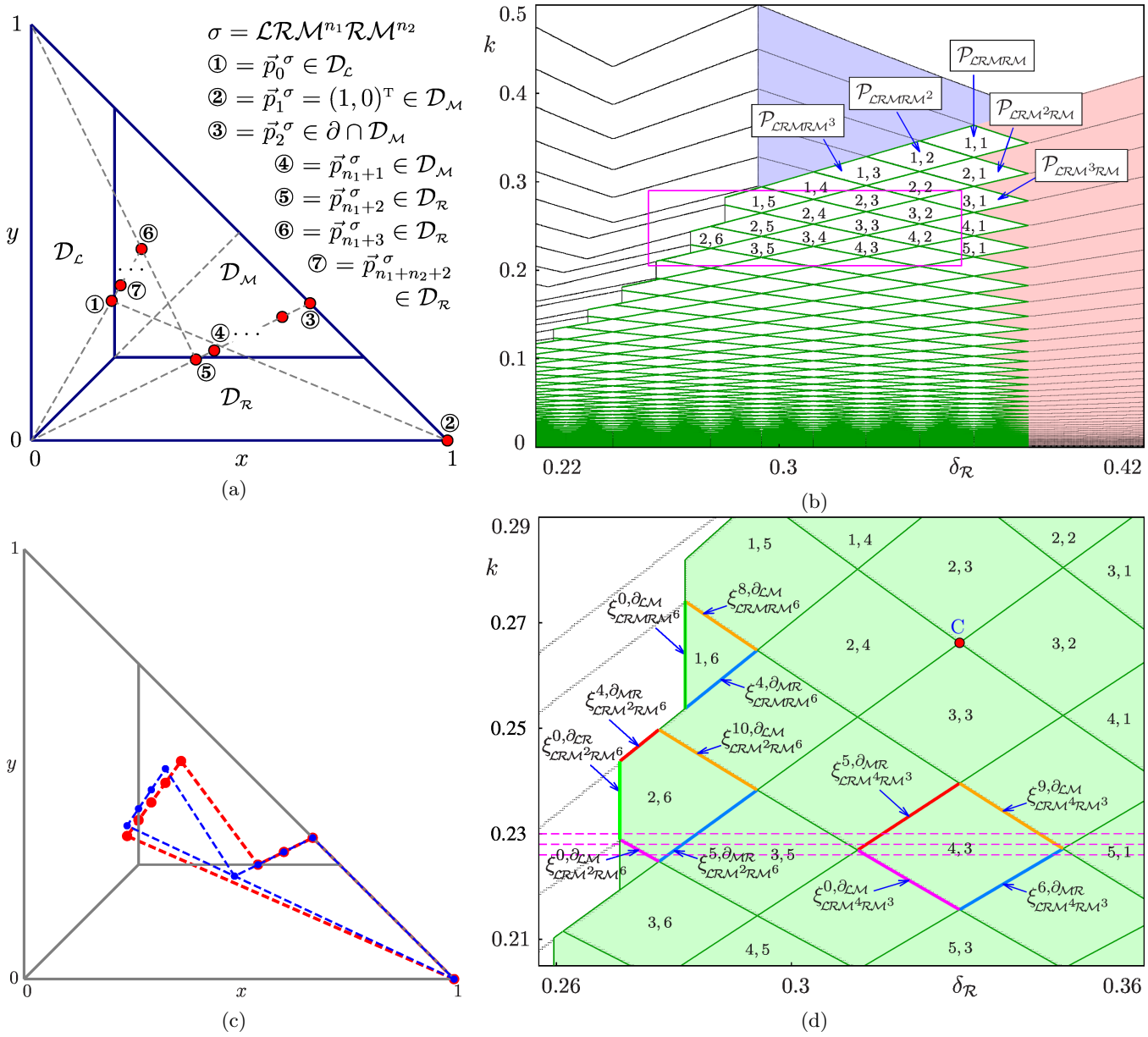

Fig. 16. (a) Mechanism leading to the appearance of cycles $\mathcal{O}_{\mathcal{LRM}^{n_1}\mathcal{RM}^{n_2}}$, $n_1, n_2 \geqslant 1$, of map (9) at $\delta_\mathcal{L} = 1$. (b) The existence regions of the cycles $\mathcal{O}_{\mathcal{LRM}^n\mathcal{R}}$, $n \geqslant 1$ are shown red; of the cycles $\mathcal{O}_{\mathcal{LR}^2\mathcal{M}^n}$, $n \geqslant 1$, blue; and of the cycles $\mathcal{O}_{\mathcal{LRM}^{n_1}\mathcal{RM}^{n_2}}$, $n_1, n_2 \geqslant 1$ green. The pairs of number specify the values n_1, n_2 of the cycle existing in the corresponding region. (c) Cycles $\mathcal{O}_{\mathcal{LRM}^3\mathcal{RM}^3}$ (blue) and $\mathcal{O}_{\mathcal{LRM}^2\mathcal{RM}^4}$ (red) at the moment of the codimension-2 border collision bifurcation occurring at $\delta_\mathcal{R} \approx 0.328609$, $k \approx 0.266171$. The corresponding parameter point is marked by C in (d). (d) Magnification of the rectangle marked in (b). Horizontal dashed lines mark the values $k = 0.226$, $k = 0.228$, and $k = 0.23$. $\delta_\mathcal{M} = 0.1$.

is necessarily located above the diagonal $y = x$, so that the last point of that sequence, i.e., the point $\vec{p}_{n_1+n_2+2}^{\,\sigma}$, is mapped in the partition $\mathcal{D}_\mathcal{L}$, i.e., on the $\vec{p}_0^{\,\sigma}$. The described mechanism leads to the following property:

Property 23. *A sufficient condition for the existence of the cycle $\mathcal{O}_\sigma$, with $\sigma = \mathcal{LRM}^{n_1}\mathcal{RM}^{n_2}$, $n_1, n_2 \geqslant 1$, is*

$$\vec{p}_0^{\,\sigma} \in \mathcal{D}_\mathcal{L} \tag{42a}$$
$$\vec{p}_1^{\,\sigma} \in \mathcal{D}_\mathcal{R} \tag{42b}$$
$$\vec{p}_{n_1+1}^{\,\sigma} \in \mathcal{D}_\mathcal{M} \tag{42c}$$
$$\vec{p}_{n_1+2}^{\,\sigma} \in \mathcal{D}_\mathcal{R} \tag{42d}$$
$$\vec{p}_{n_1+n_2+2}^{\,\sigma} \in \mathcal{D}_\mathcal{M} \tag{42e}$$

The following points of the cycle can collide the following boundaries:

- *The point* $\vec{p}_0^{\,\sigma}$ *can collide the boundary* $\partial_{\mathcal{LM}}$.
- *The point* $\vec{p}_0^{\,\sigma}$ *can collide the boundary* $\partial_{\mathcal{LR}}$.
- *The point* $\vec{p}_1^{\,\sigma}$ *can collide the boundary* $\partial_{\mathcal{MR}}$.
- *The point* $\vec{p}_{n_1+1}^{\,\sigma}$ *can collide the boundary* $\partial_{\mathcal{MR}}$.
- *The point* $\vec{p}_{n_1+2}^{\,\sigma}$ *can collide the boundary* $\partial_{\mathcal{MR}}$.
- *The point* $\vec{p}_{n_1+n_2+2}^{\,\sigma}$ *can collide the boundary* $\partial_{\mathcal{LM}}$.

This property can be proven by arguments similar to Properties 15, 18, and 21.
The expressions for the border collision bifurcations of the cycle $\mathcal{O}_{\mathcal{LR}^2\mathcal{M}^n}$, $n \geqslant 1$, is can be calculated straightforwardly:

$$\xi^{0,\partial_{\mathcal{LM}}}_{\mathcal{LRM}^{n_1}\mathcal{RM}^{n_2}} = \left\{\vec{\Delta} \mid x_0^{\mathcal{LRM}^{n_1}\mathcal{RM}^{n_2}} = k\right\} = \left\{\vec{\Delta} \mid \delta_{\mathcal{L}} = \frac{k\left(1-\varrho_{\mathcal{M}}^{n_1+n_2}\varrho_{\mathcal{R}}^2\right)}{(1-k)\varrho_{\mathcal{M}}^{n_1+n_2}\varrho_{\mathcal{R}}^2}\right\} \tag{43a}$$

$$\xi^{0,\partial_{\mathcal{LR}}}_{\mathcal{LRM}^{n_1}\mathcal{RM}^{n_2}} = \left\{\vec{\Delta} \mid x_0^{\mathcal{LRM}^{n_1}\mathcal{RM}^{n_2}} = y_0^{\mathcal{LRM}^{n_1}\mathcal{RM}^{n_2}}\right\} = \left\{\vec{\Delta} \mid \delta_{\mathcal{L}} = \frac{\delta_{\mathcal{R}}(1+\varrho_{\mathcal{M}}^{n_1}\varrho_{\mathcal{R}})}{\varrho_{\mathcal{M}}^{n_1}\varrho_{\mathcal{R}}^2}\right\} \tag{43b}$$

$$\xi^{1,\partial_{\mathcal{MR}}}_{\mathcal{LRM}^{n_1}\mathcal{RM}^{n_2}} = \left\{\vec{\Delta} \mid y_1^{\mathcal{LRM}^{n_1}\mathcal{RM}^{n_2}} = k\right\} = \left\{\vec{\Delta} \mid \delta_{\mathcal{L}} = \frac{\varrho_{\mathcal{M}}^{n_2}(\varrho_{\mathcal{M}}^{n_1}\varrho_{\mathcal{R}}(\delta_{\mathcal{R}}+k\varrho_{\mathcal{R}})+\delta_{\mathcal{R}})-k}{\varrho_{\mathcal{M}}^{n_2}(\varrho_{\mathcal{M}}^{n_1}\varrho_{\mathcal{R}}(\delta_{\mathcal{R}}+k\varrho_{\mathcal{R}})+\delta_{\mathcal{R}})}\right\} \tag{43c}$$

$$\xi^{n_1+1,\partial_{\mathcal{LM}}}_{\mathcal{LRM}^{n_1}\mathcal{RM}^{n_2}} = \left\{\vec{\Delta} \mid y_{n_1+1}^{\mathcal{LRM}^{n_1}\mathcal{RM}^{n_2}} = k\right\} = \left\{\vec{\Delta} \mid \delta_{\mathcal{L}} = \frac{\varrho_{\mathcal{M}}^{n_1-1}(\varrho_{\mathcal{M}}^{n_2}\varrho_{\mathcal{R}}(\delta_{\mathcal{R}}+k\varrho_{\mathcal{R}}\varrho_{\mathcal{M}})-\delta_{\mathcal{R}})+k}{\varrho_{\mathcal{M}}^{n_1+n_2-1}\varrho_{\mathcal{R}}(\delta_{\mathcal{R}}+k\varrho_{\mathcal{R}}\varrho_{\mathcal{M}})}\right\} \tag{43d}$$

$$\xi^{n_1+2,\partial_{\mathcal{LM}}}_{\mathcal{LRM}^{n_1}\mathcal{RM}^{n_2}} = \left\{\vec{\Delta} \mid y_{n_1+2}^{\mathcal{LRM}^{n_1}\mathcal{RM}^{n_2}} = k\right\} = \left\{\vec{\Delta} \mid \delta_{\mathcal{L}} = \frac{\varrho_{\mathcal{M}}^{n_1}(\varrho_{\mathcal{M}}^{n_2}\varrho_{\mathcal{R}}(\delta_{\mathcal{R}}+k\varrho_{\mathcal{R}})+\delta_{\mathcal{R}})-k}{\varrho_{\mathcal{M}}^{n_1+n_2}\varrho_{\mathcal{R}}(\delta_{\mathcal{R}}+k\varrho_{\mathcal{R}})}\right\} \tag{43e}$$

$$\xi^{n_1+n_2+2,\partial_{\mathcal{LM}}}_{\mathcal{LRM}^{n_1}\mathcal{RM}^{n_2}} = \left\{\vec{\Delta} \mid y_{n_1+n_2+2}^{\mathcal{LRM}^{n_1}\mathcal{RM}^{n_2}} = k\right\} = \left\{\vec{\Delta} \mid \delta_{\mathcal{L}} = \frac{k(1-\varrho_{\mathcal{M}}^{n_1+n_2-1}\varrho_{\mathcal{R}}^2\varrho_{\mathcal{M}})}{\varrho_{\mathcal{M}}^{n_1+n_2-1}\varrho_{\mathcal{R}}^2(1-k\varrho_{\mathcal{M}})}\right\} \tag{43f}$$

Clearly, the border collision bifurcations $\xi^{1,\partial_{\mathcal{MR}}}_{\mathcal{LRM}^{n_1}\mathcal{RM}^{n_2}}$ cannot occur in the case $\delta_{\mathcal{L}} = 1$. The expressions for the remaining five bifurcations in the case $\delta_{\mathcal{L}} = 1$ can easily be obtained from Eqs. (44):

$$\xi^{0,\partial_{\mathcal{LM}}}_{\mathcal{LRM}^{n_1}\mathcal{RM}^{n_2}}\Big|_{\delta_{\mathcal{L}}=1} = \left\{\vec{\Delta} \mid k = \varrho_{\mathcal{M}}^{n_1+n_2}\varrho_{\mathcal{R}}^2\right\} \tag{44a}$$

$$\xi^{0,\partial_{\mathcal{LR}}}_{\mathcal{LRM}^{n_1}\mathcal{RM}^{n_2}}\Big|_{\delta_{\mathcal{L}}=1} = \left\{\vec{\Delta} \mid \delta_{\mathcal{R}} = \frac{3}{4}\varrho_{\mathcal{M}} - \frac{1}{4\varrho_{\mathcal{M}}^{n_1}}\sqrt{6\varrho_{\mathcal{M}}^{n_1}+\varrho_{\mathcal{M}}^{2n_1}+1}\right\} \tag{44b}$$

$$\xi^{n_1+1,\partial_{\mathcal{LM}}}_{\mathcal{LRM}^{n_1}\mathcal{RM}^{n_2}}\Big|_{\delta_{\mathcal{L}}=1} = \left\{\vec{\Delta} \mid k = \varrho_{\mathcal{M}}^{n_1-1}\delta_{\mathcal{R}}\right\} \tag{44c}$$

$$\xi^{n_1+2,\partial_{\mathcal{LM}}}_{\mathcal{LRM}^{n_1}\mathcal{RM}^{n_2}}\Big|_{\delta_{\mathcal{L}}=1} = \left\{\vec{\Delta} \mid k = \varrho_{\mathcal{M}}^{n_1}\delta_{\mathcal{R}}\right\} \tag{44d}$$

$$\xi^{n_1+n_2+2,\partial_{\mathcal{LM}}}_{\mathcal{LRM}^{n_1}\mathcal{RM}^{n_2}}\Big|_{\delta_{\mathcal{L}}=1} = \left\{\vec{\Delta} \mid k = \varrho_{\mathcal{M}}^{n_1+n_2-1}\varrho_{\mathcal{R}}^2\right\} \tag{44e}$$

Therefore, the regions $\mathcal{P}_{\mathcal{LRM}^{n_1}\mathcal{RM}^{n_2}}$, $\mathcal{P}_{\mathcal{LRM}^{n_1+1}\mathcal{RM}^{n_2}}$, and $\mathcal{P}_{\mathcal{LRM}^{n_1}\mathcal{RM}^{n_2+1}}$ are adjacent in the $(\delta_{\mathcal{R}}, k)$ parameter plane with $\delta_{\mathcal{L}} = 1$, since

$$\xi^{n_1+2,\partial_{\mathcal{LM}}}_{\mathcal{LRM}^{n_1+1}\mathcal{RM}^{n_2}}\Big|_{\delta_{\mathcal{L}}=1} = \xi^{n_1+2,\partial_{\mathcal{LM}}}_{\mathcal{LRM}^{n_1}\mathcal{RM}^{n_2}}\Big|_{\delta_{\mathcal{L}}=1} \tag{45}$$

$$\xi^{0,\partial_{\mathcal{LM}}}_{\mathcal{LRM}^{n_1}\mathcal{RM}^{n_2}}\Big|_{\delta_{\mathcal{L}}=1} = \xi^{n_1+n_2+3,\partial_{\mathcal{LM}}}_{\mathcal{LRM}^{n_1}\mathcal{RM}^{n_2+1}}\Big|_{\delta_{\mathcal{L}}=1} \tag{46}$$

The bifurcation structure formed by the regions $\mathcal{P}_{\mathcal{LRM}^{n_1}\mathcal{RM}^{n_2}}$, $n_1, n_2 \geqslant 1$, in the $(\delta_{\mathcal{R}}, k)$ parameter plane with $\delta_{\mathcal{L}} = 1$ is shown in Fig. 16(b). As one can see, the regions form a kind of grid of rhomboid-like regions uniquely defined by two indexes n_1 and n_2. More precisely, we can state the following:

Property 24.
(a) For $\delta_{\mathcal{L}} = 1$ *and any* $\delta_{\mathcal{M}}$ *a non-empty region* $\mathcal{P}_{\mathcal{LRM}^{n_1}\mathcal{RM}^{n_2}}$ *exists in the* $(\delta_{\mathcal{R}}, k)$ *parameter plane for any* $n_1 \geqslant 1$ *and any* $n_2 = 1, \ldots, N_{\max}(n_1)$ *and does not exist for* $n_2 > N_{\max}(n_1)$.
(b) For any $n_1 \geqslant 1$ *the region* $\mathcal{P}_{\mathcal{LRM}^{n_1}\mathcal{RM}^{n_2}}$ *in the* $(\delta_{\mathcal{R}}, k)$ *parameter plane is confined by four border collision bifurcation curves* $\xi^{0,\partial_{\mathcal{LM}}}_{\mathcal{LRM}^{n_1}\mathcal{RM}^{n_2}}$, $\xi^{n_1+1,\partial_{\mathcal{LM}}}_{\mathcal{LRM}^{n_1}\mathcal{RM}^{n_2}}$, $\xi^{n_1+2,\partial_{\mathcal{LM}}}_{\mathcal{LRM}^{n_1}\mathcal{RM}^{n_2}}$, $\xi^{n_1+n_2+2,\partial_{\mathcal{LM}}}_{\mathcal{LRM}^{n_1}\mathcal{RM}^{n_2}}$ *iff* $n_2 < N_{\max}(n_1)$. *In general, a part of the region with the largest possible value of* n_2, *i.e.,* $\mathcal{P}_{\mathcal{LRM}^{n_1}\mathcal{RM}^{N_{\max}(n_1)}}$, *is cut off by the border collision bifurcation curve* $\xi^{0,\partial_{\mathcal{LR}}}_{\mathcal{LRM}^{n_1}\mathcal{RM}^{n_2}}$.
(c) For a fixed value of $\delta_{\mathcal{R}}$ *and* k *tending to zero,* n_1 *increases to infinity. For a fixed value of* k *and* $\delta_{\mathcal{R}}$ *decreasing,* n_1 *decreases and* n_2 *increases.*

As one can see in Fig. 16(b), at the value of $\delta_{\mathcal{M}}$ used in this figure there exist regions $\mathcal{P}_{\mathcal{LRMRM}^{n_2}}$ with $n_2 = 1, \ldots, 6$, i.e., $N_{\max}(1) = 6$. Similarly, it can be seen that $N_{\max}(2) = 7$, $N_{\max}(3) = 7$, $N_{\max}(4) = 8$, and so on. It is worth noticing that for increasing n_1 also $N_{\max}(n_1)$ increases. Moreover, it can be seen in Fig. 10(b), for k tending to zero the regions $\mathcal{P}_{\mathcal{LRM}^{n_1}\mathcal{RM}^{n_2}}$ occupy more and more space in the $(\delta_{\mathcal{R}}, k)$ parameter plane, leaving less space for

the existence regions of the cycles with the symbolic sequences containing more than two letters $\mathcal{R}$.

Property 24(b) is illustrated in Fig. 16(d). The region $\mathcal{P}_{\mathcal{LRM}^4\mathcal{RM}^3}$ represents the generic case, since $n_2 = 3 < N_{\max}(4) = 8$. Therefore, this region is confined by four border collision bifurcation boundaries, namely. $\xi^{0,\partial_{\mathcal{LM}}}_{\mathcal{LRM}^4\mathcal{RM}^3}$, $\xi^{5,\partial_{\mathcal{LM}}}_{\mathcal{LRM}^4\mathcal{RM}^3}$, $\xi^{6,\partial_{\mathcal{LM}}}_{\mathcal{LRM}^4\mathcal{RM}^3}$, and $\xi^{9,\partial_{\mathcal{LM}}}_{\mathcal{LRM}^4\mathcal{RM}^3}$. By contrast, the regions $\mathcal{P}_{\mathcal{LRMRM}^6}$ and $\mathcal{P}_{\mathcal{LRM}^2\mathcal{RM}^6}$ are not generic, as $n_2 = 6 = N_{\max}(1)$ and $n_2 = 6 = N_{\max}(2)$. The first of these regions is confined by three border collision bifurcation curves, which are indicated in the figure, and the second one by five. Note, that as the $\delta_{\mathcal{R}}$ values of the upper and of the lower corner of a region $\mathcal{P}_{\mathcal{LRM}^{n_1}\mathcal{RM}^{N_{\max}(n_1)}}$ are not identical, it is also possible that this region has four border collision bifurcation boundaries. It is also clear that the corners of the regions $\mathcal{P}_{\mathcal{LRM}^{n_1}\mathcal{RM}^{n_2}}$ represent codimension-2 border collision bifurcation points in the $(\delta_{\mathcal{R}}, k)$ parameter plane (as this plane is already particular due to $\delta_{\mathcal{L}} = 1$, in the 4D parameter space of map (9) this bifurcation has codimension 3). At the moment of this bifurcation each of four involved cycles has two points located at the borders, namely one at $\partial_{\mathcal{LR}}$ and another one at $\partial_{\mathcal{MR}}$. As an example, let us consider the bifurcation occurring at the point

$$\begin{aligned} C &= \xi^{8,\partial_{\mathcal{LM}}}_{\mathcal{LRM}^2\mathcal{RM}^4} \cap \xi^{4,\partial_{\mathcal{MR}}}_{\mathcal{LRM}^2\mathcal{RM}^4} \\ &= \xi^{4,\partial_{\mathcal{MR}}}_{\mathcal{LRM}^3\mathcal{RM}^3} \cap \xi^{8,\partial_{\mathcal{LM}}}_{\mathcal{LRM}^3\mathcal{RM}^3} \\ &= \xi^{0,\partial_{\mathcal{MR}}}_{\mathcal{LRM}^3\mathcal{RM}^2} \cap \xi^{0,\partial_{\mathcal{LM}}}_{\mathcal{LRM}^3\mathcal{RM}^2} \\ &= \xi^{0,\partial_{\mathcal{LM}}}_{\mathcal{LRM}^2\mathcal{RM}^3} \cap \xi^{4,\partial_{\mathcal{MR}}}_{\mathcal{LRM}^2\mathcal{RM}^3} \end{aligned} \tag{47}$$

marked with C in Fig. 16(d). From the four cycles undergoing border collision bifurcations at this point, namely $\mathcal{O}_{\mathcal{LRM}^2\mathcal{RM}^4}$, $\mathcal{O}_{\mathcal{LRM}^3\mathcal{RM}^3}$, $\mathcal{O}_{\mathcal{LRM}^3\mathcal{RM}^2}$, and $\mathcal{O}_{\mathcal{LRM}^2\mathcal{RM}^3}$, the first two are shown in Fig. 16(c). It can easily be seen that

$$\begin{aligned} \vec{p}_4^{\,\mathcal{LRM}^2\mathcal{RM}^4} &\in \partial_{\mathcal{MR}} \\ \vec{p}_8^{\,\mathcal{LRM}^2\mathcal{RM}^4} &\in \partial_{\mathcal{LM}} \\ \vec{p}_4^{\,\mathcal{LRM}^3\mathcal{RM}^3} &\in \partial_{\mathcal{MR}} \\ \vec{p}_8^{\,\mathcal{LRM}^3\mathcal{RM}^3} &\in \partial_{\mathcal{LM}} \end{aligned} \tag{48}$$

It is worth to emphasize that the cycles at the bifurcation moment do not coexist (in particular, since the points $\vec{p}_1, \ldots, \vec{p}_4$ of all four cycles are identical). Instead, only one of them exists, whereby which one does depends on the definition of the functions f^x, f^y at the boundaries, which have not been specified in Sec. 2.

For the transfer of the obtained results from the considered parameter plane $(\delta_{\mathcal{R}}, k)$ with $\delta_{\mathcal{L}} = 1$ to the parameter plane $(\delta_{\mathcal{R}}, \delta_{\mathcal{L}})$ with $k = k^*$ the question arises which regions $\mathcal{P}_{\mathcal{LRM}^{n_1}\mathcal{RM}^{n_2}}$ in the parameter plane $(\delta_{\mathcal{R}}, k)$ can be intersected by the line $k = k^*$. As the k-values of the left and right corners of the regions $\mathcal{P}_{\mathcal{LRM}^{n_1}\mathcal{RM}^{n_2}}$ are not identical, it is a cumbersome task to specify all possible situations. As an example, in Fig. 16(d) the line $k = k^*$ with $k^* = 0.23$ is shown. It can easily be seen that the sequence of the regions $\mathcal{P}_{\mathcal{LRM}^{n_1}\mathcal{RM}^{n_2}}$ intersected by this line is (for decreasing values of $\delta_{\mathcal{R}}$)

$$\begin{aligned} \mathcal{P}_{\mathcal{LRM}^5\mathcal{RM}} &\to \mathcal{P}_{\mathcal{LRM}^4\mathcal{RM}^2} \to \mathcal{P}_{\mathcal{LRM}^4\mathcal{RM}^3} \\ &\to \mathcal{P}_{\mathcal{LRM}^3\mathcal{RM}^4} \to \mathcal{P}_{\mathcal{LRM}^3\mathcal{RM}^5} \\ &\to \mathcal{P}_{\mathcal{LRM}^2\mathcal{RM}^6} \end{aligned} \tag{49}$$

When the value k^* is decreased to $k^* = 0.228$, this sequence is prolonged by one more region and becomes

$$\begin{aligned} \mathcal{P}_{\mathcal{LRM}^5\mathcal{RM}} &\to \mathcal{P}_{\mathcal{LRM}^4\mathcal{RM}^2} \to \mathcal{P}_{\mathcal{LRM}^4\mathcal{RM}^3} \\ &\to \mathcal{P}_{\mathcal{LRM}^3\mathcal{RM}^4} \to \mathcal{P}_{\mathcal{LRM}^3\mathcal{RM}^5} \\ &\to \mathcal{P}_{\mathcal{LRM}^2\mathcal{RM}^6} \to \mathcal{P}_{\mathcal{LRM}^2\mathcal{RM}^7} \end{aligned} \tag{50}$$

However, when k^* is decreased again, then the sequence changes not at the end but in the middle. As one can see, at $k^* = 0.228$ this sequence is given by

$$\begin{aligned} \mathcal{P}_{\mathcal{LRM}^5\mathcal{RM}} &\to \mathcal{P}_{\mathcal{LRM}^5\mathcal{RM}^2} \to \mathcal{P}_{\mathcal{LRM}^4\mathcal{RM}^3} \\ &\to \mathcal{P}_{\mathcal{LRM}^4\mathcal{RM}^4} \to \mathcal{P}_{\mathcal{LRM}^3\mathcal{RM}^5} \\ &\to \mathcal{P}_{\mathcal{LRM}^2\mathcal{RM}^6} \to \mathcal{P}_{\mathcal{LRM}^2\mathcal{RM}^7} \end{aligned} \tag{51}$$

5.4. *More than two letters $\mathcal{R}$ in the symbolic sequence*

In Sec. 5.3 we considered all families of cycles with points in all three partitions existing at $\delta_{\mathcal{L}} = 1$ for which the associated symbolic sequence contains two letters $\mathcal{R}$. In a similar way one can treat also families of cycles with more than two letters $\mathcal{R}$ in the associated symbolic sequences. To identify these families is a pure combinatorial task.

Clearly, for each number $N_{\mathcal{R}} > 2$ of letters $\mathcal{R}$ any symbolic sequence associated with a cycle existing at $\delta_{\mathcal{L}} = 1$ can be written as

$$\begin{aligned} \sigma = \mathcal{LRM}^{n_1}\mathcal{RM}^{n_2} \ldots \mathcal{RM}^{n_{N_{\mathcal{R}}}} \\ \text{with } n_j \geqslant 0,\ j = 1, \ldots, N_{\mathcal{R}} \end{aligned} \tag{52}$$

As explained above, to identify the mechanism leading to the appearance of the cycle $\mathcal{O}_\sigma$ and the border collision bifurcations occurring at the boundaries of its existence region $\mathcal{P}_\sigma$ it is necessary to

distinguish between the cases $n_j = 0$ and $n_j > 0$. Hence, a simple way to specify all cases to be considered separately is to write down $2^{N_\mathcal{R}}$ symbolic sequences $\rho = \rho_1\rho_2\dots\rho_{N_r}$ consisting of $N_\mathcal{R}$ letters $+$ and $-$, with the meaning $(\rho_j = +) \Rightarrow (n_j > 0)$ and $(\rho_j = -) \Rightarrow (n_j = 0)$. In this way we obtain for example for $N_\mathcal{R} = 3$:

$$(\rho_1\rho_2\rho_3) \Leftrightarrow \sigma$$

$$(---) \Leftrightarrow \{\mathcal{LR}^3\} \tag{53a}$$

$$(--+) \Leftrightarrow \{\mathcal{LR}^3\mathcal{M}^{n_3} \mid n_3 > 0\} \tag{53b}$$

$$(-+-) \Leftrightarrow \{\mathcal{LR}^2\mathcal{M}^{n_3}\mathcal{R} \mid n_3 > 0\} \tag{53c}$$

$$(-++) \Leftrightarrow \{\mathcal{LR}^2\mathcal{M}^{n_2}\mathcal{RM}^{n_3} \mid n_{2,3} > 0\} \tag{53d}$$

$$(+--) \Leftrightarrow \{\mathcal{LRM}^{n_1}\mathcal{R}^2 \mid n_1 > 0\} \tag{53e}$$

$$(+-+) \Leftrightarrow \{\mathcal{LRM}^{n_1}\mathcal{R}^2\mathcal{M}^{n_3} \mid n_{1,3} > 0\} \tag{53f}$$

$$(++-) \Leftrightarrow \{\mathcal{LRM}^{n_1}\mathcal{RM}^{n_2}\mathcal{R} \mid n_{1,2} > 0\} \tag{53g}$$

$$(+++) \Leftrightarrow \{\mathcal{LRM}^{n_1}\mathcal{RM}^{n_2}\mathcal{RM}^{n_3} \mid n_{1,2,3} > 0\} \tag{53h}$$

Obviously, (53a) is a single sequence corresponding to a basic cycle. Regarding other families, some statements can be provided. So, for example it can be shown that cycles corresponding to families (53e) and (53f) cannot exist for $\delta_\mathcal{L} = 1$. Hence, when investigating the part of the $(\delta_\mathcal{R}, k)$ parameter plane corresponding to cycles for which the associated symbolic sequence contains three letters $\mathcal{R}$, then five families of cycles must be considered. Clearly, a similar procedure can be applies also for any $N_\mathcal{R}$. However, the number of families grows exponentially with increasing $N_\mathcal{R}$, even if some of them can be excluded from the consideration.

6. Period adding structures

In the previous sections only the cycles were considered which have extended existence regions in the parameter plain $(\delta_\mathcal{R}, k)$ for $\delta_\mathcal{L} = 1$. It has been shown that in this plane the existence regions of these cycles are grouped according to the number of letters $\mathcal{R}$ in the associated symbolic sequences. This makes it possible to identify the cycles existing in the $(\delta_\mathcal{R}, \delta_\mathcal{L})$ parameter plane, even if the existence regions of these cycles do not cover this plane completely. Nevertheless, the knowledge about these regions build a basis for explanation of the bifurcation structure of the remaining parts the $(\delta_\mathcal{R}, \delta_\mathcal{L})$ parameter plane. In particular, between several of these regions period adding structures can be observed.

As an example, let us consider the bifurcation scenario shown in Fig. 17(a). The corresponding parameter path is marked in Fig. 12(c). As one can see in this figure, the parameter path intersects (for increasing $\delta_\mathcal{R}$) the regions $\mathcal{P}_{\mathcal{LRM}^n}$, $n = 3, 2, 1$ with periods 5, 4 and 3, respectively. By Property 17(c) for each n there is some free space between the regions $\mathcal{P}_{\mathcal{LRM}^{n+1}}$ and $\mathcal{P}_{\mathcal{LRM}^n}$. The bifurcation structure between these regions is the usual period adding: between the regions with periods 5 and 4 there is a region with period 9, between the regions with periods 4 and 3 there is a region with period 7, and so on. The symbolic sequences of the cycles forming this structure can easily be obtained by concatenation of the symbolic sequences of the cycles $\mathcal{O}_{\mathcal{LRM}^n}$. For example, as one can easily see in Fig. 17(b), the 9-cycle located in the parameter space between the cycles $\mathcal{O}_{\mathcal{LRM}^3}$ and $\mathcal{O}_{\mathcal{LRM}^2}$ is $\mathcal{O}_{\mathcal{LRM}^3\mathcal{LRM}^2}$. More general, the families of cycles with the first complexity level in this period adding structure located between the regions $\mathcal{P}_{\mathcal{LRM}^{n+1}}$ and $\mathcal{P}_{\mathcal{LRM}^n}$ can easily be obtained by replacing the letters $\mathcal{L}$ and $\mathcal{R}$ in Eq. (21) by $\mathcal{LRM}^{n+1}$ and $\mathcal{LRM}^n$, respectively. In this way we obtain the families

$$\{\mathcal{O}_{(\mathcal{LRM}^{n+1})(\mathcal{LRM}^n)^{n_1}} \mid n_1 \geqslant 1\} \tag{54a}$$

$$\{\mathcal{O}_{(\mathcal{LRM}^{n+1})^{n_1}(\mathcal{LRM}^n)} \mid n_1 \geqslant 1\} \tag{54b}$$

(see Fig. 17(a)) The families cycles with higher complexity levels can be obtained similarly. Note that a sufficient condition for the appearance of a period adding structure in the portion of the parameter space confined by the border collision bifurcation curves of two cycles colliding the border point from opposite sides in 1D discontinuous maps is proved in [Gardini *et al.*, 2014]. To our knowledge, a similar proof for 2D maps does not exist, nevertheless the observed phenomenon is the same. In the considered example, the cycles $\mathcal{O}_{\mathcal{LRM}^{n+1}}$ and $\mathcal{O}_{\mathcal{LRM}^n}$ collide the boundary $\partial_{\mathcal{LM}}$ from opposite sides, and in the portion of the parameter space confined by the border collision bifurcation curves $\xi^{n+2,\partial_{\mathcal{LM}}}_{\mathcal{LRM}^{n+1}}$ and $\xi^{0,\partial_{\mathcal{LM}}}_{\mathcal{LRM}^n}$ there exists a period adding structure issuing from the intersection point of these curves formed by the existence regions of the cycles with the symbolic sequences specified above.

It is worth noticing that the period adding structure in map 9 may involve coexisting attractors. This is particularly the case close to the diagonal $\delta_\mathcal{L} = \delta_\mathcal{R}$ of the parameter plane $(\delta_\mathcal{R}, \delta_\mathcal{L})$, since the symmetry of the map given by the Property 5 implies that in this parameter region cycles with odd periods can exist only in pairs. As an example let us consider the bifurcation scenario shown in Fig. 6(a).

As described in Sec. 4.3, the interval in which the

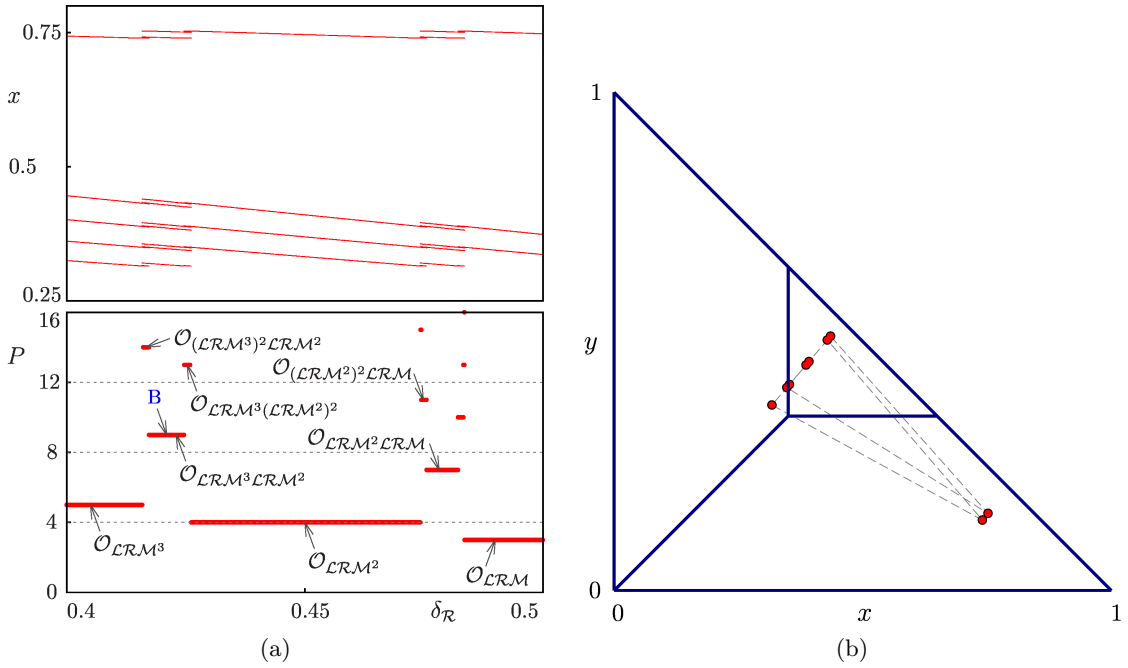

Fig. 17. (a) Period adding scenario between the regions $\mathcal{P}_{\mathcal{LRM}^n}$, $n = 3, 2, 1$. The corresponding parameter path in the $(\delta_{\mathcal{R}}, \delta_{\mathcal{L}})$ plane is marked in Fig. 12(c). Parameters $\delta_{\mathcal{L}} = 0.62$, $\delta_{\mathcal{M}} = 0.1$, $k = 0.35$. (b) Cycle $\mathcal{O}_{\mathcal{LRM}^3\mathcal{LRM}^2}$ at $\delta_{\mathcal{R}} = 0.421$ (the corresponding point is indicated in (a) by the letter B).

limit sets of the map have period 3, is belongs to the intersection $\mathcal{P}_{\mathcal{LRM}} \cap \mathcal{P}_{\mathcal{LMR}}$ (see Fig. 9(d)). Accordingly, in this interval the cycles $\mathcal{O}_{\mathcal{LRM}}$ and $\mathcal{O}_{\mathcal{LMR}}$ coexist and their basins of attraction cover the complete domain $\mathcal{D}$, as shown in Fig. 18(a). Similarly, the period 5 in the period adding cascade shown in Fig. 6(a) is related to the coexistence of the cycles $\mathcal{O}_{\mathcal{LRLMR}}$ and $\mathcal{O}_{\mathcal{RMLRL}}$ shown in Fig. 18(b). Also these cycles are symmetric to each other with respect to the diagonal $y = x$. Note that these cycles do not exist at $\delta_{\mathcal{L}} = 1$ or $\delta_{\mathcal{R}} = 1$, as the associated symbolic sequences contain two letters $\mathcal{L}$ and two letters $\mathcal{R}$.

The situation regarding the period 8 existing between the periods 3 and 5 is slightly different. It corresponds to two cycles $\mathcal{O}_{\mathcal{LRMLRLMR}}$ and $\mathcal{O}_{\mathcal{LMRLRLMR}}$ which are symmetric to each other with respect to the diagonal $y = x$. However, additionally to these cycles the cycle $\mathcal{O}_{\mathcal{RMLRMLRL}}$ exists which is symmetric in itself, as shown in Fig. 18(c). Similar structures in the state space can also be observed for higher periods: cycles with odd periods exist in pairs, symmetric to each other, while for even periods we observe pairs of cycles symmetric to each other and additionally cycles which are symmetric in itself.

Note that coexistence of cycles occurs not only in the parameter regions close to the diagonal $\delta_{\mathcal{L}} = \delta_{\mathcal{R}}$. As an example, Fig. 18(d) shows two coexisting 6-cycles observed far away from this diagonal.

7. Conclusions

In this work we considered a standard model commonly used to illustrate the Braess paradox. This paradox states that when an additional resource is added to a system formed by rational agents, then the overall performance of the system can be not only increased by also decreased. The model considered in this paper shows this effect in a particular network of roads on which cars are moving from one point to another one taking the decision which road to choose depending on the current situation on the roads. When an additional road is added to the network, the overall performance of the system may decrease.

From the mathematical point of view, a model of the considered network with two roads is given by a piecewise linear discontinuous 2D map defined on two partition. Introducing the third road corresponds in the map to the appearance of a third partition. Possible dynamics of the model on two partition and their organization in bifurcation structures have been completely understood in the previous works. In the present work we investigated the effect of introducing the third partition on these bi-

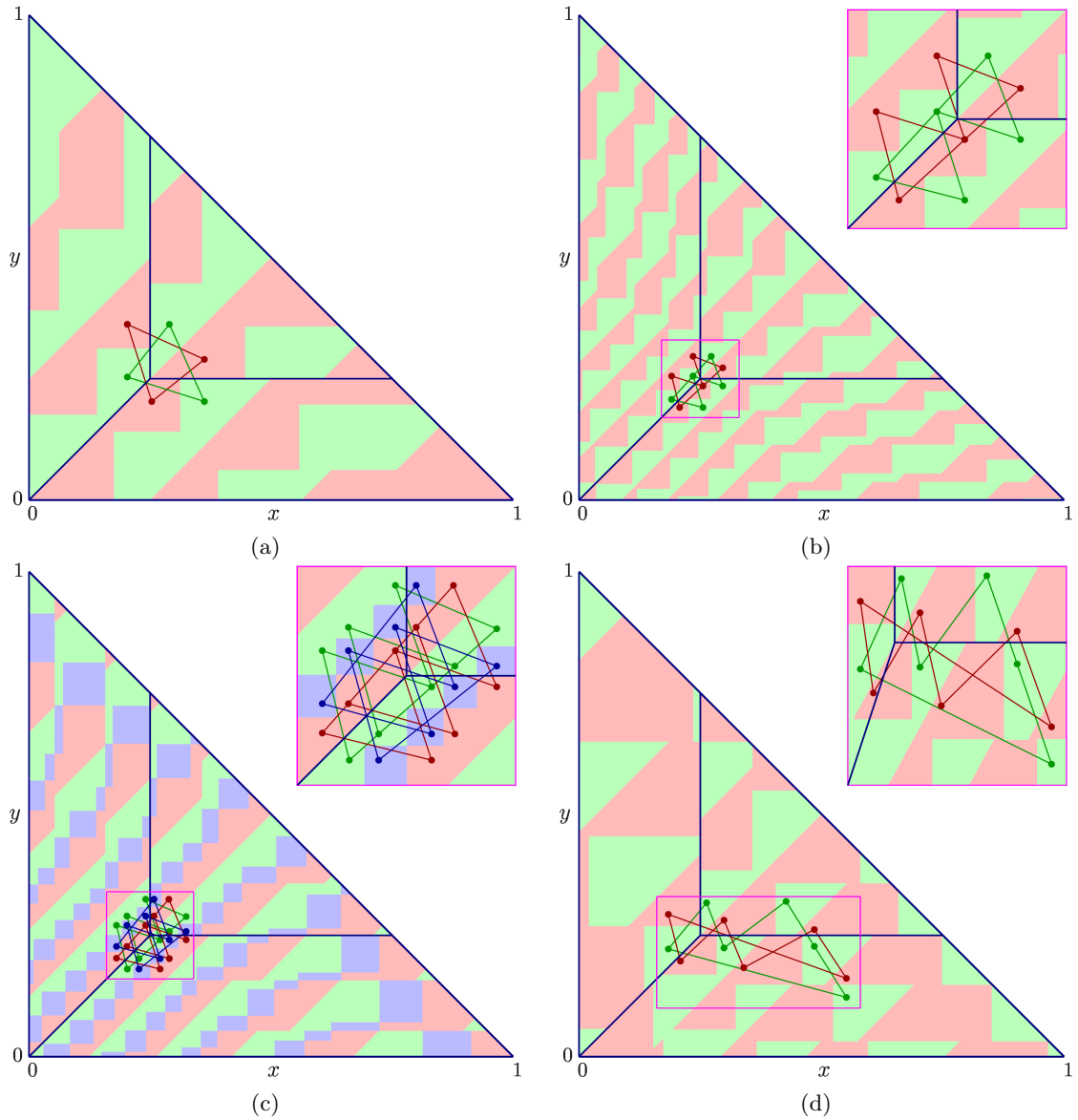

Fig. 18. Coexisting cycles of map (9) and their basins of attraction. (a) 3-cycles $\mathcal{O}_{\mathcal{LRM}}$ (green) and $\mathcal{O}_{\mathcal{RLM}}$ (red); (b) 5-cycles $\mathcal{O}_{\mathcal{LRLRM}}$ (green) and $\mathcal{O}_{\mathcal{RLRLM}}$ (red); (c) 8-cycles $\mathcal{O}_{\mathcal{LRMLRLRM}}$ (red), $\mathcal{O}_{\mathcal{RLMRLRLM}}$ (green), and $\mathcal{O}_{\mathcal{RMLRMLRL}}$ (blue); (d) 6-cycles $\mathcal{O}_{\mathcal{LRRMRM}}$ (green) and $\mathcal{O}_{\mathcal{LRMRML}}$ (red). Insets show the marked rectangles magnified. Parameters: $\delta_{\mathcal{M}} = 0.3$, $k = 0.25$, (a) $\delta_{\mathcal{L}} = \delta_{\mathcal{R}} = 0.2$, (b) $\delta_{\mathcal{L}} = \delta_{\mathcal{R}} = 0.08$, (c) $\delta_{\mathcal{L}} = \delta_{\mathcal{R}} = 0.11$, (d) $\delta_{\mathcal{L}} = 0.45$, $\delta_{\mathcal{R}} = 0.12$.

furcation structures.

It is shown that when the third partition is introduced, the bifurcation structure of the parameter plane of interest changes completely. A high number of periodicity regions appears, associated with cycles with points located in all three partitions. As any cycle of the investigated map is necessarily stable, the boundaries of these regions are given by border collision bifurcation curves. Due to the linearity of the map in all three partitions it is possible to calculate these bifurcation curves analytically for cycles of any period, provided that the symbolic sequence associated with the cycle is known. However, it turns out to be a circumstantial task to identify the regularities in the appearance of cycles in the parameter plane of interest. To solve this problem, we applied a two-step approach. First, we investigated a different parameter plane at the particular parameter values for which the investigated map has a constant value on one on the partitions. This makes it possible – at least, in principle – to identify *all* families of cycles existing in this parameter plane. Then, as a next step, the results obtained in this plane can easily be transferred back to the

original parameter plane of interest. Although set of cycles which occur in the case that map has a constant value on one on the partitions is only a subset of all possible cycles, the obtained results show how several periodicity regions appear, become split in parts and disappear. It has also been shown that the period adding structure occurring between the discussed periodicity regions may be enriched by a regular appearance of coexisting cycles.

Acknowledgments

The work of V. Avrutin was supported by the European Community within the scope of the project "Multiple-discontinuity induced bifurcations in theory and applications" (Marie Curie Action of the 7th Framework Programme). The work of U. Merlone has been performed under the auspices of COST Action IS1104 "The EU in the new complex geography of economic systems: models, tools and policy evaluation".

References

Altman, E., Kamble, V. & Kameda, H. [2008] "A Braess type paradox in power control over interference channels," *Proc. of the 6th Int. Symposium on Modeling and Optimization WiOpt 2008* (Berlin, Germany).

Avrutin, V., Schanz, M. & Gardini, L. [2010] "Calculation of bifurcation curves by map replacement," *Int. J. Bifurcat. Chaos* **20**, 3105–3135, doi:10.1142/S0218127410027581.

Bazzan, A. & Klüg, F. [2005] "Case studies on the Braess paradox: Simulating route recommendation and learning in abstract and microscopic models," *Transportation Science Part C* **13**, 299–319.

Bischi, G. I., Gardini, L. & Merlone, U. [2009a] "Impulsivity in binary choices and the emergence of periodicity," *Discrete Dynamics in Nature and Society* **Volume 2009**, Article ID 407913, 22 pages doi:10.1155/2009/407913.

Bischi, G. I., Gardini, L. & Merlone, U. [2009b] "Periodic cycles and bifurcation curves for one-dimensional maps with two discontinuities," *Journal of Dynamical Systems & Geometric Theories* **7**, 101–123.

Braess, D. [1968] "Über ein Paradoxon aus der Verkehrsplanung," *Unternehmensforschung* **12**, 258–268, (in German).

Dal Forno, A., Gardini, L. & Merlone, U. [2012] "Ternary choices in repeated games and border collision bifurcations," *Chaos Solitons and Fractals,* **45**, 294–305, doi:10.1016/j.chaos.2011.12.003.

Dal Forno, A. & Merlone, U. [2013a] "Border-collision bifurcations in a model of Braess paradox," *Mathematics and Computers in Simulation* **87**, 1–18.

Dal Forno, A. & Merlone, U. [2013b] "Border-collision bifurcations in a model of braess paradox," *Mathematics and Computers in Simulation* **87**, 1–18.

Dal Forno, A., Merlone, U. & Avrutin, V. [2014] "Dynamics in Braess paradox with non-impulsive commuters," *Discrete Dynamics in Nature and Society* **2014**, Article ID 407913, 22 pages, doi:10.1155/2009/407913.

Gardini, L., Avrutin, V. & Sushko, I. [2014] "Codimension-2 border collision bifurcations in one-dimensional discontinuous piecewise smooth maps," *Int. J. Bifurcat. Chaos* **24**, 1450024, doi:10.1142/S0218127414500242.

Gardini, L., Tramontana, F., Avrutin, V. & Schanz, M. [2010] "Border collision bifurcations in 1D piecewise-linear maps and Leonov's approach," *Int. J. Bifurcat. Chaos* **20**, 3085–3104, doi:10.1142/S021812741002757X.

Gisches, E. & Rapoport, A. [2012] "Degrading network capacity may improve performance: private versus public monitoring in the braess paradox," *Theory Decision* **73**, 267–293, doi:10.1007/s11238-010-9237-0.

Homburg, A. J. [1996] "Global aspects of homoclinic bifurcations of vector fields," *American Math. Soc.* **578**.

Keener, J. P. [1980] "Chaotic behavior in piecewise continuous difference equations," *Trans. Am. Math. Soc.* **261**, 589–604.

Korilis, Y., Lazar, A. & Orda, A. [1999] "Avoiding the Braess paradox in non-cooperative networks," *Journal of Appied Probability* **36**, 211–222.

Leonov, N. N. [1959] "On a pointwise mapping of a line into itself," *Radiofisika* **2**, 942–956, (in Russian).

Leonov, N. N. [1960] "On a discontinuous piecewise-linear pointwise mapping of a line into itself," *Radiofisika* **3**, 496–510, (in Russian).

Lin, H., Roughgarden, T., Tardos, E. & Asher, W. [2011] "Stronger bounds on braess's paradox and the maximum latency of selfish routing," *SIAM Journal on Discrete Mathematics* **25**, 1667–1686.

Lyubimov, D. V., Pikovsky, A. S. & Zaks, M. A. [1989] *Universal Scenarios of Transitions to Chaos via Homoclinic Bifurcations*, Math. Phys. Rev., Vol. 8 (Harwood Academic, London), Russian version as a Preprint (192) of Russian Academy of Science, Institute of Mechanics of Solid Matter, 1986, Sverdlovsk.

Malkevitch, J. [2011] "The price of anarchy," *Consortium* **101**, 4–10, also available:AMS Feature Column http://www.ams.org/samplings/feature-column/fcarc-anarchy, accessed: 2014-10-23.

Nagurney, A. & Boyce, D. [2005] "Preface to "On a paradox of traffic planning"," *Transportation Science* **39**, 443–445.

Panchuk, A., Sushko, I., Schenke, B. & Avrutin, V. [2013] "Bifurcation structures in a bimodal piecewise linear map: regular dynamics," *Int. J. Bifurcat. Chaos* **23**, 1330040, doi:10.1142/S0218127413300401.

Rapoport, A., Mak, V. & Zwick, R. [2006] "Navigating congested networks with variable demand: Experimental evidence," *Journal of Economic Psychology* **27**, 648–666.

Roughgarden, T. & Tardos, E. [2002] "How bad is selfish routing?" *Journal of the ACM* **49**, 236–259.

Sandholm, W. H. [2010] *Population games and evolutionary dynamics* (The MIT Press, Cambridge, MA).

Zhang, H.-F., Yang, Z., Wu, Z.-X., Wang, B.-H. & Zhou, T. [2013] "Braess's paradox in epidemic game: Better condition results in less payoff," *Scientific Reports* **3**, 3292, doi:10.1038/srep03292.